

Bcl-x_L deamidation in oncogenic tyrosine kinase signalling

Rui Zhao

SID 0716665/1

ACKNOWLEDGEMENTS

I am grateful to my colleagues who contribute to this project, particularly Dr Denis Alexander for his supervision, and the Babraham Institute, where the work was completed. Also I thank my family for their tremendous support in the last 8 years.

CONTENT

Timeline

Summary

Introduction

Chapter 1. Chronology of research interests

1.1 Oncogenic tyrosine kinase Lck^{F505Y} in murine thymocyte transformation

1.1.1 Aim and strategy

1.1.2 Kinase activity

1.1.3 Survival and cell- cycle progression

1.1.4 DNA repair and genomic instability

1.1.5 DNA damage- induced apoptosis

1.1.6 Examining the survival pathway in CD45^{-/-}Lck^{F505Y} DN thymocytes in DNA damage response

1.2 How is Bcl-x_L deamidated in DNA damage responses?

1.2.1 Elucidation of the roles of different species of Bcl-x_L by *in vitro* and *in vivo* studies

1.2.2 Is Bcl-x_L deamidation a consequence of mitochondrial apoptosis?

1.2.3 The DNA damage- NHE-1 up-regulation- intracellular alkalinisation- Bcl-x_L deamidation axis

1.3 Bcl-x_L deamidation pathway in Myeloproliferative Disorders (MPDs)

1.3.1 Why investigate Bcl-x_L deamidation pathway in MPDs?

1.3.2 Patients' sample collection and cell purification

1.3.3 Bcl-x_L deamidation pathway is inhibited in CML myeloid cells

1.3.4 BCR-ABL inhibitor Imatinib reverses the inhibition of Bcl-x_L deamidation pathway in CML myeloid cells

- 1.3.5 Imatinib does not reverse the inhibition of Bcl-x_L deamidation pathway in Imatinib- resistant CML cells that carry an E255V mutation in the BCR-ABL kinase domain
- 1.3.6 Bcl-x_L deamidation pathway is inhibited by Jak2^{V617F} in PV myeloid cells
- 1.3.7 Jak 2 inhibitor reverses the inhibition of Bcl-x_L deamidation pathway in PV myeloid cells
- 1.3.8 Bcl-x_L deamidation pathway in Jak2^{V617F}-positive Idiopathic Myelofibrosis (IMF)

1.4 Tyrosine kinases in other haematological malignancies- potential research interests and therapeutic targets

Chapter 2. Critiques/Reflection

- 2.1 Asn 52/66 issues
- 2.2 Global effects of alkalinisation
- 2.3 Protein modification in signal transduction

Chapter 3. Conclusion and Future Work

TIMELINE

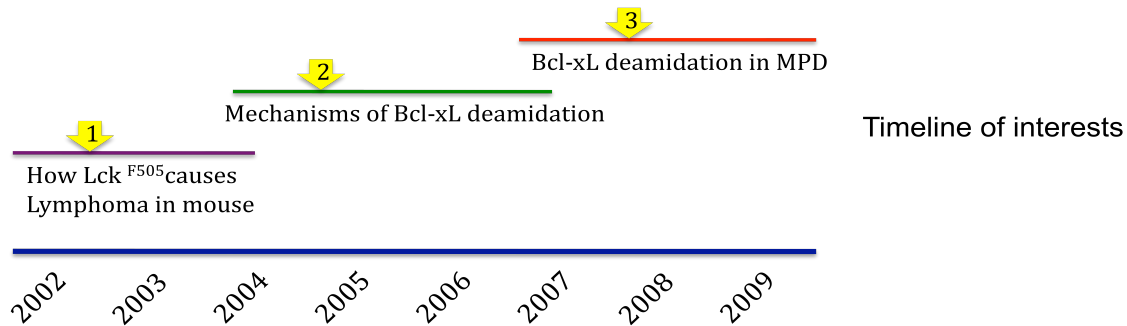


Fig 1. Key experiments in the progress of this project

The project encompassed three stages, which were represented in three time lines. A key experiment (represented as a yellow arrow symbol) in each stage, which has been critical in the development of this project, is also shown.

Key experiment 1. DNA damage-induced Bcl-x_L deamidation is inhibited by oncogenic Lck^{F505}, Fig 7A, Zhao R 2004

Key experiment 2. Bcl-x_L deamidation induced by DNA damage involves up-regulation of the NHE-1 antiport, Fig 4, Zhao R 2007

Key experiment 3. Inhibition of the NHE-1/ Bcl-x_L deamidation pathway induced by DNA damage in Chronic Myelogenous Leukaemia cells, Fig 1, Zhao R 2008

SUMMARY

I have been interested in the molecular mechanisms of Haematopoietic malignant diseases such as leukaemia and lymphoma, especially those involving oncogenic tyrosine kinases. About 30 of the 90 tyrosine kinases in the human genome have been implicated in cancer (Blume-Jensen P, 2001). The oncogenic tyrosine kinases (OTKs), such as Bcr-Abl (product of chromosomal translocations of two genes *bcr* and *abl*) in Chronic Myelogenous Leukaemia, and Erythroblastic leukaemia viral oncogene homolog 2(Erb-B2) in mammary and other cancers, mediate their transforming effects via a diverse array of signalling pathways involved in DNA damage, cell survival and cell cycle regulation (Deutsch E, 2001; Skorski T, 2002; Kumar R, 1996)

My work has been centred around the analysis of a mouse cancer model that is driven by an oncogenic tyrosine kinase – p56^{Lck-F505} expressed on CD45 knock- out background (Baker M, 2000). The investigation of this mouse model has revealed that oncogenic inhibition of deamidation of the Bcl-x_L survival protein plays a critical role in protecting thymocytes from DNA-damage induced apoptosis. Cells that would normally be eliminated due to accumulating DNA damage are instead preserved with an increasing load of double-stranded breaks, leading to genomic instability, chromosomal abnormalities and transformation. This work was published in Cancer Cell (An oncogenic tyrosine kinase inhibits DNA repair and DNA-damage-induced Bcl-x_L deamidation in T cell transformation. Zhao R, 2004). Following that I have tried to elucidate the different roles of the two deamidated species of Bcl-x_L in apoptosis, and also the molecular mechanisms of DNA damage- induced Bcl-x_L deamidation in order to understand the inhibition of Bcl-x_L deamidation by oncogenic tyrosine kinases. Recently I have shown that Bcl-x_L deamidation, whereby two critical Asn residues are converted to iso-Asp, cripples the ability of the protein to sequester pro-apoptotic BH3-only proteins such as Bim and p53- upregulated modulator of apoptosis (PUMA), thereby explaining its loss of pro-survival functionality. *In vivo*, DNA damage causes intracellular alkalinisation that is both necessary and sufficient to deamidate Bcl-x_L, promoting apoptosis: no enzyme is necessary for this process. In pre-tumourigenic thymocytes alkalinisation is blocked, so preserving Bcl-x_L in its pro-survival mode.

Furthermore murine tumours are protected from genotoxic attack by native Bcl-x_L, but enforced alkalinisation and consequent Bcl-x_L deamidation promotes apoptosis. This part of work was published in Plos Biology (DNA damage-induced Bcl-x_L deamidation is mediated by NHE-1 antiport regulated intracellular pH. Zhao R, 2007).

Through collaboration with Prof AR Green's research group at the Department of Haematology of the University of Cambridge, I have also analysed the Bcl-x_L deamidation pathway in human myeloproliferative disorders, e.g. Polycythemia vera(PV) and Chronic Myelogenous Leukaemia (CML). We found that the oncogenic tyrosine kinases involved in these disorders, i.e. Jak2^{V617F} and Bcr-Abl also inhibit the Bcl-x_L deamidation pathway in DNA damage responses. These findings shed light on potential therapeutic application of the Bcl-x_L deamidation pathway in human malignancies. This piece of work was recently published in the New England Journal of Medicine (Inhibition of the Bcl-x_L deamidation pathway in myeloproliferative disorders. Zhao R, 2008).

Overall the cited work has led to several important new insights into the molecular mechanisms involved in oncogenesis: first, that Bcl-x_L deamidation is important in the cascade of events leading from DNA damage to apoptosis; second, that oncogenic tyrosine kinases inhibit these events in both the murine and human context; third, that up-regulation of the NHE-1 antiport and consequent intracellular alkalinisation are critical events in this DNA damage-induced cascade leading to apoptosis. In the process I have demonstrated the first in vivo mechanism for the deamidation of an internal protein Asn. Essentially, a completely new and unexpected signalling pathway has been uncovered that seems to pertain to all murine and human haematopoietic cell lineages that have been investigated so far.

INTRODUCTION

Tyrosine kinases play important roles in cellular function. They normally behave as tightly regulated switches in the signal transduction network, however they also have the potential to induce oncogenic transformation.

Receptor tyrosine kinases (RTKs) such as EGFR and Erb-B2, are composed of an extracellular ligand binding domain, a transmembrane domain, and a cytoplasmic domain that contains a catalytic kinase core and regulatory sequences (Schlessinger *et al.*, 2000). RTKs have three general mechanisms to become oncogenic. Firstly, genomic rearrangements can generate fused proteins that maintain the kinase in a more stable manner; Secondly, gene amplification leads to spontaneous dimerisation that stabilizes the kinase; Finally, some RTKs acquire point mutations that allow them to dimerise and stabilize (Blume-Jensen and Hunter, 2001).

Non-receptor tyrosine kinases, such as Src, Lck and Abl, lack extracellular and transmembrane domains. Their mechanisms of oncogenic activation are varied. Some become constitutively active by fusion to a dimerising partner, while others are transformed to onco-proteins by acquiring mutations that disrupt autoinhibitory functions (Blume-Jensen and Hunter, 2001).

Oncogenic Tyrosine Kinases (OTKs) are extensively involved in cancer by promoting proliferation, invasion, and metastasis. Compared to other onco-proteins, OTKs are unique in that they tend to render cells extraordinarily resistant to DNA damage-induced apoptosis (Skorski *et al.*, 2002). This is demonstrated clinically that cancers that express OTKs are usually highly resistant to radio- and chemo- therapy. This clinical observation has attracted great interests from clinicians and researchers. The resistance, although likely contributed by several mechanisms, has been found consistently linked with markedly increased Bcl-x_L expression (Kumar *et al.*, 1996; Amarante-Mendes *et al.*, 1998; Karni *et al.*, 1999; Zamo *et al.*, 2002).

Bcl-x_L is an anti-apoptotic member of the Bcl-2 family. Like Bcl-2, Bcl-x_L is believed to act by binding and sequestering BH3-only proteins such as Bim, thereby

preventing their pro-apoptotic interactions with Bax (Cheng EH, 2001; Kuwana T, 2002). Bcl-x_L deamidation in response to DNA damage has been recently proposed as a critical switch to subvert the pro-survival function of Bcl-x_L (Deverman BE, 2002).

P56^{Lck} is a member of src family tyrosine kinases expressed predominantly in T thymocytes. Lck is constitutively located to membranes as a result of modification of amino acid residues close to the N-terminus that are sites of myristoylation/palmitoylation (Kabouridis PS, 1997). The N-terminal domain contains a di-cysteine motif that is required for association with the CD4 and CD8 coreceptors (Kim PW, 2003). As with other src-family kinases, the regulation of kinase activity/functionality is tightly controlled by conformational changes arising from binding of ligands to the SH3 and/or Sh2 domains of the kinases (Holdor AD, 1999; da Silva AJ, 1997) and by the phosphorylation and dephosphorylation of two critical tyrosine residues (Palacios EH, 2004).

Earlier studies (Koretzky GA, 1990; Shiroo M, 1992; Kishihara K, 1993; Byth KF, 1996; Mee PJ, 1999) have established both positive and negative roles for CD45 in controlling the signaling threshold of T-cell antigen receptor (TCR), thereby regulating T-cell development (Alexander DR, 2000). Mice expressing active Lck^{F505} at non-oncogenic levels develop aggressive thymic lymphomas on a CD45 null background (Baker M, 2000). CD45 suppresses the tumorigenic potential of the kinase by dephosphorylation of the Tyr394 autophosphorylation site (Baker M, 2000; Alexander DR, 2000). In CD45^{-/-} thymocytes the kinase is switched to hyperactive oncogenic state, resulting in increased resistance to apoptosis. Transformation occurs in early CD4-CD8⁻ thymocytes during the process of TCR- β chain rearrangement by a recombinase-independent mechanism (Baker M, 2000).

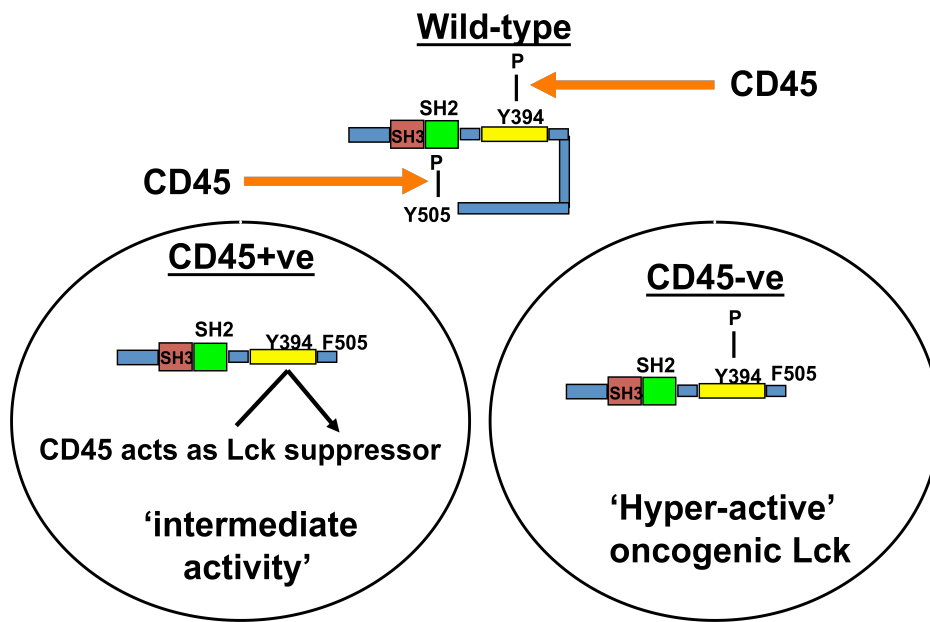


Fig 2. A model explaining the interaction between CD45 and various phosphorylated sites of p56^{Lck} in CD45+ve and CD45-ve cells. Overall CD45 acts as both a positive and negative regulator of immune cells function.

Phosphorylation of Tyr 394 increases p56^{Lck} kinase activity, while phosphorylation of Tyr 505 decreases p56^{Lck} kinase activity.

CHAPTER 1. CHRONOLOGY OF RESEARCH INTERESTS

1.1.1 Aim and strategy

The first part of my work (Zhao R, 2004) was aiming to elucidate the mechanisms involved in the tumourigenesis of CD45^{-/-} Lck^{F505} mice, progeny produced by crossing CD45^{-/-} mice and Lck^{F505} mice, instigated by the interesting phenomenon that thymic tumours develop in these mice with a 100% penetrance at a quite early age, i.e. 5-15 weeks. As a contrast, the parental CD45^{-/-} and Lck^{F505} mice do not develop tumours during their whole life span.

In an earlier published work from Dr DR Alexander's group (Baker M, 2000), CD45^{-/-} Lck^{F505} mice were phenotypically characterised, with comparisons to wild-type, CD45^{-/-} and Lck^{F505} mice in respective of the thymic development and differentiation. Higher kinase activity of Lck^{F505} was proposed to be the origin of the tumourigenesis, however the mechanisms behind this were obscure.

Intrigued by the dramatic tumour development in CD45^{-/-} Lck^{F505} mice, I joined Dr Alexander's group in early 2002, with a medical background in Haemato-oncology, hoping to discover the mechanisms entailed by the oncogenic tyrosine kinase Lck^{F505}. The strategy I used in the study was to analyse the signalling pathways that might be involved in the transformation in pre-tumourigenic double-negative (DN) thymocytes in relation to Lck^{F505} activity and function.

1.1.2 Kinase activity

Initially, the phosphorylation status and kinase activity of Lck in CD45^{-/-} Lck^{F505} DN thymocytes were analysed in detail. For technical simplicity, I took the advantage of having the above mice on Rag^{-/-} background in-house. Rag^{-/-} and Rag^{-/-}CD45^{-/-} mice only produce DN thymocytes in their thymus. It is noteworthy that it has been shown in the previous study (Baker 2000) that deletion of Rag does not confer any changes to the tumour development of CD45^{-/-} Lck^{F505} mice.

There are two regulatory sites in wild- type Lck that are important for the kinase activity: pTyr- 394 and pTyr- 505, of which pTyr- 394 is a positive regulatory site, while pTyr-505 a negative one. CD45 tyrosine phosphatase dephosphorylates both sites, keeping Lck activity at an appropriate level and with normal function. However in Lck^{F505} Tyr 505 is mutated to Phe, causing a non-regulatory site at the end of Lck. CD45 cannot dephosphorylate this site, thus the overall kinase activity in Lck^{F505} is lower than in wild- type Lck. However in the absence of CD45, i.e. CD45^{-/-}, Lck^{F505} has an increased activity (Alexander DR, 2000).

Phosphorylation studies on the immunoprecipated Lck protein from Rag^{-/-}CD45^{-/-} Lck^{F505} DN thymocytes showed an increased phosphorylation of Tyr 394 and decreased phosphorylation of Tyr 505 respectively. In vitro kinase assay on the same material revealed a 2- 3 fold increase of the kinase activity. The results were consistent with previous study and current understandings of the CD45/Lck interaction. Kinase activities in DN thymocytes can be defined as basal (Rag^{-/-}), intermediate (Rag^{-/-}CD45^{-/-} or Rag^{-/-}Lck^{F505}), or hyperactive (Rag^{-/-}CD45^{-/-} Lck^{F505}).

1.1.3 Survival and cell- cycle progression

I considered the commonest signalling pathways that might be involved in oncogenesis to start with, i.e. those relating to cellular survival and cell- cycle control. Both analyses were performed on gated DN3 and DN4 thymocytes by flow- cytometry (FACs). A pool of monoclonal antibodies conjugated with different fluorescent dyes allows analysis of DN3/ DN4 subsets with relatively small number of cells.

Not surprisingly, Rag^{-/-} thymocytes had a high level of apoptosis and a significant growth arrest due to a complete failure of β - selection and lack of pre-TCR mediated mitogenic signals. This made Rag^{-/-} mice and its CD45^{-/-} and CD45^{-/-} Lck^{F505} crosses most useful in addressing these points. Compared with Rag^{-/-}, Rag^{-/-} CD45^{-/-} thymocytes had much less apoptosis- 29.6% compared to 97.3%. While in Rag^{-/-} Lck^{F505} and Rag^{-/-} CD45^{-/-} Lck^{F505}, the reduction of apoptosis was even more significant- both of them had less than 1% of apoptotic cell in their DN3

compartment of the thymocytes. Likewise, there were more cells in G2 phase in Rag^{-/-} CD45^{-/-} than in Rag^{-/-} DN3- 7% compared to 2-4%, whilst in Rag^{-/-} Lck^{F505} and Rag^{-/-} CD45^{-/-} Lck^{F505}, cells in cycle were increased to nearly 30%.

The results described imply that the “intermediate activity” Lck in Rag^{-/-} Lck^{F505} and the “hyperactive” Lck in Rag^{-/-} CD45^{-/-} Lck^{F505} have similar effects on the survival and cell cycle progression of DN3 thymocytes, though the former is non- oncogenic and the latter is oncogenic. This suggests that “intermediate activity” Lck is sufficient for keeping the normal survival and cell cycle progression of thymocytes. Since “hyperactive” Lck has 2-3 fold increase of the kinase activity compared to “intermediate activity” Lck, this begs the question: what is the role of the increased kinase activity? There must be something extra conferred by the “hyperactive” Lck to transform the thymocytes into cancerous phenotype.

One point to argue here is that the link between kinase activity and apoptosis in DN 3 thymocytes might be casual. However, as we know Lck^{F505} mice with a higher copy number of the transgene, and consequently a higher kinase activity, develop thymic lymphoma in a way similar to CD45^{-/-} Lck^{F505} mice. The evidence demonstrates an exquisitely sensitive link between Lck kinase activity and the cellular survival and cell cycle progression of DN thymocytes.

1.1.4 DNA repair and genomic instability

It is believed that accumulation of unrepaired double strand breaks (DSBs) can cause genomic instability and secondary mutations, which are an important source of transformation. Thymocytes are known to be sensitive to genotoxic drugs and irradiation. So the DNA repair pathway is another potential candidate to investigate (Khanna KK, 2001; Richardson C, 2000).

My first test of the DNA repair pathway was to give same gamma-irradiation to the cells, then leave them to repair and measure the repair efficiency at 6h and 24h. Irradiated cells were cast into agarose plugs, and proteins were digested with proteinase K. DNA containing DSBs were separated from intact DNA by pulse field

gel electrophoresis (PFGE) technique (Bassing CH, 2003). The results were striking- wild- type, CD45^{-/-} and Lck^{F505} DN thymocytes showed similar repair efficiency at multiple time points, whilst CD45^{-/-}Lck^{F505} expressed a much more reduced repair of DSBs over a 6h or 24h time course.

The results were encouraging in the way that difference between non-oncogenic and oncogenic “hyperactive” Lck was first revealed. To ensure that this is a true phenomenon, the finding was vigorously tested with various methods.

Phosphorylation of H2AX was measured by western blots and also FACs as phosphorylated H2AX (γ H2AX) was thought to be a sensitive marker of the DSBs in the chromosomes following DNA damage (Bassing CH, 2003; Rogakou EP, 1998). The results showed a dramatic increase of γ H2AX in untreated CD45^{-/-}Lck^{F505} DN thymocytes, suggesting that at basal conditions more DSBs were accumulating in the cells, possibly due to the DNA repair deficiency.

DSBs are a source of genomic instability, which can be assessed by karyotype analysis with chromosomal painting. This was achieved through collaboration with Dr F.T. Yong at the Veterinary School of the University of Cambridge (Yang FT, 1995). In pre- tumorigenic DN thymocytes, we detected multiple chromosomal abnormalities in 5 Rag^{-/-} CD45^{-/-}Lck^{F505}, but no aberrations were found in 43 wild-type, CD45^{-/-} or Lck^{F505} DN thymocytes. In transformed cell lines from the CD45^{-/-} Lck^{F505} thymic tumours (Matt cell lines), chromosomal abnormalities were also detected. These results provided strong evidence of the genomic instability caused by the “hyperactive” Lck in CD45^{-/-}Lck^{F505} DN thymocytes.

The results together demonstrate a striking correlation between inhibition of DNA repair and genomic instability in CD45^{-/-}Lck^{F505} DN thymocytes expressing oncogenic Lck.

1.1.5 DNA damage- induced apoptosis

Since DNA repair mechanisms were inhibited in CD45^{-/-}Lck^{F505} DN thymocytes, this begged the following question: what is keeping these cells with DSBs alive; and expanding? I hypothesised whether the apoptotic pathway is disrupted in these cells.

The survival profile was analysed in the cells that were exposed to ionising irradiation or etoposide (Fig 4, Zhao R, 2004). The results showed that only in the thymocytes expressing oncogenic Lck, was there a powerful survival signal protecting the cells from apoptosis. This was a very interesting finding. It seemed that a “double whammy” mechanism was functioning behind the transformation of these cells. On the one hand, cells were prone to accumulation of DSBs, which were possible source of further mutations; on the other hand, the cells were waived from the deadly consequence, so the cells with loads of DSBs could grow, proliferate and expand.

1.1.6 Examinaing the survival pathway in CD45^{-/-}Lck^{F505} DN thymocytes in DNA damage response

In normal thymocytes, a hallmark of DNA damage is the induction and activation of p53 pathway. P53 transcription factor is up-regulated by ATM and ATR serine/threonine kinases, which are activated by DNA damage signals, probably through γ H2AX. P53, as a transcription factor, initiates apoptotic pathway mediated by Bax; and cell cycle arrest through p21^{WAF1} (Sherr CJ, 2002; Vousden KH, 2002).

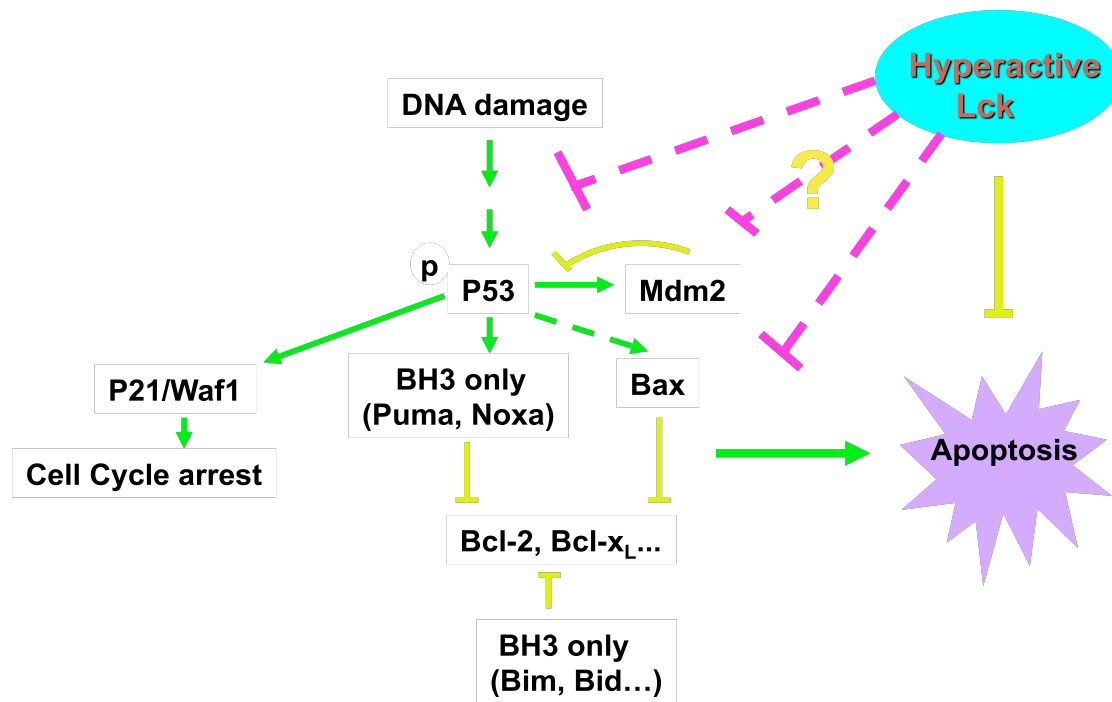


Fig 3. A diagram to show the signalling network involving p53 and downstream effectors, and putative mechanisms how hyperactive lck affects the various pathways. DNA damage induces phosphorylation of p53, which stabilises p53 and subsequently drives cells into apoptosis by promoting p21^{WAF1} mediated cell cycle arrest, inducing up-regulation of BH3-only proteins Puma and Noxa, and increasing expression of pro-apoptotic protein Bax directly. Hyperactive Lck could exert its function by targeting at the various pathways or molecules.

I compared the phosphorylation, induction of p53, and the downstream effectors Bax and p21^{WAF1} between non- oncogenic lck expressing and oncogenic lck expressing cells. On finding no significant difference in all the aspects, I concluded that the p53 machinery was functioning normally in CD45^{-/-}Lck^{F505} DN thymocytes in DNA damage response (Fig 2, Zhao R, 2004).

Moving down from p53 to the mitochondria apoptotic machinery, key molecules involved in the caspase execution cascade were also examined. In mammalian cells, cytochrome c initiates caspase activation following its release from mitochondria, it

also forms an active apoptosome complex with Apaf-1, which activates procaspase-9, which in turn activates caspase-3. Active caspase-3 can cleave poly(ADP-ribose)polymerase (PARP) to yield an inactive form of PARP.

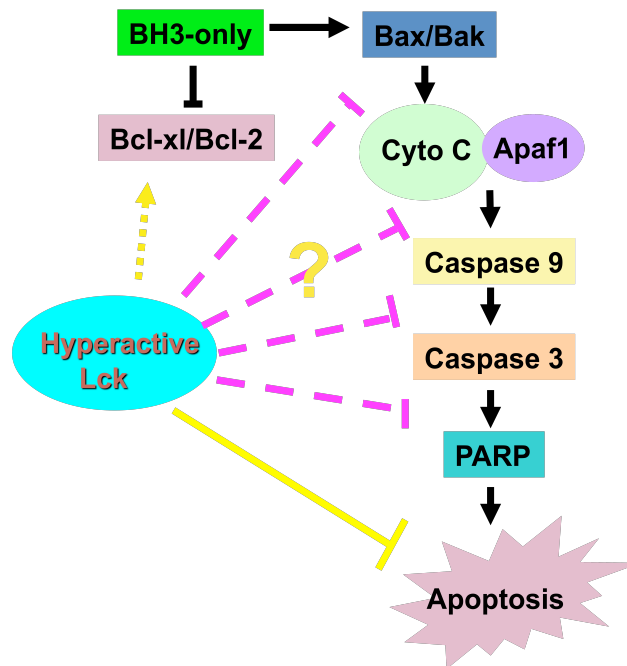


Fig 4. A diagram showing various molecules involved in the mitochondrial apoptotic pathway and the possible roles that hyperactive Lck plays in this signalling network.

Starting from PARP I found that the cleavage of PARP was clearly blocked in CD45^{-/-} Lck^{F505} DN thymocytes that were exposed to DNA damage. This suggested that caspase-3 might not be activated properly. Next, I examined caspase-3 status in these cells under the same condition, and the results were again striking- caspase-3 was not cleaved hence not activated, suggesting that the active apoptosome complex comprised of cytochrome c and Apaf-1 was not formed. This pointed to the possibility of inhibition of cytochrome c release from mitochondria, which had been

reported as a critical switch in the initiation of apoptosis (Zou H, 1999; Wang X, 2001).

In order to measure the quantity of released cytochrome c from mitochondria, subcellular fractionation on the cells was carried out and mitochondria (M) and cytosol (C) fractions were purified. The quantities of cytochrome c in these two fractions were measured by immunoblotting with an anti- cytochrome c antibody. In CD45^{-/-}Lck^{F505} DN thymocytes, cytosolic fraction of cytochrome c was greatly reduced. By re-probing the same gel- membrane with a Bax antibody, I found that Bax was mostly located in cytosolic fraction instead of mitochondrial fraction in these cells.

Bax is a BH3- only protein that translocates from cytosol to mitochondria upon apoptotic signals, promoting release of cytochrome c from mitochondria (Gross A, 1998). A conformational change in Bax precedes its translocation to mitochondria. An antibody (6A7 mab) recognises an epitope in its N- terminus that becomes exposed during apoptotic signalling (Hsu YT, 1998; Nechushtan A, 1999). I therefore examined the conformational status of Bax by utilising this antibody. Naïve Bax was immunoprecipitated by 6A7 mab, the quantity of which was then measured by immunoblotting with a Bax antibody. While in CD45^{-/-}Lck^{F505} DN thymocytes, DNA damage induced no conformational change of Bax, it was clearly opposite in wild-type, CD45^{-/-} and Lck^{F505} DN thymocytes.

Previous study on mitochondrial apoptosis and Bcl-2 family molecules suggested that anti-apoptotic proteins such as Bcl-2 and Bcl-x_L bind and sequester BH3-only proteins, e.g Bid and Bim, thereby preventing their pro-apoptotic interactions with Bax (Cheng EH, 2001; Kuwana T, 2002). As Bcl-2 levels were similar in the DN thymocytes from the four mouse lines (previous unpublished work from Dr Alexander's group), I focused my interest on Bcl-x_L, which is known to be well-expressed in immune cells. In DN thymocytes, Bcl-x_L expression was increased similarly in both Rag^{-/-} Lck^{F505} and Rag^{-/-} CD45^{-/-}Lck^{F505} mice, compared to controls. This still does not explain why tumours develop in (Rag^{-/-}) CD45^{-/-}Lck^{F505} mice, but not in (Rag^{-/-}) Lck^{F505} mice.

Interestingly Bcl-x_L deamidation in response to DNA damage had been proposed as a critical switch to subvert the pro-survival function of Bcl-x_L (Deverman BE, 2002). I therefore studied the Bcl-x_L deamidation status in response to DNA damage in the above four mouse lines. I found that Bcl-x_L deamidation was inhibited in CD45^{-/-} Lck^{F505} mice, while it clearly occurred in control mice. This result provided the most convincing evidence of how oncogenic Lck^{F505} subverted the apoptotic pathway, although the mechanism of how Bcl-x_L was deamidated *per se* was still not clear.

Protein deamidation occurs spontaneously at Asn residues, which are flanked, on the α-carboxyl side, by small non-bulky residues, such as Gly, Ala, Ser or Thr (Robinson NE, 2001). The nucleophilic attack of the peptidyl nitrogen of the Asn+1 residue onto the β-carbonyl carbon of the Asn, leads to the formation of an aspartyl succinimidyl intermediate, with the elimination of the ammonia moiety. The aspartyl succinimidyl intermediate itself is unstable and its ring can open on either side of the nitrogen atom, yielding either a normal peptide or an atypical isopeptide containing a β-linked isoaspartyl residue (isoAsp), the latter form being generally predominant (Asward DW, 2000).

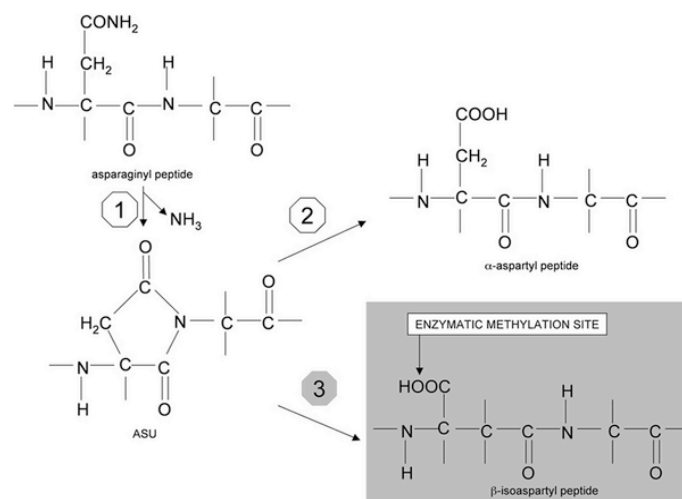


Fig 5. Mechanism for deamidation of asparaginyl residues in peptides. (Fig. from Climmino A, 2008)

(Step 1): the nitrogen of the Asn+1 residue (a Gly in the example) attacks the β-

carbonyl carbon of the Asn, thus forming the succinimidyl derivative of the peptide (ASU) with the ammonia elimination. The ASU ring can open spontaneously on either side of the nitrogen atom. In one case the α -aspartyl peptide is formed (Step 2). In the other case the β -isoaspartyl peptide does occur (Step 3).

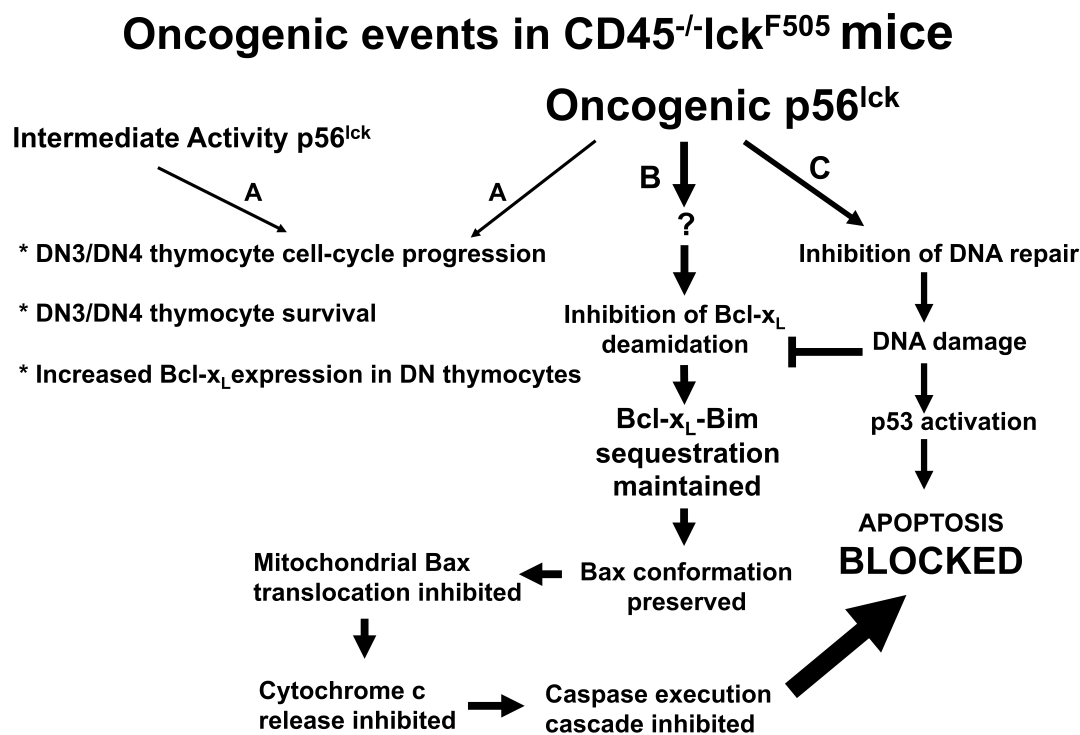


Fig 6. A model integrating the findings on the DNA damage response, cell survival and cell- cycle progression in cells with various Lck kinase activity. Pathway A refers to signals that are common to both intermediate activity Lck (as in DN CD45^{-/-}Lck^{F505} thymocytes). Pathway B and C are unique to the oncogenic hyperactive Lck found in DN CD45^{-/-}Lck^{F505} thymocytes. (Zhao R, 2007)

1.2 How is Bcl-x_L deamidated in DNA damage responses?

This is the main question to be answered in the next part of work (Zhao R, 2007). To answer this question would be the key to understanding how oncogenic tyrosine kinases interact with the Bcl-x_L deamidation pathway, and potentially, uncovering new strategies in cancer treatment.

1.2.1 Elucidation of the roles of different species of Bcl-x_L by *in vitro* and *in vivo* studies

Initial work from the Weintraub laboratory suggested that when Asn52 and Asn 66 were both mutated to Asp, Bcl-x_L lost its ability to bind that BH3-only pro-apoptotic protein Bim, thereby providing a putative link between DNA damage and apoptosis (Deverman BE, 2002). However, a secondary mutation was later identified, which, when corrected, enabled the N52D/N66D Bcl-x_L to bind Bim, casting doubt on this interpretation (Deverman BE, 2003). As the sequestration of BH3-only proteins by Bcl-x_L was thought to explain its anti-apoptotic function (Cheng EH, 2001), resolution of this question was clearly important for establishing a molecular link between DNA damage and apoptosis.

To address this point, a series of cellular and biochemical experiments were carried out. First of all, whether deamidated forms of Bcl-x_L bind to BH3-only proteins needed to be elucidated. In the previous work (Zhao R, 2004), Bim could only immuno-precipitate Bcl-x_L protein from the lysates of CD45^{-/-} Lck^{F505} thymocytes which had been treated with etoposide, and also Bcl-x_L pulled down much more Bim from the CD45^{-/-} Lck^{F505} thymocyte lysates, suggesting that deamidation crippled the ability of Bcl-x_L to bind Bim. However, Weintraub's correction showed that mutated N52D/N66D Bcl-x_L was still able to bind Bim. The discrepancy might have been caused by the following reasons: A) The amount of protein Bim may be different between CD45^{-/-} Lck^{F505} and other non-tumourigenic mice; B) DNA damage/etoposide treatment may induce different amount of Bim; and C) N52D/N66D Bcl-x_L does not bind Bim, although N52D/N66D Bcl-x_L does bind Bim. Points A and B were easily eliminated by thorough Bim/ Bcl-x_L binding experiments

(Fig7B, Zhao R, 2004; Fig 2 A& B, Zhao R, 2007), in which the native and deamidated Bcl-x_L species were also tested separately for their binding ability with Bim, and the results clearly indicated that deamidated Bcl-x_L, including both the N52D/N66D and N52-iso D/N66-iso D Bcl-x_L forms, lost most of its ability to bind Bim *in vivo*. Recombinant Bcl-x_L also lost part of its binding to Bim when one site was deamidated, and lost most of its binding when two sites were deamidated. I also tested the binding of N52D/N66D Bcl-x_L form to Bim in thymocytes, which confirmed what Weintraub's laboratory had claimed.

Collectively, the results supported the hypothesis C that N52-iso D/N66-iso D Bcl-x_L does not bind Bim, although N52D/N66D Bcl-x_L does bind Bim. If physiologically N52-iso D/N66-iso D Bcl-x_L exists as the dominant form, it would not be surprising to see that deamidated Bcl-x_L loses most of its ability to bind BH3-only proteins.

Consistently, previous literature on protein deamidation showed that when an Asn is converted to a mixture of Asp and iso-Asp, the ratio of Asp/iso-Asp is about 1:5 (Robinson NE, 2001). To confirm this was applicable to Bcl-x_L deamidation, it was necessary to measure the ratio of Asp/iso-Asp at Asn52 and Asn66. This was achieved by Mass Spectrometric analysis. Respective peptides were designed and synthesised, which encompass Asn 52/ Asn 66 and their corresponding Asp/ iso-Asp forms as identifiers of these species in the same peptides digested from recombinant Bcl-x_L. The results showed that the ratios of Asp/iso-Asp for Asn 52 and Asn66 were 10:1 and 5:1, respectively.

Taken together, my results showed that conversion of Bcl-x_L Asn 52 and Asn 66 to iso-Asp forms, but not Asp counterparts, prevented sequestration of BH3-only proteins. In fact deamidation of Bcl-x_L to iso-Asp causes greater perturbation of protein structure than conversion to Asp (Aritomi M, 1997), presumably explaining its loss of BH3-only protein binding ability.

1.2.2 Is Bcl-x_L deamidation a consequence of mitochondrial apoptosis?

Whether Bcl-x_L deamidation is a cause or a consequence of apoptosis is an obvious and important point to elucidate. Clearly if Bcl-x_L deamidation is a cause of

apoptosis, it will play a more critical role in thymic transformation than being a consequence of apoptosis.

This was addressed by using a caspase inhibitor Z-VAD-fmk, which can effectively block the occurrence of apoptosis in thymocytes (Fig 1a&b, Zhao R, 2007). In the cells treated with etoposide, and with or without Z-VAD-fmk, Bcl-x_L deamidation occurred at similar levels, suggesting that Bcl-x_L deamidation was not a consequence of apoptosis.

As Bax and Bak are required in apoptosis mediated by BH3-only proteins, I also tested whether depletion of Bax or Bak could block Bcl-x_L deamidation. Thymocytes were transfected with shRNA for Bax or Bak prior to exposure to DNA damage. As shown in Fig 1c (Zhao R, 2007), neither the depletion of Bax or Bak affected the occurrence of Bcl-x_L deamidation.

1.2.3 The DNA damage- NHE-1 up-regulation- intracellular alkalinisation- Bcl-x_L deamidation axis

How DNA damage caused Bcl-x_L deamidation was a completely unexplored area when we started to think about it in early 2006. It was not surprising though as the link between DNA damage and Bcl-x_L deamidation was just revealed in late 2002 (Deverman BE, 2002).

It has been known that protein Asn deamidation is accelerated by increased pH *in vitro*. Antiport Sodium-Hydrogen-Exchanger family member 1 (NHE-1) is responsible for maintaining the intracellular pH in thymocytes. It seemed to be the only clue to follow. The hypothesis would be that DNA damage induces NHE-1 mediated intracellular pH (pHi) change. A quick test of this hypothesis was to check whether DNA damage could induce any change in NHE-1, which could potentially cause intracellular alkalinisation.

Many types of stimuli induce phosphorylation of NHE-1 and thus increase its activity. I believed that it might be the same case in DNA damage response. Therefore I tried

to check the phosphorylation status of NHE-1 in DNA damaged thymocytes. Using a set of anti-phospho antibodies against known phosphorylation sites in NHE-1, I could not find altered phosphorylation of NHE-1 after DNA damage. However, I noticed on the western blots that the NHE-1 expression level was increased after DNA damage. It was an interesting finding although there was not much emphasis on the role of NHE-1 protein expression level in its function in previous literature.

In parallel I tried to measure the intracellular pH (pHi) before and after DNA damage. Using a pH- sensitive fluorescent dye SNARF-1, pHi can be measured by FACS. It was encouraging to find that pHi consistently was increased in DNA damaged cells. This increase in pHi was about 0.4-0.5 units, which was both necessary and sufficient to cause Bcl-x_L deamidation in the cells without exposure to DNA damage. These results were achieved by artificially changing the pHi in the cells and then examining the Bcl-x_L deamidation status.

Whether it was just a casual link between up-regulation of NHE-1 protein level and intracellular alkalinisation or whether NHE-1 up-regulation caused intracellular alkalinisation needs to be clarified before drawing a conclusion on the mechanism of Bcl-x_L deamidation. This entailed a series of experiments. In summary, I had shown (Fig 4&5, Zhao R, 2007):

- a) DNA damage- induced Bcl-x_L deamidation requires de novo protein synthesis.
- b) DNA damage causes up-regulation of NHE-1 in wild- type but not in CD45^{-/-} Lck^{F505} thymocytes.
- c) NHE-1 over-expression by retroviral transfection causes intracellular alkalinisation and Bcl-x_L deamidation.
- d) NHE-1 function blockage by specific inhibitor (DMA) blocks intracellular alkalinisation and Bcl-x_L deamidation.
- e) NHE-1 gene knock- down by shRNA also blocks intracellular alkalinisation and Bcl-x_L deamidation.

Collectively the combined evidence strongly supports a model whereby DNA damage- induced Bcl-x_L deamidation is mediated by NHE-1 antiport regulated intracellular alkalinisation. The current model is equally applicable to fully-

transformed cells- i.e. CD45^{-/-}Lck^{F505} tumour cells, and human Chronic lymphoblastic leukaemia (CLL) cells, though the former express an OTK, the latter do not.

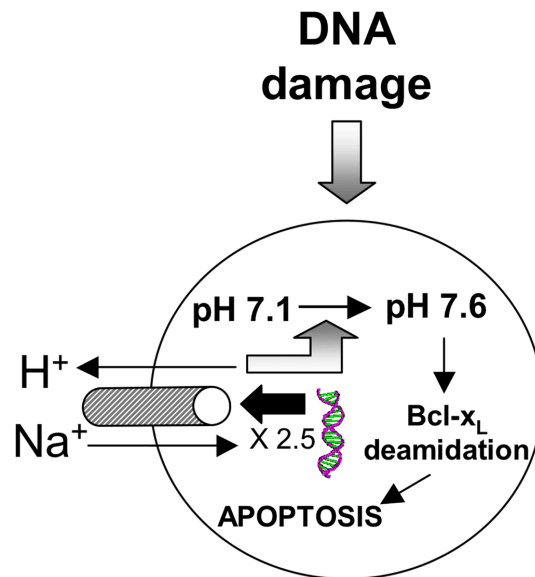


Fig 7. A novel signaling pathway triggered by DNA damage leads to the up-regulation of the NHE-1 antiport, increased intracellular pH, Bcl-x_L deamidation, and finally apoptosis. (Fig. from Zhao et al, 2007)

1.3 Bcl-x_L deamidation pathway in Myeloproliferative Disorders (MPDs)

1.3.1 Why investigate Bcl-x_L deamidation pathway in MPDs?

Bcl-x_L plays important roles in many tumour types (Amundson SA, 2000), including MPDs. My finding on deamidation of Bcl-x_L in DNA damage responses therefore have potential relevance to cancer therapy, whereby enforced alkalinisation, perhaps by amplification of NHE-1 expression, would promote Bcl-x_L deamidation, thereby triggering apoptosis.

Relevance of Bcl-x_L deamidation for human cancers associated with OTKs remained unclear, although DNA damaged- induced Bcl-x_L deamidation was intact in cell lines of osteosarcoma and cervical, bladder and ovarian cancers, and in primary human lymphoblastic leukaemia cells (Zhao R, 2007).

MPDs are good candidates for studying Bcl-x_L deamidation pathway because, as a group of human haematopoietic malignant diseases, many of them express OTKs. Among MPDs, Chronic Myeloid Leukaemia (CML) and Polycythemia vera (PV) are the two seeing most significant breakthroughs in the understanding of their pathological mechanisms. They are associated with the BCR-ABL fusion tyrosine kinase and the Janus tyrosine kinase 2 (JAK2) mutation V617F, respectively. Both disorders initially usually present with chronic diseases, but carry a risk of progression to blastic phase resembling acute leukaemia that resists further therapy (Goldman JM, 2003; Campbell PJ, 2006).

Bcl-x_L has been shown to be up-regulated in patients with CML and PV and is thought to inhibit apoptosis. BCR-ABL protein expression is associated with a reduced apoptotic response to genotoxic drugs. Moreover, quiescent CML stem cells, thought to be responsible for residual disease, are resistant to apoptosis that tyrosine kinase inhibitors induce. Collectively the combined results suggested there might be an undiscovered link between Tyrosine kinases BCR-ABL and Jak2^{V617F} and the resistance to DNA damage- induced apoptosis in CML and PV patient myeloid cells.

1.3.2 Patients' sample collection and cell purification

Access to human samples was made possible by collaboration with Prof. AR Green's research group at the Department of Haematology, Addenbrooks Hospital, University of Cambridge. The study was approved by the Cambridge and Eastern Region ethics committee. All patients involved provided written informed consent.

Cells of myeloid or lymphoid lineage were purified from peripheral blood samples. The process involves using density separation through centrifugation, followed by immunological targeting to cell surface markers combined with flow cytometry. Unlike using thymocytes from established mouse lines, human samples were precious in terms of how many cells were available and when they were available. This responsibility proved challenging but satisfying, as it constituted a particularly good model system upon which to work.

1.3.3 Bcl-x_L deamidation pathway is inhibited in CML myeloid cells

Purified myeloid/ granulocytes from normal subjects and CML patients were treated with etoposide or exposed to γ -irradiation. Then every step in the Bcl-x_L deamidation pathway was examined, i.e. NHE-1 expression level change, intracellular pH alteration, Bcl-x_L deamidation status and apoptosis of the cells. Results from 6 normal controls and 10 CML patients consistently showed that the Bcl-x_L deamidation pathway in DNA damage responses was intact in normal cells while inhibited in CML cells.

T cells purified from the same CML patient samples, as good internal controls, showed no effect on the Bcl-x_L deamidation pathway (Suppl Fig 3, Zhao R, 2008). The same CML myeloid cells were subjected to a series of 'forced alkalinisation' experiments, where cells were cultured in alkaline medium i.e. pH>8. I found that the resistance to Bcl-x_L deamidation was overcome in these cells. It suggested that the inhibition by Bcr-Abl was at the step of up-regulation NHE-1, which was same as in p56Lck^{F505}.

The dysfunction of Bcl-x_L deamidation pathway in CML cells was further examined aiming to identify the critical steps responsible. CML cells were transfected with a retroviral vector carrying NHE-1 cDNA in order to over-express NHE-1 in CML cells. These cells not only became alkalinised intracellularly, but also had more Bcl-x_L protein deamidated and subsequently apoptosed.

1.3.4 BCR-ABL inhibitor Imatinib reverses the inhibition of Bcl-x_L deamidation pathway in CML myeloid cells

Imatinib is a very effective BCR-ABL inhibitor. Its application in treating CML patients has been so successful that most CML patients will achieve complete regression. However, a small proportion of CML patients develop resistance to Imatinib by point mutation of the BCR-ABL kinase domain. In my experiments Imatinib-sensitive CML cells were either pre-treated with Imatinib or not, then were exposed to etoposide/irradiation. NHE-1 expression level and Bcl-x_L deamidation status were examined subsequently. The results were clear that Imatinib completely reversed the inhibition of Bcl-x_L deamidation in these CML cells.

1.3.5 Imatinib does not reverse the inhibition of Bcl-x_L deamidation pathway in Imatinib-resistant CML cells that carry an E255V mutation in the BCR-ABL kinase domain

Although Imatinib is known to be a very specific BCR-ABL kinase inhibitor, it also inhibits a few other kinases. Strictly speaking, the above reversion of the inhibition of Bcl-x_L deamidation pathway might possibly be due to the other effects of Imatinib.

At this point I managed to obtain an imatinib-resistant CML sample, which carried an E255V mutation in the BCR-ABL kinase domain. The same experiments were performed with this sample. Strikingly, the reversion of the Bcl-x_L deamidation pathway did not occur. Furthermore, the same cells were transfected with a NHE-1 vector using a Nucleofector kit. NHE-1 was over-expressed in these cells, which subsequently caused intracellular alkalinisation and Bcl-x_L deamidation.

This series of experiments involving Imatinib sensitive and resistant CML cells strongly support the critical role of BCR-ABL in the inhibition of Bcl-x_L deamidation pathway in CML.

1.3.6 Bcl-x_L deamidation pathway is inhibited by Jak2^{V617F} in PV myeloid cells

Likewise, in a series of similar experiments, Jak2^{V617F} in PV myeloid cells exhibited its role in blocking the DNA damage- induced NHE-1/Bcl-x_L deamidation pathway, i.e. NHE-1 up-regulation, intracellular alkalinisation, Bcl-x_L deamidation and apoptosis. T cells purified from the same PV patient samples, as good internal controls, showed no effect on the Bcl-x_L deamidation pathway (suppl Fig 3, Zhao R, 2008).

1.3.7 Jak 2 inhibitor reverses the inhibition of Bcl-x_L deamidation pathway in PV myeloid cells

Whilst there were no established specific Jak2 inhibitors available, three inhibitors with different sensitivity and specificity were used. Jak inhibitor 1 (Calbiochem) is a pan- inhibitor of Jak, TG101209 (Targagen) and AT9283 (Astex) are inhibitors currently in clinical trials, which have been shown in cellular experiments inhibiting Jak2 (Prof AR Green unpublished data).

Surprisingly all three Jak2 inhibitors all showed significant effects in inhibiting the Bcl-x_L deamidation pathway, although one of them was apparently more potent than others. Similarly the PV myeloid cells were subjected to 'forced alkalinisation' experiments. The resistance to Bcl-x_L deamidation was also overcome in these cells suggesting that the inhibition by Jak2^{V617F} is at the step of up-regulation NHE-1, which is same as p56Lck^{F505Y} and Bcr-Abl.

1.3.8 Bcl-x_L deamidation pathway in Jak2^{V617F}-positive Idiopathic Myelofibrosis (IMF)

IMF represents a sub- group of diseases in myeloproliferative disorders. Some IMF patients carry Jak2^{V617F} mutations, whereas others do not. Luckily I was able to obtain two Jak2^{V617F}-positive and two Jak2^{V617F}-negative IMF patient samples to study the Bcl-x_L deamidation pathway. The results were very encouraging- the Bcl-x_L deamidation pathway was inhibited in Jak2^{V617F}-positive IMF patient cells. This again supports the correlation of Jak2^{V617F} and the blockage of DNA damage- induced Bcl-x_L deamidation pathway in myeloproliferative disorders.

1.4 Tyrosine kinases in other haematological malignancies- potential research interests and therapeutic targets?

Eight cancer cell lines were also studied, representing different haematologic cancers associated with distinct molecular mechanisms. Among these, K562 expresses Bcr-Abl, HEL expresses Jak2^{V617F} in Jak2^{V617F} and Karpas 299 expresses NPM-ALK, a tyrosine kinase; Daudi expresses c-myc, DU528 expresses Tal1, JVM2 expresses cyclin D1, OPM2 expresses FGFR3 and DOHH2 expresses Bcl-2.

While demonstrated again that Bcr-Abl and Jak2^{V617F} inhibit the NHE-1/Bcl-x_L deamidation pathway, none of the other onco-proteins do, including tyrosine kinase NPM-ALK. So the inhibition of Bcl-x_L deamidation pathway is not a general feature of haematologic cancers and is only mediated by a sub- group of tyrosine kinases or is dependent on a particular cellular context.

CHAPTER 2. CRITIQUES/REFLECTION

2.1. Asn 52/66 issues

Original work from Weintraub laboratory suggested that deamidated Bcl-x_L does not bind to BH3- only protein Bim. However, this result was later withdrawn due to the identification of a secondary mutation in the original DNA construct used in the experiments. When the secondary mutation was corrected deamidated Bcl-x_L did bind to Bim (Deverman BE, 2003).

Interestingly, I found that whereas the ability of Bcl-x_L to bind Bim was ablated in control thymocytes exposed to DNA damage, it was strikingly retained in CD45^{-/-} Lck^{F505} thymocytes, tightly correlating with the resistance to Bcl-x_L deamidation noted in these cells.

These findings cast doubt on the model that Bcl-x_L triggers apoptosis because the sequestration of BH3-only proteins by Bcl-x_L is thought to explain its anti-apoptotic function. Resolution of this question is clearly important for establishing a molecular link between DNA damage and apoptosis. So at an early stage of my project I carried out a series of cellular and biochemical experiments to address this key point, such as, immunoprecipitation of Bim from cell lysates with a Bcl-x_L antibody or the other way around, and measuring the precipitated proteins by western blots. Recombinant His-tagged Bcl-x_L was exposed to alkaline conditions to cause partial deamidation and separated by anion exchange chromatography into purified native, singly deamidated and doubly deamidated Bcl-x_L proteins, and these different species of Bcl-x_L bound with endogenous Bim in a completely different manner, i.e. native Bcl-x_L has a maximum binding ability, doubly deamidated Bcl-x_L does not bind with Bim at all, while singly deamidated Bcl-x_L lies in between. And interestingly, both the Bcl-x_L N52A/N66A and N52D/N66D mutants maintain the complete binding ability with BH3-only proteins as the native Bcl-x_L. Given that most asparagines deamidate to iso-aspartate forms at physiological conditions in cells, it is reasonable to suggest that the change from asparagine to aspartate does not affect the binding with BH3-only proteins, but the conversion from asparagine to iso-aspartate does.

This speculation was also validated by a definitive experiment, which nevertheless, was to prove an established view, was however, critical in the interpretation of the mechanism of Bcl-x_L deamidation. Aspartate and iso-aspartate species of Bcl-x_L were separated from naturally occurred Bcl-x_L mixture by LC-MS chromatography respectively, and their quantities were compared, which confirm that more than 90% of asparagines in Bcl-x_L convert to iso-aspartates, but not aspartates.

2.2. Global effects of alkalinisation

One argument about the NHE-1/ Bcl-x_L deamidation pathway is that intracellular alkalinisation can possibly cause deamidation of other proteins. What roles do they play in apoptosis and transformation? This is a fair argument. I have been trying to address this question in different ways. The most critical evidence is that when Bcl-x_L is mutated to N52A/N66A mutant, a constitutively native form, enforced intracellular alkalinisation does not increase apoptosis. So although the global effect of alkalinisation is inevitably present, its role in apoptosis might be negligible.

The possibility of pH manipulation as a means to cancer therapy has in the past attracted intermittent interest. The pioneering work of Warberg established that tumours display acidic extracellular pH (Warberg O, 1930), although half a century later it was established that the intracellular pH of tumours is comparable with normal cells (Griffiths JR, 1991). My findings suggest that strategies for pH manipulation in anti-neoplastic therapy should continue to receive attention, albeit for reasons different from those envisaged by Warberg.

2.3. Protein modification in signal transduction

Proteins are frequently modified in signal transduction. Modification of proteins confers new function to the molecules and often the proteins with altered function play critical roles in signalling networks. Phosphorylation, methylation, sumoylation etc. have attracted more research attention and indeed demonstrated their importance in protein and cellular function. Deamidation, though universally

occurring in all proteins, has only recently been shown being involved in rapid physiological events, i.e. signal transduction of Bcl-x_L. Is it just an individual phenomenon, or revealing a completely new type of protein modification with physiological significance, needs to be elucidated.

A number of cell stress conditions have recently been linked to protein deamidation. Oxidative conditions have been considered as a way through which protein deamidation is facilitated. Protein Isoaspartate Methyltransferase (PIMT) may be able to mediate protection from apoptosis induced by Bax in a neuronal cell line by catalyzing protein methyl esterification (Cimmino A, 2008). PIMT has been shown to be able to prevent isoaspartate accumulation in the Eukaryotic Initiator Factor Binding Protein 2 (4E-BP2), an important factor in learning and memory, in the brain (Bidinosti M, 2010). Deamidation has also been involved in ubiquitination and ubiquitin- dependent degradation of peptides (Cui J, 2010)

CHAPTER 3. CONCLUSION AND FUTURE WORK

Protein deamidation is a naturally occurring process, which increases protein turnover, and has been proposed as a molecular timer of biological events (Robinson NE, 2001). However, the significance of protein deamidation to the cell has never been firmly established. It has been suggested, in respect to the regulation of DNA damage-induced apoptosis, Bcl-x_L deamidation may serve as a chronometric buffer, affording the cell time to reverse low-level genotoxic stress-induced events (Deverman BE, 2002). Rapid deamidation of Bcl-x_L induced by DNA damage indicates that the deamidation "clock" is a dynamic process that can be regulated in vivo by biological events (Zhao R, 2007).

Bcl-x_L is an important pro-survival protein whose potency is emphasised by its protection of a wide range of tumour cells from genotoxic attack (Amarante-Mendes et al., 1998; Amundson et al., 2000; Brumatti et al., 2003). The role of Bcl-x_L deamidation in the transformation of OTK- expressing cells is particularly critical, as it explains how these cells gain their survival advantage under extreme conditions- i.e. cytotoxic drugs or gamma-radiation. It also explains why these cells, once they become cancerous, are notoriously resistant to chemo- or radiotherapy.

It is interesting that a few OTKs inhibit the NHE-1/Bcl-x_L deamidation pathway, whereas others do not. Further study is needed given the vast number of OTKs involved in human cancer. Finally whether it is applicable to target at the NHE-1/Bcl-x_L deamidation pathway warrants attention, although variances are predictable due to biological/cellular complexity.

Future work

There are a number of lines of work that need to be done in order to understand the relationship between OTKs and the NHE-1/Bcl-x_L deamidation pathway, and hopefully, to be able to manipulate the components involved in oncogeneis to generate potential new cancer therapy.

The hypothesis that inhibition of DNA-damage induced alkalisation and Bcl-x_L deamidation causes transformation needs to be vigorously tested.

Firstly, what is the role of NHE-1 in tumourigenesis? This can be achieved by generating new transgenic/ knock-in mouse models based on the CD45^{-/-}p56^{lck-Y505F} mouse model. If we can express NHE-1 in the CD45^{-/-}p56^{lck-Y505F} mouse in a regulatory manner, i.e. tetracycline- controlled expression, then we can observe whether NHE-1 up-regulation can prevent tumour development, and, whether NHE-down- regulation can induce tumour relapse. Tumour growth monitoring can be achieved by using the immunofluorescence/illuminescence technique, which itself will require careful design of the molecular tags.

Secondly, is prevention of Bcl-x_L deamidation sufficient for transformation? Blockade of the Bcl-x_L deamidation pathway plays an important role in the transformation driven by three OTKs - Lck^{Y505F}, Bcr-abl and Jak2^{V617F}. Whether Bcl-x_L deamidation is directly involved in the transformation process needs to be validated *in vivo*. One way of doing this is to generate a mouse model with the two asparagines in Bcl-x_L replaced by Alanines so that they are not able to deamidate, i.e. a mouse model with a constitutively “native” Bcl-x_L. If this mouse is crossed with an OTK model, i.e. CD45^{-/-}p56^{lck-Y505F}, then the role of Bcl-x_L deamidation can be tested by subjecting the live mice to DNA damage and monitor tumour occurrence etc.

How NHE-1 expression is regulated following DNA damage also needs to be studied. This is still a mystery so far. NHE-1 expression and modification have been studied in the context of various stimuli, such as growth factors, cytokines, homeostasis, etc. But the link between DNA damage and NHE-1 has not been paid much attention, probably due to the fact that NHE-1, as an antiport, was mainly investigated in cardiovascular diseases (Fliegel L, 2001)

Lacking this important information, it is impossible to understand how the oncogenic tyrosine kinases (e.g. Lck^{Y505F}, Bcr-abl and Jak2^{V617F}) carry out their abnormal function and drive the transformation of the cells. The increased expression level of NHE-1 could be caused at various stages: 1) messenger RNA level - transcriptional

or mRNA stability, and 2) protein level – translational or protein stability. My preliminary data show that DNA damage triggers increased NHE-1 mRNA levels in wild-type thymocytes, but not in the thymocytes transformed by hyper- active Lck^{F505} (Appendix Fig 7). This suggests that the up-regulation of NHE-1 in response to DNA damage is caused at least in part by increased mRNA. NHE-1 antiport is a well- characterised protein, and regulation of NHE-1 expression in response to multiple stimuli other than DNA- damage has been extensively investigated (Dyck JR, 1995; Yang W, 1996). These investigations have established that NHE-1 expression is mainly regulated by transcription, and a number of transcription binding sites for these other stimuli have been identified in the promoter region of the NHE-1. So it is not premature to hypothesise that in DNA damaged cells NHE-1 increases expression level by transcriptional mechanism.

There is plenty to discover in this completely untouched area- such as, the responsive elements in NHE- promoter and the transcription factors that are critical in initiating the transcription in response to DNA damage signals; the inhibitory mechanisms employed by the OTKs to block the transcription, etc.

Thirdly, but not lastly, any other proteins that could be deamidated by the DNA damage induced intracellular alkalinisation?

A large percentage of proteins deaminate to a substantial extent during their biological life times (Nordhoff E, 1999). Among these spontaneous protein deamidation processes, Bcl-x_L deamidation is the first example of rapid protein deamidation triggered by genotoxic stress, and playing a central role in the regulation of biological process. Other protein deamidation processes might also be promoted following DNA damage. There could be a plenary of molecules with various roles in cellular physiology that are regulated by deamidation.

APPENDIX

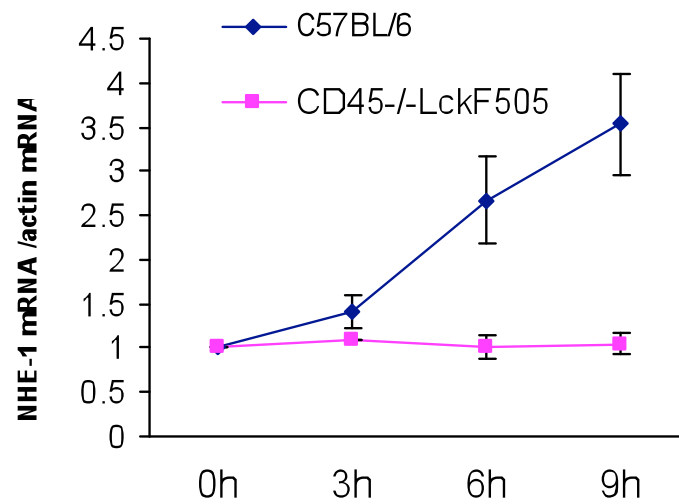


Fig 8. Quantitative RT-PCR results showing the NHE-1 mRNA level (mean values \pm SD, n=3) in C57BL/6 and CD45^{-/-} Lck^{F505} thymocytes at time 0, 3, 6, 9 h of etoposide treatment. The RT-PCR were run on Bio-Rad Chromo4, and NHE-1 mRNA is normalised for actin mRNA.

REFERENCES

- Alexander, D. R. (2000). The CD45 tyrosine phosphatase: a positive and negative regulator of immune cell function. *Semin Immunol* 12, 349-359.
- Alexander, D. R. (2004). Oncogenic tyrosine kinases, DNA repair and survival: the role of Bcl-xL deamidation in transformation and genotoxic therapies. *Cell Cycle* 3, 584-587.
- Amarante-Mendes, G. P., McGahon, A. J., Nishioka, W. K., Afar, D. E., Witte, O. N., and Green, D. R. (1998). Bcl-2-independent Bcr-Abl-mediated resistance to apoptosis: protection is correlated with up regulation of Bcl-xL. *Oncogene* 16, 1383-1390.
- Amundson, S. A., Myers, T. G., Scudiero, D., Kitada, S., Reed, J. C., and Fornace, A. J., Jr (2000). An informatics approach identifying markers of chemosensitivity in human cancer cell lines. *Cancer Res* 60, 6101-6110.
- Aritomi, M., Kunishima, N., Inohara, N., Ishibashi, Y., Ohta, S., and Morikawa, K. (1997). Crystal structure of rat Bcl-xL. Implications for the function of the Bcl-2 protein family. *J Biol Chem* 272, 27886-27892.
- Baker, M., Gamble, J., Tooze, R., Higgins, D., Yang, F. T., O'Brien, P. C., Coleman, N., Pingel, S., Turner, M., and Alexander, D. R. (2000). Development of T-leukaemias in CD45 tyrosine phosphatase-deficient mutant lck mice. *EMBO J* 19, 4644-4654.
- Bassing, C. H., Suh, H., Ferguson, D. O., Chua, K. F., Manis, J., Eckersdorff, M., Gleason, M., Bronson, R., Lee, C., and Alt, F. W. (2003). Histone H2AX: a dosage-dependent suppressor of oncogenic translocations and tumors. *Cell* 114, 359-370.
- Bidinosti, M., Martineau, Y., Frank, F., and Sonenberg, N. Repair of isoaspartate formation modulates the interaction of deamidated 4E-BP2 with mTORC1 in brain. *J Biol Chem* 285, 19402-19408.
- Blume-Jensen, P., and Hunter, T. (2001). Oncogenic kinase signalling. *Nature* 411, 355-365.
- Byth, K. F., Conroy, L. A., Howlett, S., Smith, A. J., May, J., Alexander, D. R., and Holmes, N. (1996). CD45-null transgenic mice reveal a positive regulatory role for CD45 in early thymocyte development, in the selection of CD4+CD8+ thymocytes, and B cell maturation. *J Exp Med* 183, 1707-1718.
- Campbell, P. J., and Green, A. R. (2006). The myeloproliferative disorders. *N Engl J Med* 355, 2452-2466.

Cheng, E. H., Wei, M. C., Weiler, S., Flavell, R. A., Mak, T. W., Lindsten, T., and Korsmeyer, S. J. (2001). BCL-2, BCL-X(L) sequester BH3 domain-only molecules preventing BAX- and BAK-mediated mitochondrial apoptosis. *Mol Cell* 8, 705-711.

da Silva, A. J., Li, Z., de Vera, C., Canto, E., Findell, P., and Rudd, C. E. (1997). Cloning of a novel T-cell protein FYB that binds FYN and SH2-domain-containing leukocyte protein 76 and modulates interleukin 2 production. *Proc Natl Acad Sci U S A* 94, 7493-7498.

Cimmino, A., Capasso, R., Muller, F., Sambri, I., Masella, L., Raimo, M., De Bonis, M. L., D'Angelo, S., Zappia, V., Galletti, P., and Ingrosso, D. (2008). Protein isoaspartate methyltransferase prevents apoptosis induced by oxidative stress in endothelial cells: role of Bcl-XI deamidation and methylation. *PLoS One* 3, e3258.

Cui, J., Yao, Q., Li, S., Ding, X., Lu, Q., Mao, H., Liu, L., Zheng, N., Chen, S., and Shao, F. Glutamine deamidation and dysfunction of ubiquitin/NEDD8 induced by a bacterial effector family. *Science* 329, 1215-1218.

Deutsch, E., Dugray, A., AbdulKarim, B., Marangoni, E., Maggiorella, L., Vaganay, S., M'Kacher, R., Rasy, S. D., Eschwege, F., Vainchenker, W., *et al.* (2001). BCR-ABL down-regulates the DNA repair protein DNA-PKcs. *Blood* 97, 2084-2090.

Deverman, B. E. (2003). Erratum to: Bcl-xL deamidation is a critical switch in the regulation of the response to DNA damage. *Cell* 115, 503.

Deverman, B. E., Cook, B. L., Manson, S. R., Niederhoff, R. A., Langer, E. M., Rosova, I., Kulans, L. A., Fu, X., Weinberg, J. S., Heinecke, J. W., *et al.* (2002). Bcl-xL deamidation is a critical switch in the regulation of the response to DNA damage. *Cell* 111, 51-62.

Dyck, J. R., and Fliegel, L. (1995). Specific activation of the Na⁺/H⁺ exchanger gene during neuronal differentiation of embryonal carcinoma cells. *J Biol Chem* 270, 10420-10427.

Dyck, J. R., Silva, N. L., and Fliegel, L. (1995). Activation of the Na⁺/H⁺ exchanger gene by the transcription factor AP-2. *J Biol Chem* 270, 1375-1381.

Fliegel, L. (2001). Regulation of myocardial Na⁺/H⁺ exchanger activity. *Basic Res Cardiol* 96, 301-305.

Goldman, J. M., and Melo, J. V. (2003). Chronic myeloid leukemia--advances in biology and new approaches to treatment. *N Engl J Med* 349, 1451-1464.

Griffiths, J. R. (1991). Are cancer cells acidic? *Br J Cancer* 64, 425-427.

Gross, A., Jockel, J., Wei, M. C., and Korsmeyer, S. J. (1998). Enforced dimerization of BAX results in its translocation, mitochondrial dysfunction and apoptosis. *EMBO J* 17,

3878-3885.

Holdorf, A. D., Green, J. M., Levin, S. D., Denny, M. F., Straus, D. B., Link, V., Changelian, P. S., Allen, P. M., and Shaw, A. S. (1999). Proline residues in CD28 and the Src homology (SH)3 domain of Lck are required for T cell costimulation. *J Exp Med* 190, 375-384.

Hsu, Y. T., and Youle, R. J. (1998). Bax in murine thymus is a soluble monomeric protein that displays differential detergent-induced conformations. *J Biol Chem* 273, 10777-10783

Kabouridis, P. S., Magee, A. I., and Ley, S. C. (1997). S-acylation of LCK protein tyrosine kinase is essential for its signalling function in T lymphocytes. *EMBO J* 16, 4983-4998.

Karni, R., Jove, R., and Levitzki, A. (1999). Inhibition of pp60c-Src reduces Bcl-XL expression and reverses the transformed phenotype of cells overexpressing EGF and HER-2 receptors. *Oncogene* 18, 4654-4662.

Khanna, K. K., and Jackson, S. P. (2001). DNA double-strand breaks: signaling, repair and the cancer connection. *Nat Genet* 27, 247-254.

Kim, P. W., Sun, Z. Y., Blacklow, S. C., Wagner, G., and Eck, M. J. (2003). A zinc clasp structure tethers Lck to T cell coreceptors CD4 and CD8. *Science* 301, 1725-1728.

Kishihara, K., Penninger, J., Wallace, V. A., Kundig, T. M., Kawai, K., Wakeham, A., Timms, E., Pfeffer, K., Ohashi, P. S., Thomas, M. L., and et al. (1993). Normal B lymphocyte development but impaired T cell maturation in CD45-exon6 protein tyrosine phosphatase-deficient mice. *Cell* 74, 143-156.

Koretzky, G. A., Picus, J., Thomas, M. L., and Weiss, A. (1990). Tyrosine phosphatase CD45 is essential for coupling T-cell antigen receptor to the phosphatidyl inositol pathway. *Nature* 346, 66-68.

Kumar, R., Mandal, M., Lipton, A., Harvey, H., and Thompson, C. B. (1996). Overexpression of HER2 modulates bcl-2, bcl-XL, and tamoxifen-induced apoptosis in human MCF-7 breast cancer cells. *Clin Cancer Res* 2, 1215-1219.

Kuwana, T., Mackey, M. R., Perkins, G., Ellisman, M. H., Latterich, M., Schneider, R., Green, D. R., and Newmeyer, D. D. (2002). Bid, Bax, and lipids cooperate to form supramolecular openings in the outer mitochondrial membrane. *Cell* 111, 331-342.

Li, X., Liu, Y., Kay, C. M., Muller-Esterl, W., and Fliegel, L. (2003). The Na⁺/H⁺ exchanger cytoplasmic tail: structure, function, and interactions with tescalcin. *Biochemistry* 42, 7448-7456.

Mee, P. J., Turner, M., Basson, M. A., Costello, P. S., Zamoyska, R., and Tybulewicz, V. L. (1999). Greatly reduced efficiency of both positive and negative selection of thymocytes in

CD45 tyrosine phosphatase-deficient mice. *Eur J Immunol* 29, 2923-2933.

Nechushtan, A., Smith, C. L., Hsu, Y. T., and Youle, R. J. (1999). Conformation of the Bax C-terminus regulates subcellular location and cell death. *EMBO J* 18, 2330-2341.

Nordhoff, E., Krogsdam, A. M., Jorgensen, H. F., Kallipolitis, B. H., Clark, B. F., Roepstorff, P., and Kristiansen, K. (1999). Rapid identification of DNA-binding proteins by mass spectrometry. *Nat Biotechnol* 17, 884-888.

Palacios, E. H., and Weiss, A. (2004). Function of the Src-family kinases, Lck and Fyn, in T-cell development and activation. *Oncogene* 23, 7990-8000.

Richardson, C., and Jasin, M. (2000). Frequent chromosomal translocations induced by DNA double-strand breaks. *Nature* 405, 697-700.

Rieder, C. V., and Fliegel, L. (2003). Transcriptional regulation of Na⁺/H⁺ exchanger expression in the intact mouse. *Mol Cell Biochem* 243, 87-95.

Robinson, N. E., and Robinson, A. B. (2001). Molecular clocks. *Proc Natl Acad Sci U S A* 98, 944-949.

Rogakou, E. P., Pilch, D. R., Orr, A. H., Ivanova, V. S., and Bonner, W. M. (1998). DNA double-stranded breaks induce histone H2AX phosphorylation on serine 139. *J Biol Chem* 273, 5858-5868.

Schlessinger, J. (2000). Cell signaling by receptor tyrosine kinases. *Cell* 103, 211-225.

Sherr, C. J., and McCormick, F. (2002). The RB and p53 pathways in cancer. *Cancer Cell* 2, 103-112.

Shiroo, M., Goff, L., Biffen, M., Shivnan, E., and Alexander, D. (1992). CD45 tyrosine phosphatase-activated p59fyn couples the T cell antigen receptor to pathways of diacylglycerol production, protein kinase C activation and calcium influx. *EMBO J* 11, 4887-4897.

Skorski, T. (2002). Oncogenic tyrosine kinases and the DNA-damage response. *Nat Rev Cancer* 2, 351-360.

Takehara, T., and Takahashi, H. (2003). Suppression of Bcl-xL deamidation in human hepatocellular carcinomas. *Cancer Res* 63, 3054-3057.

Vousden, K. H., and Lu, X. (2002). Live or let die: the cell's response to p53. *Nat Rev Cancer* 2, 594-604.

Wang, X. (2001). The expanding role of mitochondria in apoptosis. *Genes Dev* 15, 2922-2933.

warberg, o. (1930). The mechanism of tumours. In, (London: Constable press), p. 327p.

- Weintraub, S. J., and Deverman, B. E. (2007). Chronoregulation by asparagine deamidation. *Sci STKE* 2007, re7.
- Weintraub, S. J., Manson, S. R., and Deverman, B. E. (2004). Resistance to antineoplastic therapy. The oncogenic tyrosine kinase-Bcl-x(L) axis. *Cancer Cell* 5, 3-4.
- Yang, F. T., Lord, B. I., and Hendry, J. H. (1995). Gamma irradiation of the fetus damages the developing hemopoietic microenvironment rather than the hemopoietic progenitor cells. *Radiat Res* 141, 309-313.
- Yang, W., Dyck, J. R., Wang, H., and Fliegel, L. (1996). Regulation of NHE-1 promoter in mammalian myocardium. *Am J Physiol* 270, H259-266.
- Yang, W., Wang, H., and Fliegel, L. (1996). Regulation of Na⁺/H⁺ exchanger gene expression. Role of a novel poly(dA.dT) element in regulation of the NHE1 promoter. *J Biol Chem* 271, 20444-20449.
- Zamo, A., Chiarle, R., Piva, R., Howes, J., Fan, Y., Chilosi, M., Levy, D. E., and Inghirami, G. (2002). Anaplastic lymphoma kinase (ALK) activates Stat3 and protects hematopoietic cells from cell death. *Oncogene* 21, 1038-1047.
- Zhao, R., Follows, G. A., Beer, P. A., Scott, L. M., Huntly, B. J., Green, A. R., and Alexander, D. R. (2008). Inhibition of the Bcl-xL deamidation pathway in myeloproliferative disorders. *N Engl J Med* 359, 2778-2789.
- Zhao, R., Oxley, D., Smith, T. S., Follows, G. A., Green, A. R., and Alexander, D. R. (2007). DNA damage-induced Bcl-xL deamidation is mediated by NHE-1 antiport regulated intracellular pH. *PLoS Biol* 5, e1.
- Zhao, R., Yang, F. T., and Alexander, D. R. (2004). An oncogenic tyrosine kinase inhibits DNA repair and DNA-damage-induced Bcl-xL deamidation in T cell transformation. *Cancer Cell* 5, 37-49.
- Zou, H., Li, Y., Liu, X., and Wang, X. (1999). An APAF-1.cytochrome c multimeric complex is a functional apoptosome that activates procaspase-9. *J Biol Chem* 274, 11549-11556.

Published Work

Rui Zhao

DNA Damage–Induced Bcl-x_L Deamidation Is Mediated by NHE-1 Antiport Regulated Intracellular pH

Rui Zhao¹, David Oxley², Trevor S. Smith², George A. Follows³, Anthony R. Green³, Denis R. Alexander^{*1}

1 Laboratory of Lymphocyte Signalling and Development, The Babraham Institute, Babraham, Cambridge, United Kingdom, **2** Protein Technologies Laboratory, The Babraham Institute, Babraham, Cambridge, United Kingdom, **3** Department of Haematology, University of Cambridge, Hills Road, Cambridge, United Kingdom

The pro-survival protein Bcl-x_L is critical for the resistance of tumour cells to DNA damage. We have previously demonstrated, using a mouse cancer model, that oncogenic tyrosine kinase inhibition of DNA damage–induced Bcl-x_L deamidation tightly correlates with T cell transformation in vivo, although the pathway to Bcl-x_L deamidation remains unknown and its functional consequences unclear. We show here that rBcl-x_L deamidation generates an iso-Asp⁵²/iso-Asp⁶⁶ species that is unable to sequester pro-apoptotic BH3-only proteins such as Bim and Puma. DNA damage in thymocytes results in increased expression of the NHE-1 Na/H antiport, an event both necessary and sufficient for subsequent intracellular alkalinisation, Bcl-x_L deamidation, and apoptosis. In murine thymocytes and tumour cells expressing an oncogenic tyrosine kinase, this DNA damage–induced cascade is blocked. Enforced intracellular alkalinisation mimics the effects of DNA damage in murine tumour cells and human B-lineage chronic lymphocytic leukaemia cells, thereby causing Bcl-x_L deamidation and increased apoptosis. Our results define a signalling pathway leading from DNA damage to up-regulation of the NHE-1 antiport, to intracellular alkalinisation to Bcl-x_L deamidation, to apoptosis, representing the first example, to our knowledge, of how deamidation of internal asparagine residues can be regulated in a protein in vivo. Our findings also suggest novel approaches to cancer therapy.

Citation: Zhao R, Oxley D, Smith TS, Follows GA, Green AR, et al. (2007) DNA damage–induced Bcl-x_L deamidation is mediated by NHE-1 antiport regulated intracellular pH. *PLoS Biol* 5(1): e1. doi:10.1371/journal.pbio.0050001

Introduction

The deamidation of internal asparaginyl and glutaminyl protein residues has attracted increasing attention over the past decade as a modification leading to significant changes in protein function [1,2]. The protein deamidation rates of more than 18,000 proteins have been computed, containing 230,000 individual asparaginyl residues, generating Asn half-lives of less than 1 d to 50 y or more [3,4]. Protein deamidation has broad biological implications, ranging from changes in the specificity of antigen presentation [5], to modifications in eye lens proteins [6], to the activation of RhoA by cytotoxic necrotizing factor [7], to aging [1], to name but a few examples.

The deamidation of Gln proceeds both enzymatically and nonenzymatically in physiological systems, whereas only the nonenzymatic deamidation of internal Asn residues has been reported, involving conversion to Iso-Asp:Asp in a ratio of about 3:1, with the precise ratio depending on the environment of the Asn residue [1,8]. Deamidation of both Gln and Asn residues in vitro can be greatly accelerated by exposure to either acid or alkaline pH, with minima in the range pH 4–6. Until recently, it was assumed that Asn protein deamidation rates in vivo were set up by a “fixed clock” that was defined only by the primary, secondary, and tertiary structures of proteins that specified the half-life of the particular Asn residue in question. However, this view has been radically changed by the recent observation that DNA damage induces the relatively rapid deamidation of the pro-survival protein Bcl-x_L in an osteosarcoma cell line system [9], indicating that the deamidation “clock”, far from being fixed,

is a dynamic process that can be regulated in vivo by biologically critical events. Bcl-x_L deamidation in response to DNA damage occurs at two internal Asn residues (Asn⁵² and Asn⁶⁶), causing a characteristic retardation on SDS-polyacrylamide gel electrophoresis (PAGE) gels [9–12]. Initial work from the Weintraub laboratory suggested that when Asn⁵² and Asn⁶⁶ are both mutated to Asp, then Bcl-x_L loses its ability to bind to the BH3-only pro-apoptotic protein Bim, thereby providing a putative linkage between DNA damage and apoptosis [9]. However, a secondary mutation was later identified, which, when corrected, enabled the N52D/N66D Bcl-x_L to bind Bim, casting doubt on this interpretation [13].

Using a different model system, we have previously implicated the oncogene-mediated inhibition of DNA damage–induced Bcl-x_L deamidation in the transformation of murine thymocytes [14,15]. Our transgenic mouse model of T cell lymphoma was generated by crossing mice lacking

Academic Editor: Douglas Green, St. Jude Children’s Research Hospital, United States of America

Received: June 6, 2006; **Accepted:** October 25, 2006; **Published:** December 19, 2006

Copyright: © 2007 Zhao et al. This is an open-access article distributed under the terms of the Creative Commons Attribution License, which permits unrestricted use, distribution, and reproduction in any medium, provided the original author and source are credited.

Abbreviations: B-CLL, B-lineage chronic lymphoblastic leukemia; CHX, cycloheximide; DMA, 5-(N,N’-dimethyl)-amiloride; DN, double negative; Etop, etoposide; FACS, fluorescence activated cell sorter; IR, irradiation; OTK, oncogenic tyrosine kinase; PBMC, peripheral blood mononuclear cells; pH_i, intracellular pH; pH_e, extracellular pH; PI, propidium iodide

* To whom correspondence should be addressed. E-mail: denis.alexander@bbsrc.ac.uk

Author Summary

Cell survival and cell death (apoptosis) are controlled by a finely tuned ensemble of pro-survival and pro-apoptotic proteins. When the two types of protein are balanced, cells survive. But if the pro-survival proteins dominate, there is a danger that cells with damaged DNA will stay alive, leading to malignancy. One of the key pro-survival proteins, Bcl-x_L, acts by blocking the actions of pro-apoptotic proteins. We show here that DNA damage results in an important modification of Bcl-x_L. Specifically, when the amide groups are removed from two critical asparagine (amino acid) residues, Bcl-x_L can no longer block pro-apoptotic proteins, leading to cell death. Surprisingly, Bcl-x_L deamidation is catalysed not by an enzyme, but by increased pH inside the cell due to the up-regulation of an NHE-1 transporter that moves positive ions across the cell membrane. Indeed, artificially increasing pH causes Bcl-x_L deamidation and apoptosis in the absence of initial DNA damage. Exploring this novel pathway may ultimately suggest approaches to cancer therapy, especially when malignant cells are resistant to chemotherapy or radiotherapy.

expression of the CD45 tyrosine phosphatase with a line expressing a nononcogenic level of the mutant lck^{F505} tyrosine kinase [16]. All the *CD45^{-/-}lck^{F505}* progeny develop aggressive T cell lymphomas at the early CD4⁺CD8⁻ stage of thymic development, typically at 5–12 wk of age. The absence of CD45-mediated dephosphorylation results in hyperphosphorylation of positive regulatory p56^{lck} pTyr-394, causing hyperactivation of the kinase and triggering oncogenesis [15]. The model enables the investigation of the earliest oncogenic events in primary pretumorigenic thymocytes. Inhibition of DNA repair in *CD45^{-/-}lck^{F505}* mice leads to DNA damage, genomic instability, and chromosomal aberrations detectable in primary CD4⁺CD8⁻ thymocytes before transformation. Despite a normal p53 response, DNA damage-induced apoptosis is suppressed in pretumorigenic thymocytes, correlating with the inhibition of Bcl-x_L deamidation, the preservation of Bcl-x_L binding to Bim, and the inhibition of cytochrome c release and the apoptotic caspase execution cascade. Therefore, we proposed that Bcl-x_L deamidation is a critical switch in oncogenic kinase-induced T cell transformation, and we suggested that Bcl-x_L deamidation to an Iso-Asp⁵²/Iso-Asp⁶⁶ version, rather than the mutant N52D/N66D version investigated by the Weintraub laboratory, might be the key step in disabling the antiapoptotic functions of the protein [14,15].

Neither in the osteosarcoma cell line work [9] nor in our own work based on primary thymocytes [15] has there been any indication as to how DNA damage might induce Bcl-x_L deamidation. Neither have there been previous reports in the literature showing how protein Asn deamidation in general might be regulated in vivo; we address here this question. We confirm that Bcl-x_L deamidation does indeed destroy its ability to sequester pro-apoptotic proteins such as Bim and Puma, thereby establishing a clear molecular link between DNA damage, Bcl-x_L deamidation, and apoptosis. Surprisingly, DNA damage-triggered deamidation in primary wild-type cells is mediated not enzymatically, but by intracellular alkalinisation caused by increased expression of the NHE-1 Na⁺/H⁺ exchanger (antiport), events blocked by expression of the oncogenic tyrosine kinase (OTK). In the case of either murine or human cancer cells, enforced alkalinisation

triggers Bcl-x_L deamidation, crippling its ability to provide protection from the pro-apoptotic consequences of DNA damage, thereby indicating possible novel approaches to cancer therapy.

Results

DNA Damage-Induced Bcl-x_L Deamidation Does Not Depend on Mitochondrial Apoptosis

An important consideration is whether DNA damage-induced Bcl-x_L deamidation in murine thymocytes is a cause or consequence of thymic apoptosis. Figure 1 shows that whereas the addition of the caspase inhibitor Z-VAD-fmk, as expected, inhibited DNA damage-induced apoptosis in murine thymocytes (Figure 1A), no inhibition of DNA damage-induced Bcl-x_L deamidation was observed in cell aliquots taken from the same thymic cultures (Figure 1B). It is known that in the absence of Bax and Bak, BH3-only proteins are unable to induce apoptosis [17]. We therefore used short hairpin RNA (shRNA) to deplete Bax and Bak from CD4⁺CD8⁻ (double-negative, DN) thymocytes, confirmed that depletion was sufficient to block caspase 9 cleavage (Figure S1A), and showed that DNA damage-induced Bcl-x_L deamidation proceeded normally in the absence of Bax and Bak (Figure 1C). We also showed that Bcl-x_L deamidation was clearly detectable within 3–6 h after the instigation of DNA damage, and proceeded in parallel with increased apoptosis (Figure S1B and S1C). These results show that Bcl-x_L deamidation is not caused by mitochondrial apoptosis and are consistent with a role for deamidation upstream of the apoptotic executor pathway. Further data presented below establish a more direct causal relationship between Bcl-x_L deamidation and apoptosis in DNA damaged thymocytes.

Bcl-x_L Deamidation In Situ Involves Conversion of Asn⁵²/Asn⁶⁶ to Iso-Asp⁵²/Iso-Asp⁶⁶, Preventing Sequestration of Bim and Puma

We previously noted that whereas the ability of Bcl-x_L to bind Bim was ablated in control thymocytes exposed to DNA damage, it was strikingly retained in pretumorigenic *CD45^{-/-}lck^{F505}* thymocytes, tightly correlating with the resistance to Bcl-x_L deamidation noted in these cells [15]. However, work from the Weintraub laboratory suggests that deamidated Bcl-x_L still binds Bim [13], thereby casting doubt on the model that Bcl-x_L deamidation triggers apoptosis. Because the sequestration of BH3-only proteins by Bcl-x_L is thought to explain its anti-apoptotic function [18], resolution of this question is clearly important for establishing a molecular link between DNA damage and apoptosis. We therefore carried out a series of cellular and biochemical experiments to address this key point.

Figure 2A shows that Bcl-x_L measured in whole cell lysates from pretumorigenic *CD45^{-/-}lck^{F505}* murine thymocytes is resistant to deamidation following γ irradiation, consistent with our previous findings [15]. Immunoprecipitation of the pro-apoptotic protein Bim, followed by immunoblotting for Bcl-x_L, revealed that Bim sequestered only the N52/N66 Bcl-x_L and failed to bind the slower migrating deamidated protein (Figure 2A, upper panel), although the amount of Bim in each immunoprecipitate was comparable (Figure 2A, lower panel). Because the BH3-only protein Puma, not Bim,

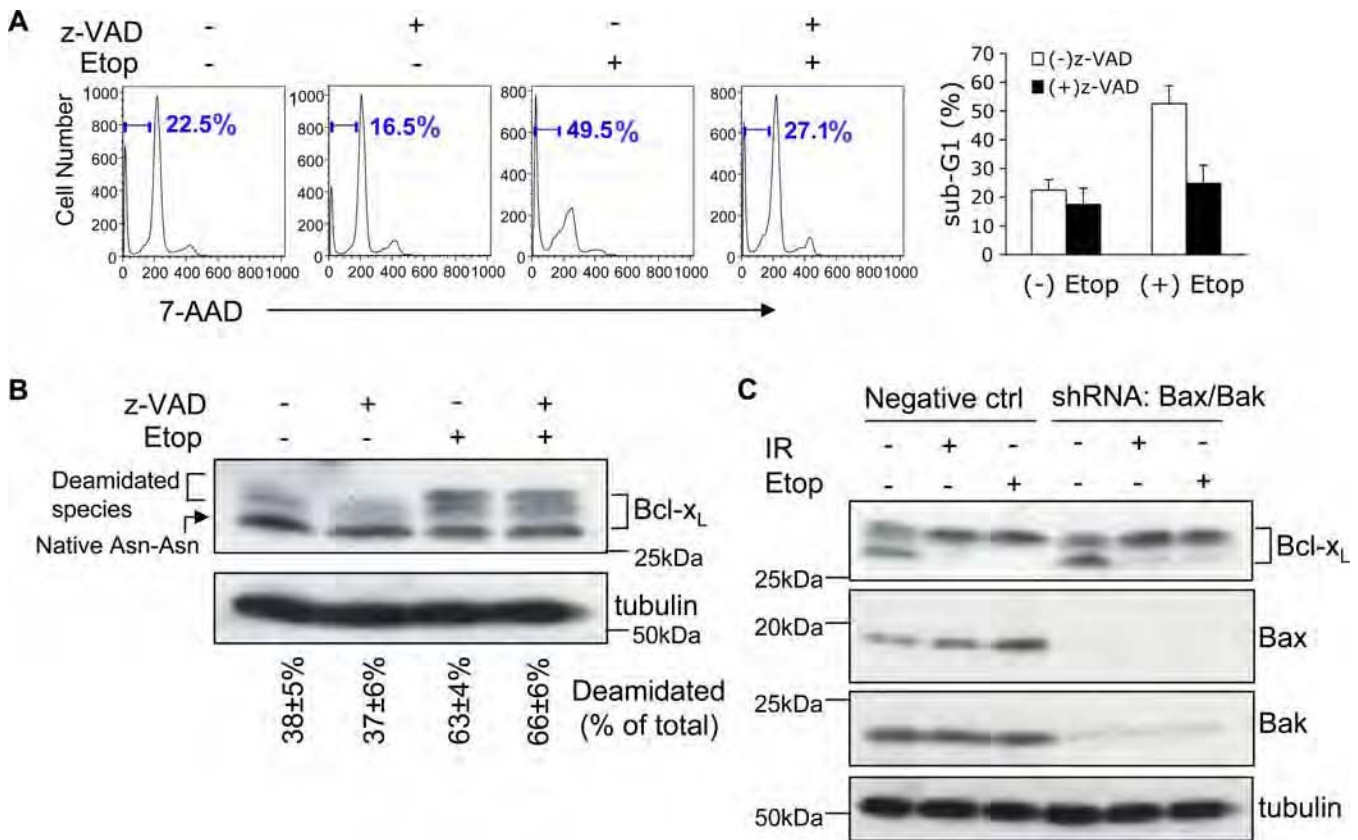


Figure 1. DNA Damage-Induced Bcl-x_L Deamidation Is Mitochondrial Apoptosis-Independent

(A) Wild-type thymocytes were pre-incubated with or without Z-VAD-fmk (200 μM), and were then cultured with or without etoposide for 24 h, harvested, and apoptosis was measured by measuring the sub-G1 peak by flow cytometry. The histograms (right panel) represent mean values ± SD (*n* = 3).

(B) Aliquots of the cells from (A) incubated in the presence or absence of Z-VAD-fmk (200 μM) were analysed for the expression of Bcl-x_L and tubulin (as loading control) by immunoblotting. The upper and lower bands of Bcl-x_L were quantified and expressed as a percentage of total Bcl-x_L. The percentages shown below each lane are means ± SD (*n* = 3).

(C) Plasmids of shRNA Bax (GFP) and shRNA Bak (DsRed) were cotransfected into purified DN thymocytes using an Amaxa nucleofactor kit. 48 h later, GFP⁺ DsRed⁺ cells were purified by flow cytometry and treated with etoposide (Etop, 25 μM) for 30 h or exposed to irradiation (IR, 5 Gy) followed by 30 h in culture. DN thymocytes transfected with negative control plasmids were treated in parallel. Cells were then processed for immunoblotting with Bcl-x_L antibody. The immunoblot was reprobed for Bax and Bak to check the efficiency of gene knockdown. Tubulin was also reprobed as a loading control. doi:10.1371/journal.pbio.0050001.g001

plays a major role in DNA-damage triggered apoptosis [19,20], we also showed that both Puma and Bim are found in Bcl-x_L immunoprecipitates from etoposide treated CD45^{-/-} Lck^{F505} thymocytes, whereas sequestration is ablated in wild-type cells, correlating with Bcl-x_L deamidation (Figure 2B). A comparable result was obtained when Puma immunoprecipitates were blotted for Bcl-x_L (Figure S2A). Therefore, deamidated Bcl-x_L appears unable to sequester BH3-only proteins.

To confirm the results using intact thymocytes, we carried out *in vitro* biochemical experiments. Recombinant purified His-tagged Bcl-x_L was exposed to alkaline conditions to cause partial deamidation and separated by anion-exchange chromatography into three peaks (Figure 2C, peaks A, B and C). Mass spectrometric analysis revealed an increase of 1 Da for peak B relative to peak A, and a further increase of 1 Da for peak C relative to peak B (Figure 2C). On SDS-PAGE gels, peak A Bcl-x_L migrated slightly faster than the more acidic peaks B and C (Figure 2D), reproducing the characteristic profile of N52/N66 Bcl-x_L and its deamidated versions found

in our cellular studies (Figure 1B). It has already been demonstrated that these migratory shifts are not caused by phosphorylation [9,12]. In fact, deamidation of a single Asn increases protein mass by 1 Da, at the same time increasing its net negative charge, confirming that the shifts are due to deamidation. Importantly, when the three species of rBcl-x_L were tested for their ability to bind to Bim in wild-type thymic lysates, only peak A bound Bim effectively, whereas binding to peak B rBcl-x_L was reduced by 88% ± 2% and completely ablated using peak C rBcl-x_L (Figure 2D, upper panel). Figure 2E shows that the Asp⁵²/Asp⁶⁶ version of Bcl-x_L, or the Ala⁵²/Ala⁶⁶ version that cannot be deamidated, does still bind both Bim and Puma, consistent with the correction published by the Weintraub laboratory [13]. We therefore determined whether rBcl-x_L Asn⁵² and Asn⁶⁶ convert mainly to Asp or to iso-Asp upon alkali treatment. Consistent with previous results [8], Figure 2F and Figure S3 show that the ratios of iso-Asp:Asp conversion for Asn⁵² and Asn⁶⁶ are 10:1 and 5:1, respectively. Kinetic analysis revealed that deamida-

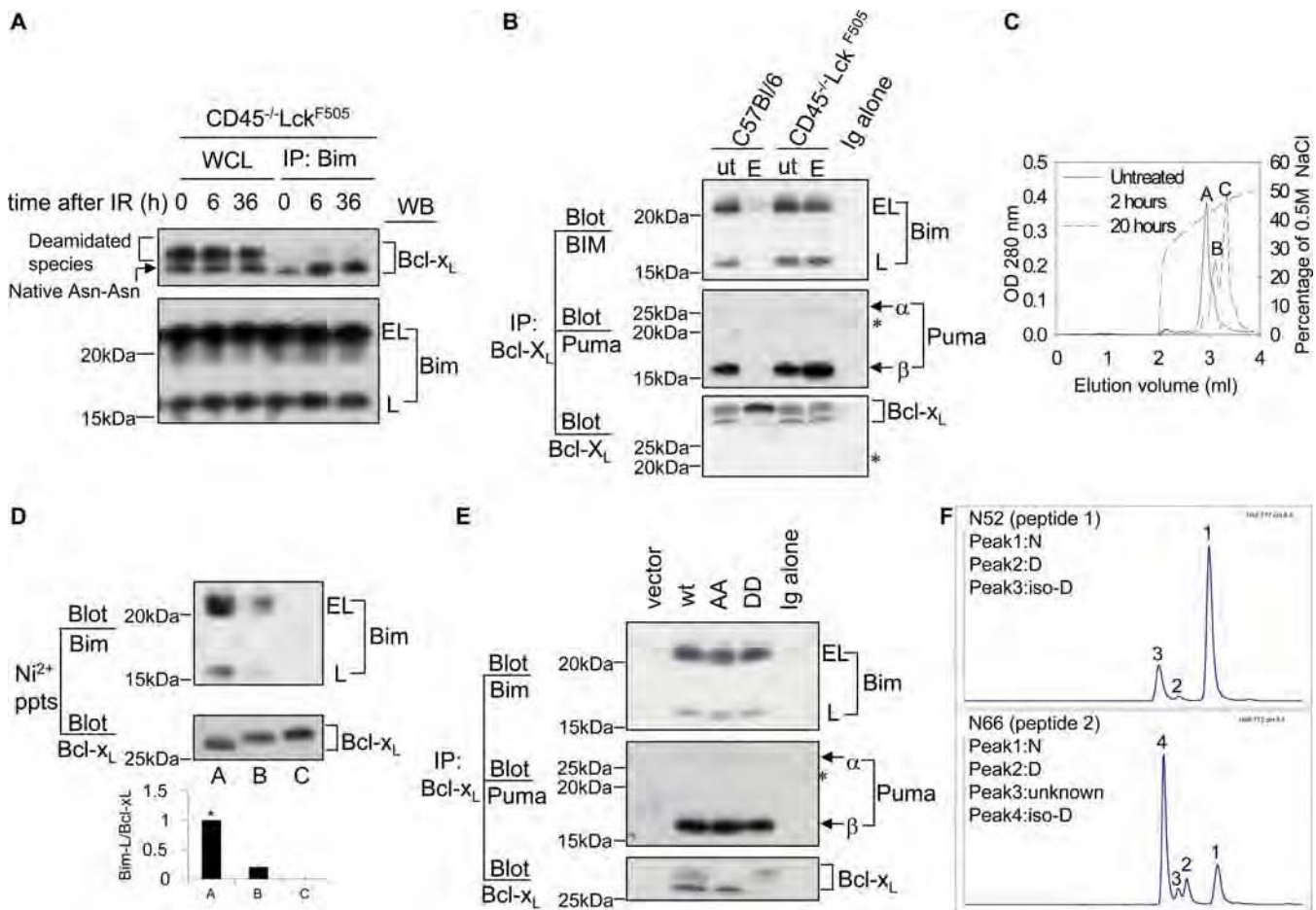


Figure 2. Deamidation Disrupts the Sequestration of BH3-Only Proteins by Bcl-x_L

(A) Bim binds to the native (Asn-Asn) but not deamidated forms of Bcl-x_L. Wild-type (C57BL/6) thymocytes (1.5×10^7) were exposed to 5 Gy irradiation (IR) and then maintained in culture for the times shown, after which cells were lysed and either separated as whole cell lysates (WCL) or as Bim immunoprecipitates, followed by immunoblotting for either Bcl-x_L or for Bim. Bim migrates as “extra-long” (EL) or “long” (L) forms.

(B) Bcl-x_L was immunoprecipitated from lysates derived from purified DN thymocytes treated with/without etoposide (ut/E), followed by immunoblotting for Bim or Puma. The asterisk indicates the light chain of the Bcl-x_L antibody used for immunoprecipitation.

(C) Anion exchange chromatography of purified rBcl-x_L. Sample A was untreated; samples B and C were exposed to pH 8.8 at 37 °C for 2 h and 20 h, respectively. The Figure illustrates superimposed elution profiles for each sample. Peaks A, B, and C had molecular masses of 25, 015.6; 25, 016.4, and 25, 017.2, respectively.

(D) Bim binds to native but not to deamidated rBcl-x_L. The three different forms of Bcl-x_L (A, B, and C) purified by anion-exchange column chromatography shown in (C) were incubated in wild-type thymic lysates (1.5×10^7 cell equivalents) at 4 °C for 2 h and then precipitated using nickel beads. The precipitated products were immunoblotted for Bim and Bcl-x_L. Quantification of the Bim-L/Bcl-x_L ratios \pm SD from three independent experiments is shown in the histogram, with the lane A ratio normalised to 1 (*).

(E) Primary thymocytes were retrovirally transduced with empty vector or Bcl-x_L constructs (wild-type, N52A-N66A, or N52D-N66D). Bcl-x_L was immunoprecipitated from lysates derived from 1.5×10^6 sorted GFP-positive cells per lane, followed by immunoblotting for Bim or Puma. Note that in the vector lane, at this exposure endogenous Bcl-x_L is not visible because of the small number of cells used. The asterisk indicates the light chain of the Bcl-x_L antibody used for immunoprecipitation.

(F) Peptides SDVEENRTEAPEGTESEMETPSAINGNPSW (peptide 1) and HLADSPAVNGATGHSSSL (peptide 2), and the corresponding deamidated forms, containing the putative deamidation sites N52 and N66, respectively, were generated by digestion of rBcl-x_L with chymotrypsin. The chromatographic conditions used for the separation of the peptides in the LC-MS analyses were optimised so as to resolve the Asn, Asp, and iso-Asp forms of peptides 1 and 2. The Asp and iso-Asp forms of the two peptides were identified by spiking an aliquot of a digestion mixture with Asp- or iso-Asp-containing synthetic peptides prior to LC-MS (Figure S3). The chromatograms show LC-MS analyses at time point 72 h of the rBcl-x_L base treatment. For both peptides, the major deamidation product is the iso-Asp form; the iso-Asp:Asp ratios are approximately 10:1 for N52 and 5:1 for N66. The unknown peak 3 in peptide 2 could be an isomer of peak 2 or peak 4.

doi:10.1371/journal.pbio.0050001.g002

tion of Asn⁶⁶ to iso-Asp is much faster than for Asn⁵² (unpublished data).

Taken together, our results show that conversion of Bcl-x_L Asn⁵² and Asn⁶⁶ to iso-Asp, but not Asp, prevents sequestration of BH3-only proteins. Peak B represents rBcl-x_L deamidated at either Asn⁵² or Asn⁶⁶, whereas peak C is deamidated at both sites (Figure 2C and 2D). Deamidation to iso-Asp causes greater perturbations of protein structure

than conversion to Asp [1,8], presumably explaining the loss of BH3-only protein binding.

DNA Damage-Induced Bcl-x_L Deamidation and Apoptosis Is Mediated by Intracellular Alkalinisation

Until now, the in vivo mechanism for the deamidation of internal protein Asn residues has not been described for any protein. Because protein Asn deamidation is accelerated by

increased pH *in vitro*, we investigated intracellular pH change (pH_i) as a possible regulatory mechanism in thymocytes. Figure 3A shows that after DNA damage, the pH_i of live wild-type CD4⁺CD8⁺ thymocytes increased to 7.55, whereas no change was observed in pretumorigenic cells. But is that increase sufficient to cause Bcl-x_L deamidation? To address this question, we incubated wild-type thymocytes in the pH range of 7.2–8.0 for 20 h in the presence of the Na⁺ ionophore monensin to ensure complete equilibration of pH_i and extracellular pH (pH_e), and to neutralize acidic intracellular compartments [21], and we then assessed the extent of Bcl-x_L deamidation. Figure 3B shows that whereas only 22.5% ± 3.2% was deamidated at pH 7.2, this increased to 56.1% ± 3.8% at pH 7.6 and 67.0% ± 4.5% at pH 8.0. Therefore, a rise in pH_i comparable with that observed after DNA damage (Figure 3A) is sufficient to cause substantial deamidation. Furthermore, the addition of Z-VAD-fmk to thymic cultures following DNA damage did not inhibit their alkalisation (Fig. 3C), showing that the rise in pH_i is not downstream of caspase activation. To investigate Bcl-x_L deamidation, pH_i, and apoptosis in parallel, we manipulated pH_i values artificially by incubating cells at varying pH_e values in the absence of monensin. The left panel of Figure 3D shows that when DNA damage was induced in wild-type thymocytes, Bcl-x_L deamidation could be largely prevented by artificially maintaining the pH_i at 7.1 (value shown in Figure 3E, left panel), thereby reducing the percentage of apoptotic CD4⁺CD8⁺ thymocytes by 2-fold relative to those incubated at physiological pH (Figure 3F, left panel). Conversely, Figure 3D (right panel) shows that the resistance to Bcl-x_L deamidation observed in DNA-damaged pretumorigenic thymocytes could be completely overcome by artificially increasing the pH_i to 7.55 or above (Figure 3E, right panel), correlating with a 2-fold increase in the percentage of apoptotic CD4⁺CD8⁺ thymocytes relative to those incubated at physiological pH (Figure 3F, right panel). Interestingly, enforced alkalisation alone in the absence of DNA damage caused a marked increase in Bcl-x_L deamidation in the OTK expressing thymocytes (Figure 3D, right panel), with a concomitant increase in apoptosis (Figure 3F, right panel), albeit at a level lower than with DNA damage, perhaps reflecting the somewhat lower pH_i values achieved under these conditions (Figure 3E, right panel).

We considered that the tight correlation between pH_i, Bcl-x_L deamidation, and apoptosis might nevertheless be coincidental and that enforced alkalisation might be inducing apoptosis by a mechanism independent of Bcl-x_L deamidation. Mutant Bcl-x_L Ala⁵²/Ala⁶⁶ or Asp⁵²/Asp⁶⁶, both of which sequester BH3-only proteins (Figure 2E), were therefore over-expressed in wild-type CD4⁺CD8⁺ thymocytes by retroviral transduction prior to enforced alkalisation by incubation in media at pH 8.0 or 8.5. Figure 3G (middle panel) shows that, as expected, the Ala⁵²/Ala⁶⁶ mutant migrates as the lower nondeamidated version of Bcl-x_L, whereas Asp⁵²/Asp⁶⁶ migrates as the more negatively charged deamidated version. Interestingly, in the cells expressing these mutant forms of Bcl-x_L, the apoptosis induced by enforced alkalisation was reduced 4-fold compared to cells transduced with empty vector, or more than 2-fold in comparison with the wild-type protein (Figure 3G, right panel), which of course undergoes deamidation in response to alkali treatment. These results show that Bcl-x_L

in a version able to sequester BH3-only proteins protects thymocytes from an enforced increase in pH_i. Nevertheless, protection was not absolute, suggesting that Bcl-x_L may not be the only mechanism protecting cells from apoptosis triggered by alkalisation. As a further control, we have confirmed that Bcl-x_L isolated from wild-type thymocytes exposed to a high pH buffer can no longer sequester Bim (Figure S2B), thereby mimicking the effects of DNA damage (Figure 2A).

Taken overall, these results demonstrate that intracellular alkalisation following DNA damage is both necessary and sufficient for nonenzymatic Bcl-x_L deamidation, that the oncogenic suppression of Bcl-x_L deamidation in pretumorigenic thymocytes is caused by inhibition of alkalisation, and that versions of Bcl-x_L competent for BH3-only protein sequestration are sufficient per se to protect cells from apoptosis at alkaline pH_i.

DNA Damage-Induced Alkalisation, Bcl-x_L Deamidation, and Apoptosis are Mediated by Increased NHE-1 Antiport Expression

We next investigated the molecular mechanisms leading from DNA damage to the regulation of pH_i and subsequent Bcl-x_L deamidation. Figure 4A shows that *de novo* protein synthesis is essential for Bcl-x_L deamidation following DNA damage in wild-type thymocytes. Because the NHE-1 Na/H antiport is a well-established regulator of pH_i [22] and has previously been implicated in the regulation of thymic apoptosis [23], we measured its expression in wild-type thymocytes after DNA damage and found that the NHE-1 level increased 2.5-fold within 5 h, whereas this increase was completely suppressed in pretumorigenic thymocytes (Figure 4B). No inhibition of increased NHE-1 expression in wild-type thymocytes was observed following addition of the Z-VAD-fmk caspase inhibitor (Figure S4A) nor following depletion of Bax and Bak from the cells (Figure S4B). We therefore carried out a further series of experiments to demonstrate that there was a direct causal linkage between the regulation of NHE-1 expression, pH_i, Bcl-x_L deamidation, and apoptosis. Given that the OTK blocks DNA-damage induced NHE-1 expression in pretumorigenic thymocytes, this provides a powerful system for examining the consequences of experimentally enforcing NHE-1 expression in these cells by retroviral transduction. As Figure 4C illustrates (upper panel), an enforced 2-fold–3-fold increase in NHE-1 expression in pretumorigenic thymocytes, without DNA damage, restored Bcl-x_L deamidation to a level comparable to that observed in a retrovirally transduced wild-type control in five separate experiments, thereby bypassing the OTK-mediated inhibition in deamidation. Overexpression of NHE-1 increased both pH_i and apoptosis to comparable levels in both pretumorigenic and wild-type thymocytes (Figure 4C, lower panels). These results suggest that increased NHE-1 expression per se is sufficient to cause increased pH_i, Bcl-x_L deamidation and apoptosis. To address this question further, we used the selective NHE-1 inhibitor 5-(N,N'-dimethyl)-amiloride (DMA) to block the actions of the antiport following its increased expression on thymocytes upon DNA damage. Figure 4D shows that DMA prevented the alkalisation of wild-type thymocytes following DNA damage (top left panel), their apoptosis (top right panel), and Bcl-x_L

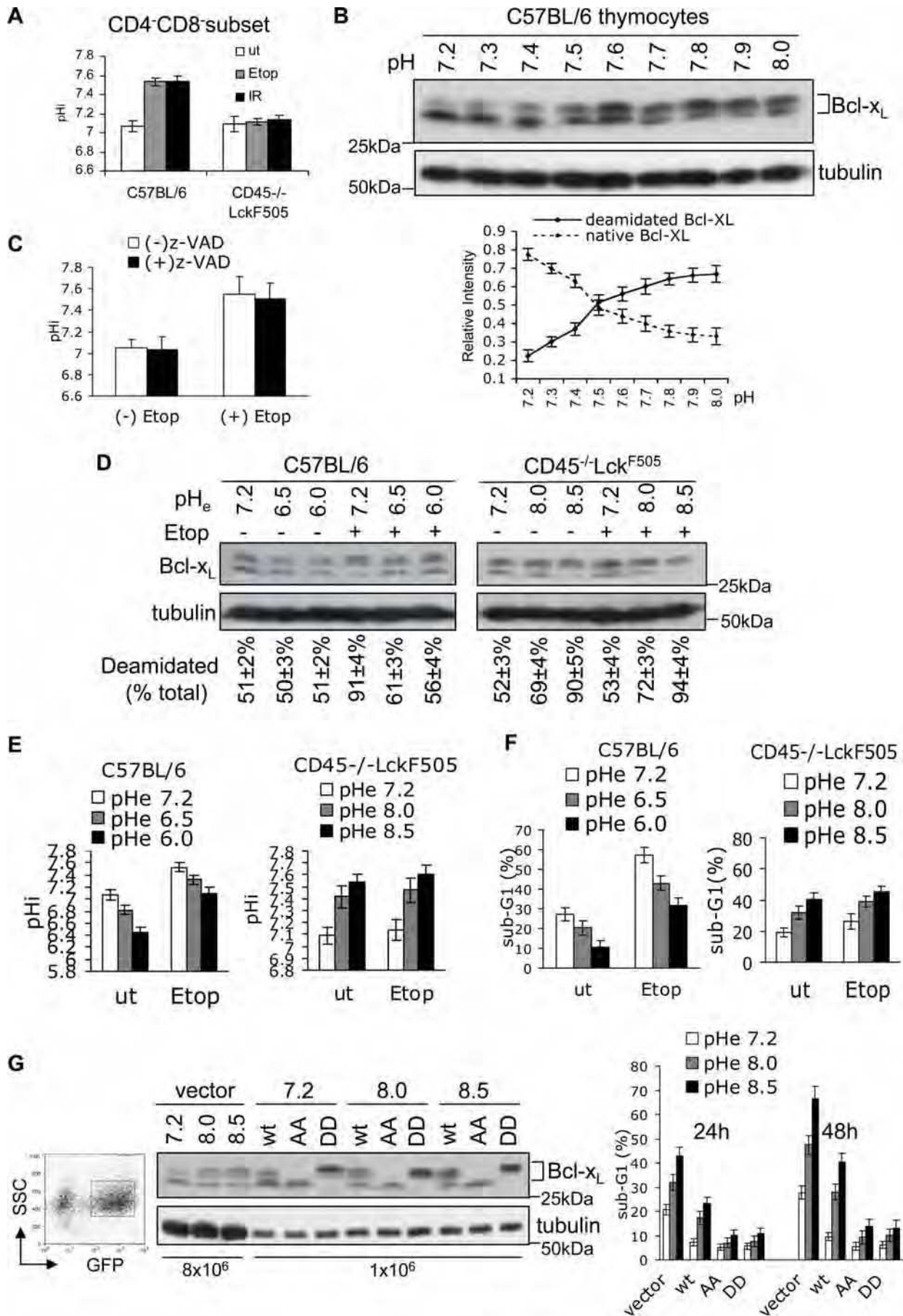


Figure 3. DNA Damage Causes Intracellular Alkalinisation and Subsequent Bcl-x_L Deamidation

(A) Intracellular alkalinisation occurs following DNA damage in wild-type but not in pretumorigenic *CD45^{-/-}Lck^{F505}* thymocytes. Cells were treated with etoposide (Etop) for 20 h or exposed to 5 Gy of irradiation (IR) and then maintained in culture for 20 h. pH_i was measured using SNARF by FACS in the gated live CD4⁺CD8⁺ subset. The histograms represent mean values \pm SD ($n = 5$).

(B) Enforced intracellular thymic alkalinisation causes Bcl-x_L deamidation. Wild-type thymocytes were maintained in RPMI-1640/10% bovine fetal calf serum buffered at the indicated pH with Tris-HCl for 20 h in the presence of 20 μ M monensin prior to lysis and immunoblotting for Bcl-x_L. To minimize any deamidation produced during the gel-running process, the resolving gel buffer was adjusted to pH 8.0 in this experiment. The mean ratio of the lower band (native Bcl-x_L) or upper band (deamidated Bcl-x_L) to the total (upper plus lower bands) is shown in the graph (lower panel). The error bars represent SD ($n = 3$). Note that deamidation becomes prominent at pH 7.5.

(C) Aliquots of the cells from Figure 1A incubated in the presence or absence of Z-VAD-fmk (200 μ M) were analysed for pH_i. The histograms represent mean values \pm SD ($n = 3$).

(D) Wild-type or *CD45^{-/-}Lck^{F505}* pretumorigenic thymocytes were cultured for 24 h in media at the pH shown without monensin, with or without etoposide, and then analysed for Bcl-x_L deamidation by immunoblotting. The upper and lower bands were quantified and the percentage of upper bands in total Bcl-x_L calculated. The percentages shown below each lane are means \pm SD ($n = 5$).

(E) Aliquots of cells used in (D) were assessed for pH_i by FACS. The histograms show the pH_i of live gated CD4⁺CD8⁺ thymocytes from five independent experiments \pm SD. The pH_e values refer to the pH values of the extracellular media.

(F) Apoptosis of aliquots of the cells from (D) was analysed by FACS. The histogram shows the sub-G1 peak (%) of CD4⁺CD8⁺ thymocytes from five independent experiments \pm SD.

(G) Wild-type (wt), N52A-N66A (AA), N52D-N66D (DD) Bcl-x_L, and empty vector were retrovirally transduced into thymocytes. GFP-positive cells were FACS sorted (left panel) and cultured in media with the pH_e shown for 24 h or 48 h, then processed for immunoblotting with Bcl-x_L antibody (middle panel). Note that 8×10^6 and 1×10^6 cell equivalents were loaded per lane for the empty vector (lanes 1–3) and Bcl-x_L (lanes 4–12) transfectants, respectively, such that the endogenous Bcl-x_L is invisible in lanes 4–12. The histogram (right panel) shows mean apoptosis (sub-G1) values \pm SD generated from five independent experiments.

doi:10.1371/journal.pbio.0050001.g003

deamidation (lower panel), correlating with increased survival (Figure S5A).

To extend these findings, we also used shRNA to deplete thymocytes of NHE-1 protein (Figure S6A). NHE-1 knock-down almost completely blocked the actions of DNA damage in causing Bcl-x_L deamidation (Figure 5A), intracellular alkalinisation (Figure 5B), or apoptosis (Figure 5C and Figure S6B). We measured apoptosis by two different methods to ensure that DNA damage-induced cell death following retroviral transduction was by apoptosis and not by necrosis. Figure 5C and Figure S6B illustrate that double staining for Annexin V and propidium iodide (PI) followed by FACS analysis revealed a major increase in Annexin V⁺ PI⁺ (apoptotic) cells following transduction with the negative control shRNA followed by either γ irradiation or treatment with etoposide, whereas there was no increase in apoptotic cells above baseline in the cells depleted of NHE-1: DNA damage-induced apoptosis was blocked 100%. Comparable results were obtained by measuring the sub-G1 peak by FACS (unpublished data) and NHE-1 depletion also correlated with increased survival (Figure S5B).

We considered that post-translational modification of the NHE-1 antiport, in addition to regulation of its expression, might also be involved in mediating the DNA damage response. For example, a number of serine kinases have been shown to regulate NHE-1 phosphorylation and activity [24,25], so we investigated the pSer and pThr levels in NHE-1 immunoprecipitates from irradiated wild-type and pretumorigenic thymocytes, but the basal level of phosphorylation did not change after DNA damage and was comparable between the two cell types (Figure S6C). Nevertheless, we cannot formally exclude the possibility that not all pSer/pThr sites were recognised by the cocktail of monoclonal antibodies (mAbs) used. Taken together, our findings therefore suggest that the increased expression of the NHE-1 transporter is both necessary and sufficient for DNA damage-induced alkalinisation, Bcl-x_L deamidation, and apoptosis in wild-type thymocytes, and that the suppression of these three parameters in pretumorigenic thymocytes is caused by oncogenic inhibition of the DNA damage-triggered increase in NHE-1 expression.

Enforced Alkalinisation Causes Increased Bcl-x_L Deamidation and Apoptosis in Murine and Human Cancer Cells

The experiments illustrated in Figures 1–5 were all carried out on wild-type or primary pretumorigenic *CD45^{-/-}Lck^{F505}* thymocytes. Signalling pathways can be markedly different in fully transformed cells compared to their pretransformed counterparts. We therefore wondered whether *CD45^{-/-}Lck^{F505}* T cell tumour cells, which develop from CD4⁺CD8⁺ thymocytes [16], might display a comparable set of properties. Figure S7 shows that this was indeed the case: murine tumour cells resistant to genotoxic insult at physiological pH_i values can be sensitised to die by enforced alkalinisation leading to Bcl-x_L deamidation. Furthermore, a modest rise in pH_i following incubation in a mildly alkaline buffer produces levels of Bcl-x_L deamidation and apoptosis in murine tumour cells comparable to those observed by adding a DNA damaging reagent to wild-type thymocytes incubated at physiological pH.

Chronic lymphocytic leukaemia (CLL) is the most common adult haematological malignancy in the Western world and, like many cancers, is characterised by the development of drug resistance. We therefore determined whether genotoxic treatment in vitro of primary human B lineage CLL (B-CLL) cells might cause increased NHE-1, alkalinisation, Bcl-x_L deamidation, and apoptosis, as in primary murine thymocytes (Figures 3–5), or whether this might be inhibited, as with the murine cancer cells (Figure S7). In addition, we examined the consequences for these parameters of incubating cancer cells in alkaline pH buffers. To perform these investigations, we divided each sample of patient cancer cells into nine aliquots that were either untreated, subjected to γ irradiation, or exposed to etoposide, followed by incubation at pH 7.2, pH 8.0, or pH 8.5 for 24 h. Each aliquot was then further subdivided into three samples to measure pH_i, Bcl-x_L deamidation, and apoptosis. As expected, exposure of cells to mildly alkaline buffers generated pH_i values that displayed some variation between samples from different patients within a narrow range. The 18 values per patient obtained from 10 different patients, the mean values calculated for each pH_e value considered separately, and representative

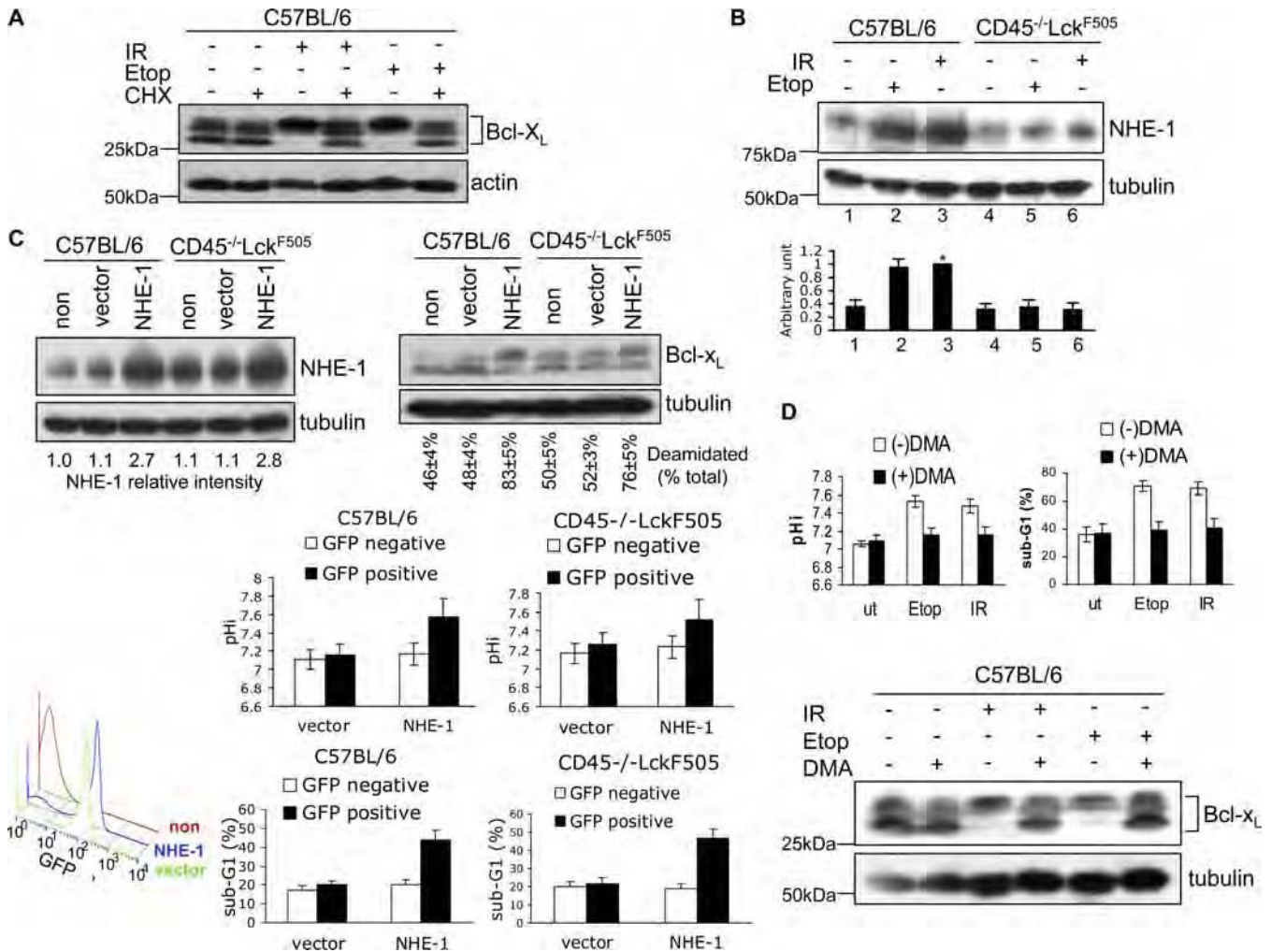


Figure 4. Bcl-x_L Deamidation Induced by DNA Damage Involves Up-Regulation of the NHE-1 Na/H Antiporter

(A) Bcl-x_L deamidation induced by DNA damage requires de novo protein synthesis. Wild-type thymocytes were either treated with etoposide for 24 h (Etop), or exposed to 5 Gy of irradiation (IR) and then maintained in culture for 24 h, with or without 0.5 μM cycloheximide (CHX). Cell lysates were processed by immunoblotting for Bcl-x_L or β-actin (loading control).

(B) DNA damage causes up-regulation of NHE-1 in wild-type but not in CD45^{-/-}Lck^{F505} thymocytes. Wild-type or CD45^{-/-}Lck^{F505} thymocytes were either treated with etoposide (Etop) for 5 h, or exposed to 5 Gy of irradiation (IR) and then maintained in culture for 5 h before immunoblotting for NHE-1 or tubulin (loading control). The histogram shows the quantification of relative NHE-1 expression levels SD from five independent experiments. Lane 3 was defined as 1 (*).

(C) Migri-NHE-1 or empty Migri vector were transduced into wild-type or pretumorigenic CD45^{-/-}Lck^{F505} thymocytes. 72 h after the first round of infection, cells were immunoblotted for NHE-1 and Bcl-x_L. NHE-1 expression levels (NHE-1 relative intensity) were normalised for loading using tubulin values. Deamidation was calculated as in Figure 1B. The lower left FACS histogram shows the infection efficiency for nontransfected (non), empty-vector transfected (vector), or NHE-1 transfected (NHE-1) cells as percentage GFP-positive cells. The lower right histograms show the mean pH_i and apoptosis (sub-G1) values ± SD (n = 5) analysed on GFP-negative and positive cells.

(D) The NHE-1 inhibitor DMA blocks DNA damage-induced alkalisation (top left panel), Bcl-x_L deamidation (lower panel) and apoptosis (top right panel) in wild-type thymocytes. Thymocytes were treated with Etoposide for 24 h, or exposed to 5 Gy of irradiation and then maintained in culture for 24 h, with or without 200 μM DMA. pH_i was measured by FACS on live CD4⁺CD8⁻ cells, and the sub-G1 peak was analysed by FACS on CD4⁺CD8⁻ cells to assess apoptosis. The histograms represent mean values ± SD (n = 3).

doi:10.1371/journal.pbio.0050001.g004

Bcl-x_L deamidation results from a single patient are illustrated in Figure 6A, Figure S8A, and Figure S8B, respectively. Interestingly, unlike the murine tumour cells expressing an OTK, the B-CLL cells behaved somewhat more like wild-type thymocytes in that DNA damage at physiological pH_e caused a mean increase of pH_i of 0.22 units, an 8% increase in Bcl-x_L deamidation, and an 18% increase in the number of cells undergoing apoptosis (Figure 6A and Figure S8A), compared to the higher thymocyte values of 0.45 pH_i units, 40% increase, and 37% increase, respectively (Figure 3). The human cancer cell values for these parameters

were greatly increased at alkaline pH_e, generating tight correlations between increasing pH_i, Bcl-x_L deamidation, and apoptosis (*r* values shown in Figure 6A). Thus, a mean increased pH_i of 0.5 correlated with 1.7-fold and 2.4-fold increases in Bcl-x_L deamidation and apoptosis, respectively. It is also striking that enforced intracellular alkalisation alone (by 0.3 pH_i units), in the absence of experimentally induced DNA damage, was itself sufficient to increase Bcl-x_L deamidation and apoptosis by 1.5-fold and 1.8-fold, respectively. This point is further illustrated by the gray shaded area shown in Figure 6A, which encompasses the overlap in sub-G1

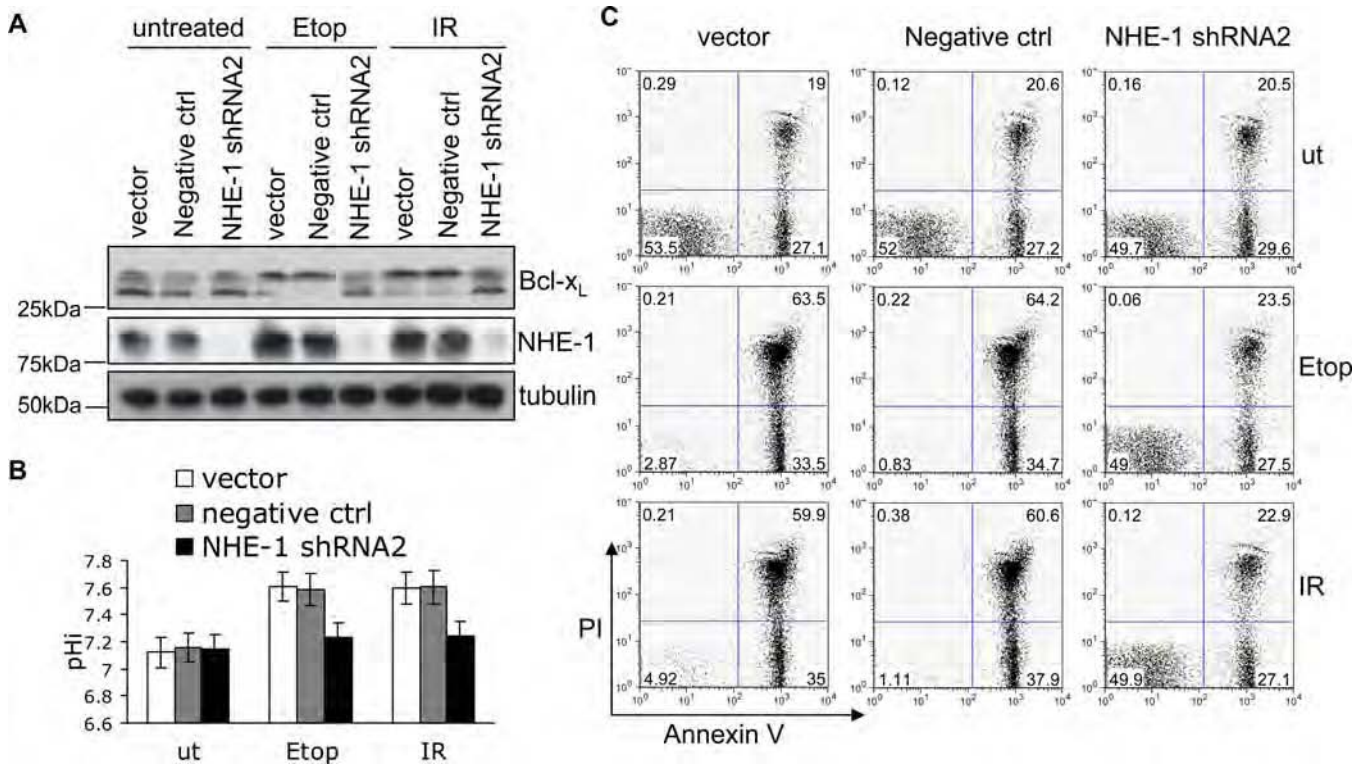


Figure 5. NHE-1 Knockdown Blocks DNA Damage-Induced Bcl-x_L Deamidation and Apoptosis

(A) Empty vector, negative control, or NHE-1shRNA2 were transduced into wild-type thymocytes, then treated with Etoposide (Etop) or irradiation (IR) prior to immunoblotting for NHE-1 and Bcl-x_L.

(B) Aliquots of the cells from (A) were analysed for pH_i. The histogram represents mean values \pm SD ($n = 3$).

(C) Aliquots of the cells from (A) were analysed for apoptosis by Annexin V/PI staining using flow cytometry, as illustrated in a representative experiment (total $n = 5$). The numbers shown are the percentage of cells in each quadrant. Histograms summarising the percentage of apoptotic cells (Annexin V⁺PI⁺) and dead cells (Annexin V⁺PI⁺) are shown in Figure 6B.

doi:10.1371/journal.pbio.0050001.g005

(apoptosis) values that were obtained either by DNA damage at physiological pH or by enforced alkalinisation without DNA damage. Conversely, incubation of B-CLL cells at lower pH inhibited DNA damage-induced Bcl-x_L deamidation and apoptosis (Figure 6B). Therefore with respect to enforced changes in pH_i, the B-CLL cells behaved in a comparable way to both murine thymocytes and tumour cells. A small increase in pH_i induced by incubation in alkaline buffer in the absence of induced DNA damage generated as much, if not more, Bcl-x_L deamidation and apoptosis as that triggered by genotoxic attack at physiological pH_e.

NHE-1 expression in response to DNA damage was investigated in a further six B-CLL patients. Figure 6C shows by immunoblotting (right panel) that there was some variation between patients, but that in all cases (left panel), etoposide caused increased NHE-1 expression by 3 h, achieving optimal values by 6–9 h ranging from 1.9-fold–2.6-fold over basal levels. These increases correlate with the observed increases in Bcl-x_L deamidation and apoptosis in patients' cells (Figure 6A) and at the 2.6-fold level, at least, are comparable with the increases observed in wild-type thymocytes (Figure 4B). Furthermore, DNA damage-induced Bcl-x_L deamidation in B-CLL cells was prevented by addition of either cycloheximide (CHX) (Figure S8C) or DMA (Figure S8D), establishing a possible linkage between DNA damage, NHE-1 function, and Bcl-x_L deamidation in human cancer cells.

Discussion

It has previously been suggested that Bcl-x_L deamidation is critical in the signalling pathway that leads from DNA damage to apoptosis [9]. This interpretation was based to a large degree on the observation that N52D/N66D Bcl-x_L, one of the species generated by deamidation, can no longer exert anti-apoptotic activity nor sequester the pro-apoptotic protein Bim. However, a secondary mutation in the N52D/N66D Bcl-x_L construct was later discovered, which, when corrected, restored binding, thereby casting doubt on the initial interpretation of the physiological significance of Bcl-x_L deamidation [13]. We now propose that the initial finding was correct, but for the wrong reason. Our results indicate that the major Bcl-x_L species generated by deamidation in situ is not Asp⁵²/Asp⁶⁶ but iso-Asp⁵²/iso-Asp⁶⁶, which is consistent with the well-established biochemistry of Asn deamidation [1], and that this species is unable to sequester Bim or Puma (Figure 2 and Figure S2). The introduction of iso-Asp into the disordered loop in which these residues are located is expected to cause greater conformational change than Asp, because of the redirection of the peptide backbone through β carboxyl groups, as indicated by the known structural and functional changes that occur in proteins upon conversion of Asn to iso-Asp residues [26,27]. The structural importance of protein iso-Asp residues is likewise underlined by the expression of the putative repair enzyme

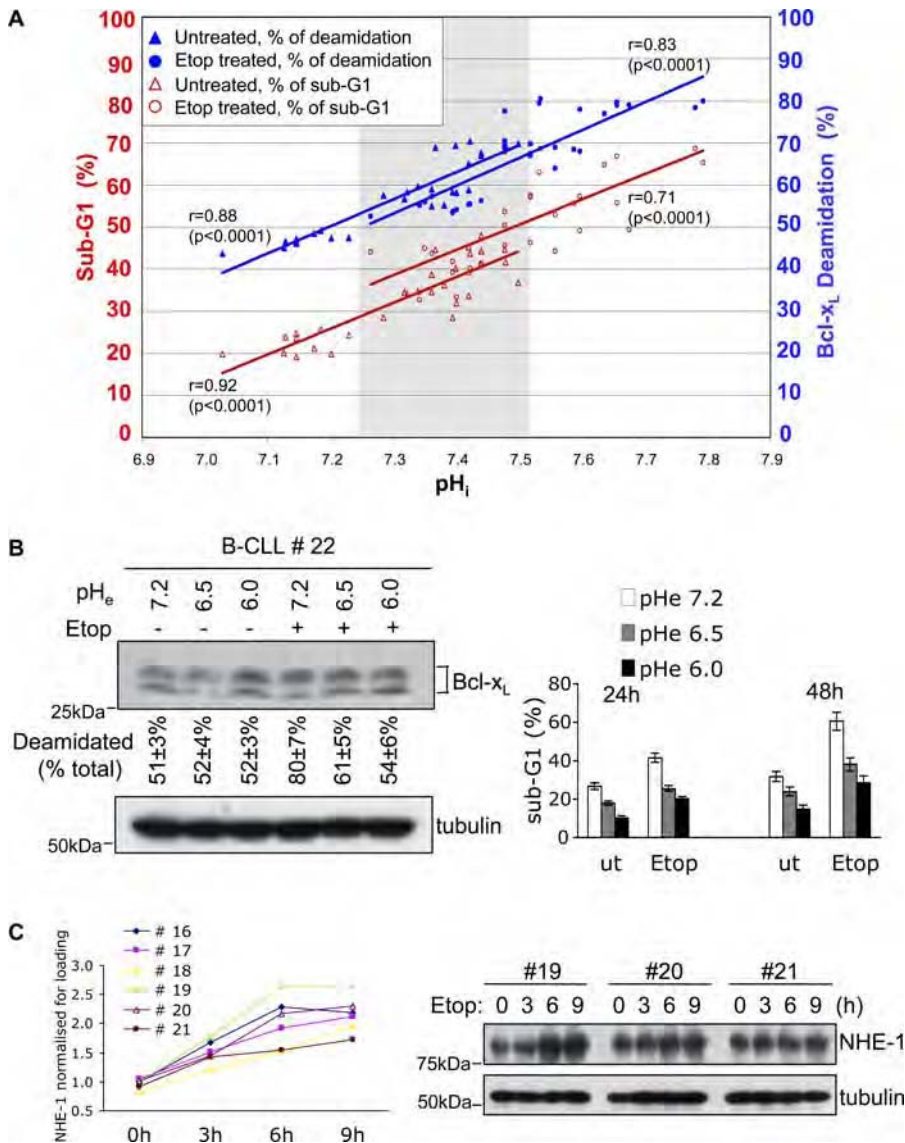


Figure 6. DNA Damage Induces NHE-1 Expression, and Enforced Alkalinisation Promotes Apoptosis of Human B-CLL cells

(A) Enforced alkalinisation of cancer cells from patients ($n = 10$) with B-CLL causes Bcl-x_L deamidation and associated cell death. Treatment with etoposide (Etop) *in vitro* further amplifies cell death. Patients' cells (PBMC, in the range 85%–95% CD19⁺B220⁺) were incubated at pH_e values of 7.2, 8.0, or 8.5, and the pH_i values were monitored by SNARF-1 staining using flow cytometry. Apoptosis was evaluated by measurement of sub-G1 peaks using flow cytometry. The data shows pooled results from ten patients via 30 values per treatment condition: due to identical values, some symbols overlap. The correlation coefficients (r) of deamidation or sub-G1 versus pH_i are shown for each treatment. The p value (significance) for each correlation is shown in parentheses. The correlation coefficients of sub-G1 versus deamidation are $r = 0.92$ ($p < 0.0001$) for untreated cells and $r = 0.87$ ($p < 0.0001$) for etoposide treated cells.

(B) Purified PBMC from B-CLL patients were cultured for 24 h in media at the pH shown, with/without etoposide for 48 h, and then analysed for Bcl-x_L deamidation by immunoblotting (left panel). The upper and lower bands were quantified and the upper deamidated Bcl-x_L band was expressed as a percentage of total Bcl-x_L. The percentages shown below each lane are means \pm SD ($n = 4$). The same cell aliquots cultured in RPMI/10% FCS for 24 h or 48 h were analysed for apoptosis by sub-G1 staining (right panel).

(C) Assessment of NHE-1 expression in B-CLL patients' samples following exposure to etoposide for the times shown. Representative immunoblotting results are shown for three patients in the right panel and the values for six patients (normalized for tubulin loading) are graphed in the left panel. doi:10.1371/journal.pbio.0050001.g006

L-isoaspartate O-methyltransferase which converts iso-Asp to Asp residues: its deletion has striking effects on protein functions [28–30]. Furthermore, comparison of the crystal structures of native rat Bcl-x_L with its deamidated version has revealed significant differences [10]; the structural implications of introducing iso-Asp residues into the disordered loop environment of Asn⁵²/Asn⁶⁶ merits further work.

We have identified critical elements in the signalling pathway leading from DNA damage to Bcl-x_L deamidation

in thymocytes and have shown, as Figure 7A illustrates, that deamidation is induced upon DNA damage by up-regulation of the NHE-1 antiporter and consequent intracellular alkalinisation (Figures 3–5). To the best of our knowledge, this represents the first description of a molecular mechanism for the regulation of protein internal Asn deamidation in cells. Our results are consistent with the failure, until now, to identify genes encoding internal protein Asn deamidases [1]. The regulation of NHE-1 antiporter function is complex,

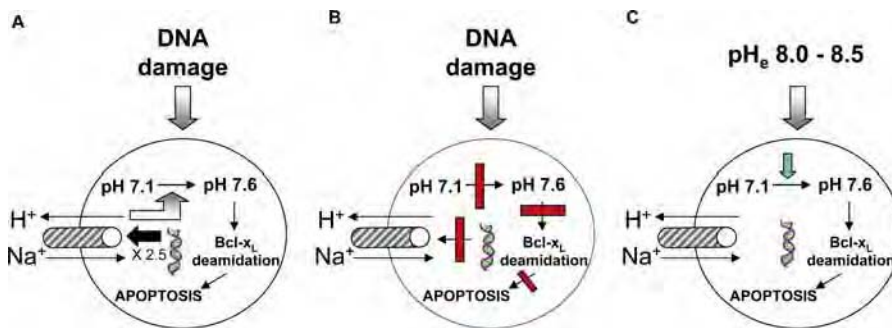


Figure 7. Models Illustrating the Linkage Between DNA Damage, the NHE-1 Antiporter, Alkalinisation, Bcl-x_L Deamidation, and Apoptosis in Wild-Type and Cancer Cells

(A) In wild-type thymocytes, DNA damage causes increased NHE-1 expression and a consequent rise in intracellular pH, Bcl-x_L deamidation, and apoptosis. (B) In pretumorigenic thymocytes expressing an OTK, the DNA damage-induced rise in NHE-1 expression is blocked, preventing alkalinisation, Bcl-x_L deamidation, and apoptosis. (C) Enforced alkalinisation of murine tumour cells, or human B-CLL cells, causes Bcl-x_L deamidation and subsequent apoptosis, even in the absence of external genotoxic attack.

doi:10.1371/journal.pbio.0050001.g007

involving modulation of its expression, phosphorylation, and binding of regulatory proteins [24,25,31]. Our data are consistent with a model in which DNA damage causes alkalinisation by a direct 2–3-fold increase in NHE-1 expression (Figures 4B and 6C), although we cannot exclude the possibility that undetected changes in phosphorylation might shift the pH dependence of the antiporter to a more alkaline range as described for myocardial tissue [32]. Furthermore, the calcineurin B homologous protein 1 (CHP-1) has been characterised as an essential cofactor for NHE-1 in normal tissues [33], whereas its CHP-2 homologue is up-regulated in transformed cells [34], so regulation of these proteins might also be involved in activation of the antiporter. Intracellular NHE-1 mediated alkalinisation has previously been implicated in the regulation of HL-60 cell apoptosis [35] and in apoptosis after trophic factor withdrawal [24]. In our present work, it is clear that the alkalinising effects of DNA damage can be mimicked simply by overexpressing NHE-1 on wild-type thymocytes in the absence of DNA damage (Figure 4C). Furthermore, either inhibition or depletion of the antiporter blocks DNA damage induced alkalinisation, Bcl-x_L deamidation, and apoptosis (Figures 4D, 5A–5C, and Figure S8D).

The direct role played by the deamidation of Bcl-x_L to its iso-Asp⁵²/iso-Asp⁶⁶ version in the signalling pathway from DNA damage to apoptosis is supported by the finding that either the N52D/N66D or N52A/N66A Bcl-x_L mutants, which still bind BH3-only proteins (Figure 2E), protect thymocytes from dying upon enforced intracellular alkalinisation (Figure 3G). An alternative hypothesis involves the generation of new BH3-only family members as a consequence of alkalinisation, which compete for binding to Bcl-x_L, thereby displacing Bim and Puma. However, such a hypothesis does not explain why the Bcl-x_L mutants that still bind BH3-only proteins retain their anti-apoptotic potency at high pH (Figure 3G).

The striking blockade in DNA damage-induced NHE-1 expression, alkalinisation, Bcl-x_L deamidation, and apoptosis noted in *CD45*^{−/−}*lck*^{F505} pretumorigenic thymocytes (Figures 3 and 4), together with the reversal of this blockade by enforced expression of NHE-1 (Figure 4C), provide strong support for the model illustrated in Figure 7B. The oncogenic hyperactive p56^{lck-Y505F} tyrosine kinase [15] must inhibit one

or more steps on the pathway from DNA damage to increased NHE-1 expression, a mechanism that is under active investigation. We have previously demonstrated in pretumorigenic thymocytes a tight correlation between inhibition of Bcl-x_L deamidation, resistance to DNA damage induced apoptosis, and oncogenesis, suggesting that the consequent accumulation of DNA-damaged thymocytes is critical in the transforming process [14,15]. It therefore seems conceivable that the OTK-induced inhibition of NHE-1 is likewise important in thymic transformation, and further in vivo work will be necessary to investigate this possibility.

The resistance to genotoxic attack by *CD45*^{−/−}*lck*^{F505} murine tumour cells correlates, as in their pretumorigenic counterparts, with the inhibition of DNA damage-induced NHE-1 antiporter expression, alkalinisation, Bcl-x_L deamidation, and apoptosis (Figure S7), which is an apparent example of “oncogene addiction”, whereby oncogene expression continues to be important for survival [36]. By contrast, DNA damage of human B-CLL cells, which should not express OTKs, triggered increased NHE-1 expression and apoptosis, achieving levels comparable with wild-type thymocytes (Figure 6C). However, enforced alkalinisation of either the murine (Figure S7) or human (Figure 6) cancer cells triggered significant increases in Bcl-x_L deamidation and apoptosis, even in the absence of genotoxic attack (Figure 7C). In the case of the B-CLL cells, we cannot yet exclude the possibility that the tight correlation observed between these events does not reflect causal efficacy, and further work will be necessary to elucidate this point. In any event, the key issue for cancer cell therapy in this context is not whether inhibition of Bcl-x_L deamidation is involved in the initial transforming process, but whether Bcl-x_L is the main prosurvival protein protecting the tumour cells from the normal consequences of DNA damage. An extensive literature suggests that Bcl-x_L does indeed play this role in many tumour types [37]. For example, the down-regulation of Bcl-x_L promoted the apoptosis of KARPAS-299 cells derived from a patient with anaplastic large cell lymphoma [38], and down-regulation of Bcl-x_L suppresses the tumourigenic potential of the causative NPM-ALK oncogenic fusion protein in vivo [39]. Knockdown of Bcl-x_L also significantly reduces the viability of pancreatic cancer cells to tumour necrosis factor α (TNF-α)– and

TNF- α - related apoptosis-inducing ligand (TRAIL)-mediated apoptosis by antitumour drugs [40]. Furthermore, Bcl-x_L deamidation is inhibited in hepatocellular carcinomas, which are highly resistant to genotoxic treatments [11]. Our findings therefore have potential relevance to cancer therapy, whereby enforced alkalinisation, perhaps by amplification of NHE-1 expression, would promote Bcl-x_L deamidation, thereby triggering apoptosis.

The pioneering work of Warburg [41] established that tumours display acidic extracellular pH, although more than half a century passed before it was clearly established that the intracellular pH of tumour cells is comparable with normal cells [42]. Warburg's legacy has included intermittent interest in the possibility of pH manipulation as a means to cancer therapy. Our findings not only establish that protein deamidation can be regulated by intracellular pH change in vivo, but they also suggest that strategies for pH manipulation in antineoplastic therapy should continue to receive attention, albeit for reasons different from those envisaged by Warburg.

Materials and Methods

Mice. All mice were bred and housed in specific pathogen-free conditions in the animal facility at The Babraham Institute, Cambridge, United Kingdom. The p56^{Lck-F505} (PLGF-A) transgenic mice [43] and the CD45^{-/-} and CD45^{-/-}lck^{F505} mice have been previously described [16].

Reagents and antibodies. Etoposide, CHX, DMA, PI, monensin, nigericin, and goat-anti-rat immunoglobulin-agarose were from Sigma (St. Louis, Missouri, United States); protein A-sepharose and protein G-sepharose were from Amersham (Uppsala, Sweden); SNARF-1 was from Molecular Probes (Eugene, Oregon, United States); Z-VAD-fmk was from Santa Cruz Biotechnology. The following antibodies were used for Western Blotting: Bim (559685) from Pharmingen (San Diego, California, United States); Bcl-x_L (610212) and NHE-1 (clone 54) from Transduction Lab (New Jersey, United States); Puma (ab9643) from Abcam (Cambridge, United Kingdom); Bax (06-499) and Bak (06-536) from Upstate (New York, United States); Caspase-9 (9504) from Cell Signaling (Beverly, Massachusetts, United States); phosphoserine detection kit from Calbiochem (Darmstadt, Germany); β actin and α tubulin from Sigma.

Recombinant Bcl-x_L analysis. Image clone (2823873) containing the sequence for human Bcl-x_L was obtained from the MRC gene service (United Kingdom). The DNA coding amino acids 1–196 (of 233) was amplified by PCR and cloned into pENTR/D-TOPO (Invitrogen, Carlsbad, California, United States). The DNA was sequenced and the insert subcloned into pDEST17 (coding for a hexa-histidine tag) and transformed into *Escherichia coli* expression host DE3 (Novagen, Madison, Wisconsin, United States). Recombinant Bcl-x_L (His^N terminal tagged) was expressed in *E. coli* and purified using Co²⁺ chelation beads so that rapid elution could be performed at pH 7.0 to prevent deamidation. After anion exchange purification, three peaks (A, B, and C) were collected. Aliquots (1 μ l) of each peak were desalted for mass spectrometric analysis by solid-phase microextraction on C4 Zip Tips (Millipore, Billerica, Massachusetts, United States) and the proteins eluted with 0.1% formic acid/50% aqueous acetonitrile (1 μ l) directly into a nanospray tip (Protana Engineering, Odense, Denmark). The nanospray tip was inserted into a nano-electrospray ion source (Protana Engineering) attached to a quadrupole time-of-flight (TOF) mass spectrometer (Qstar Pulsar i, Applied Biosystems-MDS Sciex, Foster City, California, United States) and full scan TOF spectra were acquired at an ionization potential of 900V for 5 min over the mass/charge (*m/z*) range of 500–2000 atomic mass units. The mass spectrometric data were averaged and deconvoluted using the Bayesian Protein Reconstruct function in BioAnalyst software (Applied Biosystems). For nickel precipitation, each rBcl-x_L species was added to C57BL/6 thymocyte lysates for 2 h at 4 °C at pH 7.2, and Ni²⁺ beads were used to precipitate the rBcl-x_L and complexed Bim.

Mass spectrometric analysis of Bcl-x_L peptides. Samples of native and base-treated rBcl-x_L (0.1 μ g/ μ l) were digested with chymotrypsin (sequencing grade, 10 ng/ μ l; Roche, Basel, Switzerland) in 0.1 M ammonium acetate pH 6.2 containing 0.1% octylglucoside for 16 h at

30 °C. These digestion conditions were chosen after careful optimisation to give good and consistent yields of the peptides SDVEENRTEAPEGTESEMETPSAINGNPSW (peptide 1) and HLAD-SPAVNGATGHSSSL (peptide 2), containing the putative deamidation sites N52 and N66, respectively, but without inducing further deamidation. Aliquots of the digestion mixtures were analysed by liquid chromatography mass spectrometry (LC-MS) on a quadrupole TOF mass spectrometer (Qstar pulsar i, Applied Biosystems-MDS Sciex), with online separation by reversed-phase nano-LC. Peptides were eluted from the column (0.075 mm \times 100 mm, Vydac C18) with a gradient of 5%–35% acetonitrile (containing 10 mM ammonium acetate pH 5.3) over 30 min at a flow rate of 250 nl/min. During the development phase of the methodology, the mass spectrometer was operated in MS/MS mode to conclusively identify the peptide digestion products and to confirm the sites of deamidation as N52 and N66. Once the identities of the peptides had been established, the mass spectrometer was operated in MS mode for subsequent analyses.

For relative quantification of specific peptides, peak areas were obtained from extracted ion chromatograms of the monoisotopic mass of the corresponding pseudomolecular ions. These were: 816.60 ([M+4H]⁴⁺ peptide 1), 816.85 ([M+4H]⁴⁺ peptide 1 deamidated), 574.28 ([M+3H]³⁺ peptide 2), and 574.61 ([M+3H]³⁺ peptide 2 deamidated). The chromatographic conditions used for the separation of the peptides in the LC-MS analyses were optimised so as to resolve the Asn, Asp, and iso-Asp forms of peptides 1 and 2. The Asp and iso-Asp forms of the two peptides were identified by spiking an aliquot of a digestion mixture with Asp- or iso-Asp-containing synthetic peptides prior to LC-MS.

DNA damage treatments. Freshly isolated thymocytes were irradiated with 10 Gy using a caesium source or treated with etoposide in DMSO at a concentration of 25 μ M for murine cells, or 50 μ M for B-CLL cells, for the times indicated. Carrier DMSO was added to control cells.

Immunoblotting and immunoprecipitation. Cells were lysed in 50 mM HEPES (pH 7.2), 150 mM NaCl, 1mM EDTA, 0.2% NP-40, and complete protease inhibitors. Cell lysates were resolved by standard Laemmli's SDS-PAGE (pH 8.8) unless otherwise stated. For immunoprecipitations: rat Bim antibody (Oncogene, San Diego, California, United States) was coated to goat-anti-rat immunoglobulin-agarose; rabbit Puma antibody was coated to protein A-sepharose; mouse NHE-1 antibody was coated to protein G-sepharose; rabbit Bcl-x_L antibody was coated to goat-anti-rabbit immunoglobulin-agarose. Lysates were precleared with the appropriate agarose. Quantification of immunoblots was carried out using a phosphorimager (Fuji FLA3000, <http://www.fujifilm.com>).

Intracellular pH measurement. Intracellular pH was measured using a standard ratiometric method with a pH-sensitive fluorophore SNARF-1 by flow cytometry [44]. Briefly, cells in phosphate-buffered saline (PBS) were loaded with 10 μ M SNARF-1 for 40 min at 37 °C, followed by washing and incubation in PBS at room temperature for 30 min prior to measurement of pH_i. pH calibration was carried out using high potassium buffer with 10 μ M nigericin. FACS data were analysed using Flowjo software to obtain the ratio based on the FI3/FI2 channels. It should be noted that SNARF-1 measurements provide the average pH_i of the intracellular environment in a cell population including, presumably, the contribution of acidified intracellular compartments. However, even if such compartments contribute slightly to the mean pH_i values measured, in this work, it is the change in pH_i that is most important. This point was also addressed by neutralising acidic compartments using monensin in some experiments.

Measurement of apoptosis. Cells were stained with 20 μ g/ml PI (with 50 μ g/ml RNase A) and analysed by flow cytometry, gating on the CD4⁺CD8⁺ subset as necessary. The sub-G1 peak was quantified as a measure of apoptosis. In addition, apoptosis was measured using the Annexin-V-Fluos Staining Kit (Roche) according to the protocol provided. To measure the percentage of dead cells, PI was used at 0.5 μ g/ml.

Generation of Bcl-x_L mutants. Mouse Bcl-x_L cDNA was kindly provided by S. Korsmeyer (Howard Hughes Medical Institute, Harvard Medical School, Boston, Massachusetts, United States). N52A-N66A and N52D-N66D mutants were made using the Quick-Change Site-Directed Mutagenesis Kit from Stratagene (La Jolla, California, United States) according to the instructions provided. The sequences of the constructs were confirmed by DNA sequencing.

Retroviral gene knockdown and overexpression. Murine CD4⁺CD8⁺ thymocytes were purified and cultured in the presence of interleukin-4 (IL-4) and PdBu as described [15]. The Suppressor-Retro kit was purchased from Imgenex (San Diego, California, United States), and NHE-1 shRNA sequences were designed using the "siRNA

tool” from the company’s website. Five selected sequences were cloned into pSuppressorRetro. The sequence of NHE-1 shRNA2 is 5'-GAAACAAAGCGCTCCATCAAC-3'. Retroviral production and infection were performed according to the protocol provided. For overexpression, NHE-1 or Bcl-x_L (wild-type, N52A-N66A, and N52D-N66D) cDNA were amplified with AccuPrime Pfx DNA polymerase (Invitrogen), and cloned into XhoI and EcoRI sites of the multiple cloning sites of the MigRI vector [45] upstream of an internal entry site followed by enhanced green fluorescent protein (EGFP). The sequences of the inserts were verified by DNA sequencing. The plasmids were transfected into ϕ NX cells using Lipofectamine (Invitrogen). Viral infection of CD4⁺CD8⁺ thymocytes was performed by spinoculation (1,200 g for 90 min at 30 °C). To achieve high efficiency of gene transduction, the infection was repeated every 24 h for 2–3 d. GFP-positive cells were sorted by flow cytometry using a FACSAria.

Bax, Bak double knockdown. The SureSilencing shRNA kit for Bax and Bak was purchased from SuperArray (Frederick, Maryland, United States). One plasmid from each kit was screened out for the best gene ablation efficiency by transient transfection. The shRNA sequence for Bax is TCAGGATCGTCCACCAAGAA, and the shRNA sequence for Bak is GGGCTTAGGACTTGGTTTGT. To enrich the cells transfected with both plasmids which express GFP, the GFP sequence in the shRNA:Bak plasmid was replaced by DsRed using the SmaI restriction site before GFP and the AgeI restriction site after GFP. ShRNA:Bax-GFP and shRNA:Bak-DsRed were cotransfected into primary thymocytes using the Amaxa mouse T cell nucleofactor kit (Amaxa Biosystems, Koeln, Germany). Cells positive for both GFP and DsRed were sorted by flow cytometry and used for subsequent experiments.

B-CLL patients’ cell purification. B-CLL donor peripheral blood was centrifuged through Lymphoprep (Axis-Shield PoC, Oslo, Norway), and the interphase peripheral blood mononuclear cells (PBMCs) were harvested for subsequent experiments. The purity of PBMCs was routinely checked by staining with antibodies CD3-Cy5, CD19-Fitc, and B220-PE and was analysed by flow cytometry.

Statistics. The Pearson coefficient of correlation (SPSS package, Chicago, Illinois, United States) was used to analyse the correlation between variables within the same group of data.

Supporting Information

Figure S1. DNA Damage-Induced Bcl-x_L Deamidation Correlates with the Kinetics of Thymic Apoptosis

(A) The membrane from Figure 1C was stripped and reprobed with caspase-9 antibody. Cleavage of caspase-9 following DNA damage was inhibited in Bax/Bak knock-down thymocytes.
(B) Wild-type thymocytes were cultured in RPMI-1640/10% bovine fetal calf serum with 25 μ M etoposide for the times shown, and aliquots of cells from each time point were stained with 7-AAD and analysed by flow cytometry to estimate the percentage of cells undergoing apoptosis (sub-G1 peak expressed as a % of total cells). The data illustrate a representative experiment and the mean values \pm SD from five independent experiments are quantified in (B) (blue bars).
(C) Aliquots of cells from the experiments shown in (A) were analysed for Bcl-x_L expression by immunoblotting, and the membrane was reprobed with tubulin (loading control). The upper bands (deamidated) and lower band (native) of Bcl-x_L were quantified using a phosphorimager, and the percentages of upper bands in comparison to the total (upper plus lower bands) were calculated. The mean values \pm SD from five independent experiments are shown in the histogram (red line).

Found at doi:10.1371/journal.pbio.0050001.sg001 (976 KB TIF).

Figure S2. Deamidation Disrupts the Sequestration of BH3-Only Proteins by Bcl-x_L

(A) Puma binds to the native but not deamidated form of Bcl-x_L. Either wild-type (1.5×10^7 , lanes 3 and 4) or pretumorigenic *CD45^{-/-}Lck^{F505}* thymocytes (1.5×10^7 , lanes 5 and 6) were treated as in Figure 2A, and cells were lysed and subjected to immunoprecipitation with Puma antibody, followed by blotting with either Bcl-x_L or Puma antibodies. Lane 1 is a wild-type thymocyte whole cell lysates (WCLs) control to facilitate comparison of native and deamidated forms of Bcl-x_L. The asterisk indicates the light chain of the Puma antibody used for immunoprecipitation.
(B) Deamidated Bcl-x_L from alkali treated thymocytes no longer binds to Bim. Wild-type thymocytes were incubated in neutral (pH 7.0) or

alkaline (pH 9.0) buffer at 37 °C for 24 h. Bim was immunoprecipitated from WCLs and WCL samples. Bim immunoprecipitates and Bim-depleted lysates were then separated and immunoblotted for either Bcl-x_L or Bim.

Found at doi:10.1371/journal.pbio.0050001.sg002 (944 KB TIF).

Figure S3. The Asp and iso-Asp Forms of Bcl-x_L Chymotryptic Peptides 1 and 2 Were Identified by Spiking an Aliquot of a Digestion Mixture with Asp- or iso-Asp-Containing Synthetic Peptides Before LC-MS

Peptides SDVEENRTEAPEGTESEMETPSAINGNPSW (peptide 1) and HLADSPAVNGATGHSSSL (peptide 2) and the corresponding deamidated forms, which contain the putative deamidation sites N52 and N66, respectively, were generated by digestion of rBcl-x_L with chymotrypsin. The chromatographic conditions used for the separation of the peptides in the LC-MS analyses were optimised so as to resolve the Asn, Asp, and iso-Asp forms of peptides 1 and 2. The Asp and iso-Asp forms of the two peptides were identified by spiking an aliquot of a digestion mixture with Asp- or iso-Asp-containing synthetic peptides prior to LC-MS as shown. The chromatograms show LC-MS analyses at time point 72 h of the rBcl-x_L base treatment.

Found at doi:10.1371/journal.pbio.0050001.sg003 (1.1 MB TIF).

Figure S4. DNA Damage-Induced NHE-1 Up-Regulation Is Mitochondrial Apoptosis-Independent

(A) Aliquots of the cells from Figure 1A incubated in the presence or absence of Z-VAD-fmk (200 μ M) were analysed for the expression of NHE-1 and tubulin (as loading control) by immunoblotting.
(B) Aliquots of the cells from Figure 1C were analysed for the expression of NHE-1 by immunoblotting. Tubulin was reprobed as loading control.

Found at doi:10.1371/journal.pbio.0050001.sg004 (645 KB TIF).

Figure S5. Thymocytes Treated with DMA or Transduced with NHE-1 siRNA Display a Survival Advantage In Vitro Following DNA Damage

(A) Purified double-negative (DN) thymocytes treated with/without DMA, etoposide, or irradiation were cultured in vitro. At 24 h, 48 h, or 72 h, an aliquot of cells was analysed by PI staining (0.5 μ g/ml) using flow cytometry; PI-positive cells represent dead cells.
(B) Purified DN thymocytes transduced with NHE-1 shRNA2 or empty vector were treated with or without etoposide and irradiation and then cultured in vitro. At 24 h, 48 h, or 72 h, an aliquot of cells was analysed as in (A).

Found at doi:10.1371/journal.pbio.0050001.sg005 (431 KB TIF).

Figure S6. Supplementary Information for NHE-1 Knockdown and Phosphorylation Analysis.

(A) Knockdown of NHE-1 by shRNA. NHE-1 shRNA (shRNA1–5), negative control, and empty vector were transduced into wild-type thymocytes. Immunoblotting for NHE-1 and tubulin showed that shRNA2 is the most potent shRNA2 inhibiting NHE-1 expression; soshRNA2 was used in subsequent experiments.
(B) The histograms summarise the percentage of apoptotic cells (Annexin V⁺PI⁺) and dead cells (Annexin V⁺PI⁺) from the experiment illustrated in Figure 5C. The data are means based on five independent experiments.
(C) The Ser phosphorylation of the NHE-1 antiport remains unchanged following DNA damage. Wild-type or *CD45^{-/-}Lck^{F505}* thymocytes were exposed to 5 Gy of irradiation and maintained in culture for the times shown. NHE-1 immunoprecipitates were then immunoblotted for p-Ser (16B4). The membrane was stripped and reprobed for total NHE-1. The histogram shows the relative quantification of p-Ser \pm SD from three independent experiments. Lane 1 was defined as 1 (*). Note that immunoblotting with one additional p-Ser antibody and two additional p-Thr antibodies gave comparable results to those shown here.

Found at doi:10.1371/journal.pbio.0050001.sg006 (1.0 MB TIF).

Figure S7. Primary Tumour Cells Are Resistant to DNA Damage-Induced Bcl-x_L Deamidation and Apoptosis, but Enforced Alkalinisation Overcomes this Resistance.

(A) DNA damage-induced Bcl-x_L deamidation is inhibited in *CD45^{-/-}Lck^{F505}* tumour cells. Wild-type, *CD45^{-/-}Lck^{F505}* pretumorigenic, and *CD45^{-/-}Lck^{F505}* tumour cells were either treated with etoposide for 24 h or exposed to 5 Gy of irradiation and then cultured for 24 h. Cells were lysed and subjected to immunoblotting for Bcl-x_L or tubulin (loading control).
(B) Intracellular alkalinisation and apoptosis induced by DNA

damage are both inhibited in *CD45*^{−/−}*Lck*^{F505} tumour cells. pH_i (upper panel) and apoptosis (lower panel) were analysed as in Figure 3A and Figure 1A.

(C) DNA damage causes up-regulation of NHE-1 in wild-type but not in *CD45*^{−/−}*Lck*^{F505} tumour cells. Wild-type thymocytes or *CD45*^{−/−}*Lck*^{F505} tumour cells were either treated with etoposide (Etop) for 5 h or exposed to 5 Gy of irradiation and then maintained in culture for 5 h, followed by immunoblotting for NHE-1 or tubulin. The histogram shows the quantification of NHE-1 expression from five independent experiments SD. Lane 3 was defined as 1(*).

(D) *CD45*^{−/−}*Lck*^{F505} tumour cells were cultured in the media with the pH_e as shown without monensin, treated with irradiation or etoposide, and analysed for Bcl-x_L deamidation by immunoblotting. The percentage deamidation was calculated as in Figure 1B.

(E) Aliquots of the cells used for (D) were assessed for pH_i.

(F) Aliquots of the cells used for (D) were assessed for apoptosis. The histograms represent mean values ± SD (*n* = 3).

(A) shows that Bcl-x_L deamidation following DNA damage was suppressed in primary tumour cells to the same extent as in pretumorigenic thymocytes 24 h after inducing DNA damage, although after 48 h, the inhibition of deamidation was somewhat less (68.1% ± 5.2% inhibition in tumour cells compared to 96.2% ± 3.8% in pretumorigenic thymocytes, unpublished data). Likewise, alkalisation (B, upper panel), apoptosis (B, lower panel) and increased NHE-1 expression (C) were all suppressed in tumour cells to nearly the same extent as in pretumorigenic thymocytes. Furthermore, in the absence of monensin, extracellular buffers at pH 8.0–8.5 forced pH_i values of 7.5–7.7 (E) triggering Bcl-x_L deamidation (D) and apoptosis (F). It is particularly striking that incubation in buffer at pH 8.0, for example, which achieves a pH_i value of 7.43, triggers 66.4% and 36.6% levels of Bcl-x_L deamidation and apoptosis, respectively, irrespective of whether, in addition, DNA damage was induced by etoposide or by γ irradiation. These results show that murine tumour cells resistant to genotoxic insult at physiological pH_i values can be sensitised to die by enforced alkalisation leading to Bcl-x_L deamidation.

Found at doi:10.1371/journal.pbio.0050001.sg007 (1.3 MB TIF).

Figure S8. Inhibition of NHE-1 Synthesis by CHX or Inhibition of NHE-1 Function by DMA in B-CLL Cells Blocks DNA Damage-Induced Bcl-x_L Deamidation

(A) Replotting of data from Figure 6A to show the absolute mean

values SD (*n* = 10) for Bcl-x_L deamidation (right panel) and apoptosis (left panel) obtained at each of the three extracellular pH values investigated. The numbers at the top of each bar represent the mean pH_i values measured in the cells incubated at the pH_e values shown. (B) A representative Bcl-x_L Western blot from the B-CLL samples analysed in Figure 6A is shown.

(C) B-CLL patients' PBMCs were treated with/without CHX, etoposide, and irradiation as in Figure 4A, 48 h later cells were subjected to immunoblotting for Bcl-x_L. A representative blot from four independent experiments is shown. Tubulin was reprobed as loading control.

(D) B-CLL patients' PBMCs were treated with/without DMA, etoposide, and irradiation as in Figure 4D, 48 h later cells were subjected to immunoblotting for Bcl-x_L. A representative blot from four independent experiments is shown. Tubulin was reprobed as loading control.

Found at doi:10.1371/journal.pbio.0050001.sg008 (1.2 MB TIF).

Accession Numbers

The GenBank (<http://www.ncbi.nlm.nih.gov/Genbank>) accession numbers for proteins discussed in this paper are: Bcl-x_L (BC019307), Bim (NM009754), NHE-1 (BC052708), and Puma (U82987).

Acknowledgments

We are grateful to the late Professor S. Korsmeyer for the provision of a reagent, to Cindy Webb for animal husbandry, to Geoff Morgan for help with the FACS facility, to Anne Segonds-Pichon for advice in statistical analysis, and to Klaus Okkenhaug for suggestions on the manuscript.

Author contributions. RZ and DRA conceived and designed the experiments. RZ, DO, and TSS performed the experiments. RZ, DO, and TSS analyzed the data. GAF and ARG contributed reagents/materials/analysis tools. DRA wrote the paper.

Funding. Financial support was provided by the Biotechnology and Biological Sciences Research Council and Association for International Cancer Research.

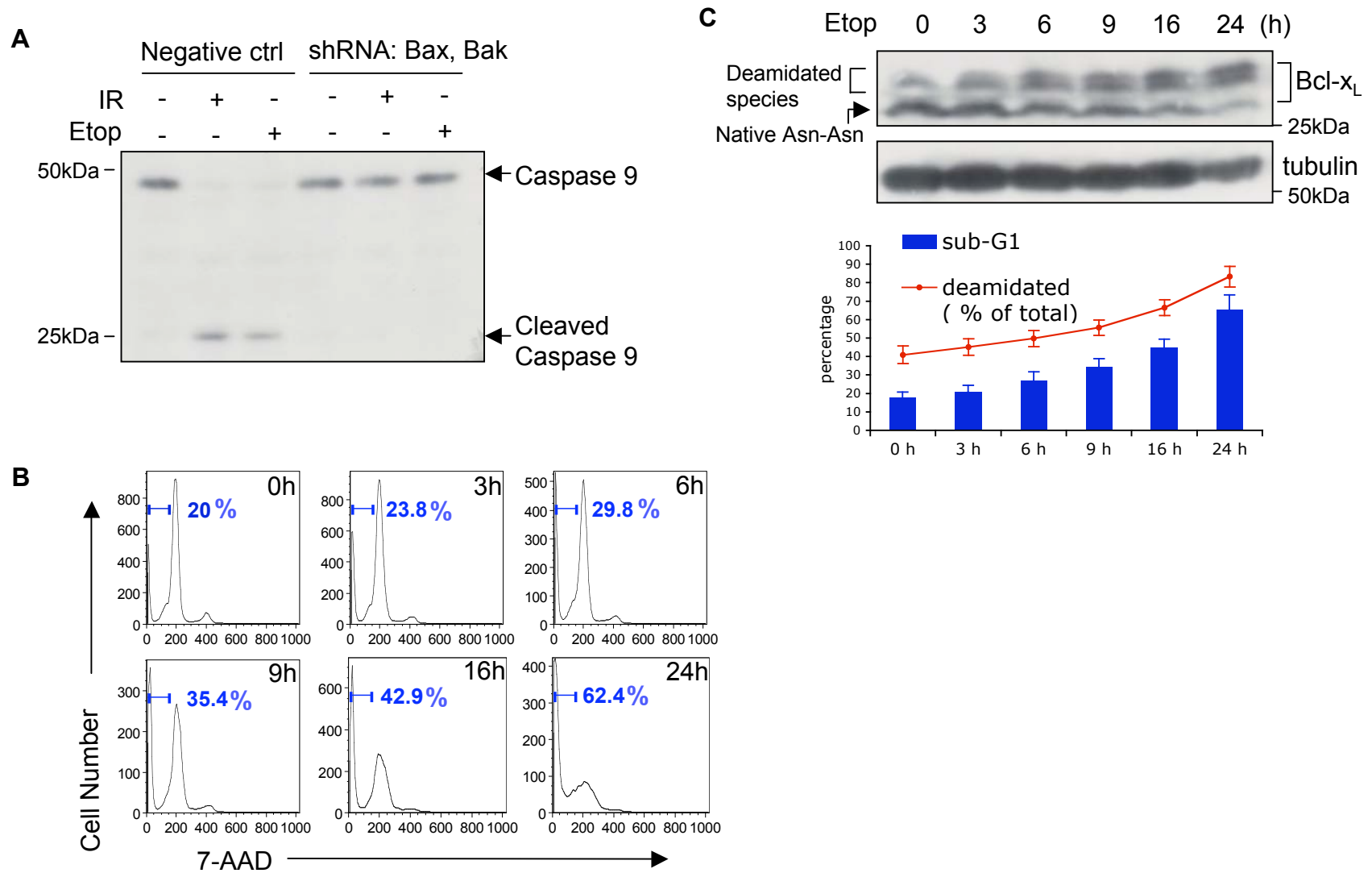
Competing interests. The authors have declared that no competing interests exist.

References

- Robinson NE, Robinson AB (2004) Molecular clocks: Deamidation of asparaginyl and glutaminyl residues in peptides and proteins. Cave Junction (Oregon): Althouse Press, 419 p.
- Chao X, Muff TJ, Park SY, Zhang S, Pollard AM, et al. (2006) A receptor-modifying deamidase in complex with a signaling phosphatase reveals reciprocal regulation. *Cell* 124: 561–571.
- Robinson NE (2002) Protein deamidation. *Proc Natl Acad Sci U S A* 99: 5283–5288.
- Robinson NE, Robinson ZW, Robinson BR, Robinson AL, Robinson JA, et al. (2004) Structure-dependent nonenzymatic deamidation of glutaminyl and asparaginyl pentapeptides. *J Pept Res* 63: 426–436.
- Moss CX, Matthews SP, Lamont DJ, Watts C (2005) Asparagine deamidation perturbs antigen presentation on class II MHC molecules. *J Biol Chem* 280: 18,498–18,503.
- Hanson SR, Hasan A, Smith DL, Smith JB (2000) The major in vivo modifications of the human water-insoluble lens crystallins are disulfide bonds, deamidation, methionine oxidation and backbone cleavage. *Exp Eye Res* 71: 195–207.
- Hoffmann C, Pop M, Leemhuis J, Schirmer J, Aktories K, et al. (2004) The *Yersinia pseudotuberculosis* cytotoxic necrotizing factor (CNFY) selectively activates RhoA. *J Biol Chem* 279: 16026–16032.
- Aswad DW, Paranandi MV, Schurter BT (2000) Isoaspartate in peptides and proteins: Formation, significance, and analysis. *J Pharm Biomed Anal* 21: 1129–1136.
- Deverman BE, Cook BL, Manson SR, Niederhoff RA, Langer EM, et al. (2002) Bcl-x_L deamidation is a critical switch in the regulation of the response to DNA damage. *Cell* 111: 51–62.
- Aritomi M, Kunishima N, Inohara N, Ishibashi Y, Ohta S, et al. (1997) Crystal structure of rat Bcl-x_L. Implications for the function of the Bcl-2 protein family. *J Biol Chem* 272: 27886–27892.
- Takehara T, Takahashi H (2003) Suppression of Bcl-x_L deamidation in human hepatocellular carcinomas. *Cancer Res* 63: 3054–3057.
- Chang CY, Lin YM, Lee WP, Hsu HH, Chen EI (2006) Involvement of Bcl-X(L) deamidation in E1A-mediated cisplatin sensitization of ovarian cancer cells. *Oncogene* 25: 2656–2665.
- Deverman BE, Cook BL, Manson SR, Niederhoff RA, Langer EM, et al. (2003) Erratum: Bcl-x_L deamidation is a critical switch in the regulation of the response to DNA damage. *Cell* 115: 503.
- Alexander DR (2004) Oncogenic tyrosine kinases, DNA repair and survival: The role of Bcl-x(L) deamidation in transformation and genotoxic therapies. *Cell Cycle* 3: 584–587.
- Zhao R, Yang FT, Alexander DR (2004) An oncogenic tyrosine kinase inhibits DNA repair and DNA damage-induced Bcl-x_L deamidation in T cell transformation. *Cancer Cell* 5: 37–49.
- Baker M, Gamble J, Tooze R, Higgins D, Yang FT, et al. (2000) Development of T-leukaemias in CD45 tyrosine phosphatase-deficient mutant lck mice. *EMBO J* 19: 4644–4654.
- Lindsten T, Thompson CB (2006) Cell death in the absence of Bax and Bak. *Cell Death Differ* 13: 1272–1276.
- Cheng EH, Wei MC, Weiler S, Flavell RA, Mak TW, et al. (2001) BCL-2, BCL-X(L) sequester BH3 domain-only molecules preventing BAX- and BAK-mediated mitochondrial apoptosis. *Mol Cell* 8: 705–711.
- Villunger A, Michalak EM, Coultas L, Mullauer F, Bock G, et al. (2003) p53- and drug-induced apoptotic responses mediated by BH3-only proteins puma and noxa. *Science* 302: 1036–1038.
- Jeffers JR, Parganas E, Lee Y, Yang C, Wang J, et al. (2003) Puma is an essential mediator of p53-dependent and -independent apoptotic pathways. *Cancer Cell* 4: 321–328.
- Mollenhauer HH, Morre DJ, Rowe LD (1990) Alteration of intracellular traffic by monensin; mechanism, specificity and relationship to toxicity. *Biochim Biophys Acta* 1031: 225–246.
- Lagadic-Gossmann D, Huc L, Lecureur V (2004) Alterations of intracellular pH homeostasis in apoptosis: Origins and roles. *Cell Death Differ* 11: 953–961.
- Tsao N, Lei HY (1996) Activation of the Na⁺/H⁺ antiporter, Na⁺/HCO₃[−]/CO₃^{2−} cotransporter, or Cl[−]/HCO₃[−] exchanger in spontaneous thymocyte apoptosis. *J Immunol* 157: 1107–1116.
- Khaled AR, Moor AN, Li A, Kim K, Ferris DK, et al. (2001) Trophic factor withdrawal: p38 mitogen-activated protein kinase activates NHE1, which induces intracellular alkalization. *Mol Cell Biol* 21: 7545–7557.
- Putney LK, Denker SP, Barber DL (2002) The changing face of the Na⁺/H⁺ exchanger, NHE1: Structure, regulation, and cellular actions. *Annu Rev Pharmacol Toxicol* 42: 527–552.

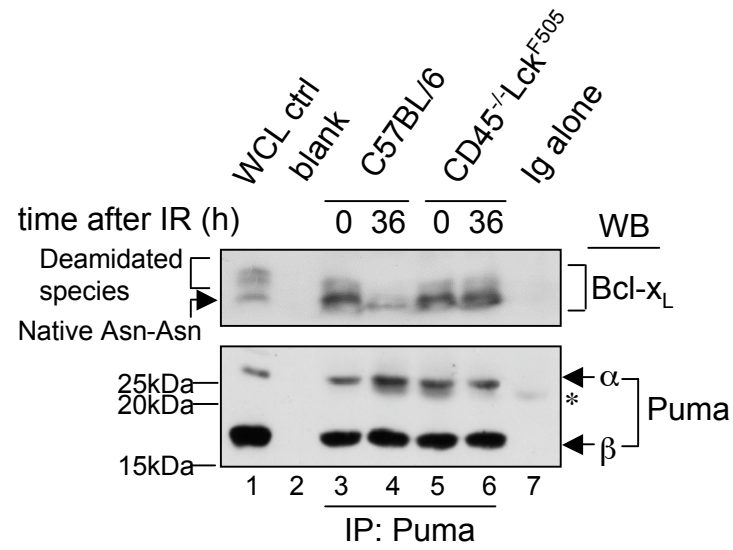
26. Capasso S, Di Donato A, Esposito L, Sica F, Sorrentino G, et al. (1996) Deamidation in proteins: The crystal structure of bovine pancreatic ribonuclease with an isoaspartyl residue at position 67. *J Mol Biol* 257: 492–496.
27. Noguchi S, Miyawaki K, Satow Y (1998) Succinimide and isoaspartate residues in the crystal structures of hen egg-white lysozyme complexed with tri-N-acetylchitotriose. *J Mol Biol* 278: 231–238.
28. Kim E, Lowenson JD, MacLaren DC, Clarke S, Young SG (1997) Deficiency of a protein-repair enzyme results in the accumulation of altered proteins, retardation of growth, and fatal seizures in mice. *Proc Natl Acad Sci U S A* 94: 6132–6137.
29. Young AL, Carter WG, Doyle HA, Mamula MJ, Aswad DW (2001) Structural integrity of histone H2B in vivo requires the activity of protein L-isoaspartate O-methyltransferase, a putative protein repair enzyme. *J Biol Chem* 276: 37161–37165.
30. Reissner KJ, Aswad DW (2003) Deamidation and isoaspartate formation in proteins: Unwanted alterations or surreptitious signals? *Cell Mol Life Sci* 60: 1281–1295.
31. Slepko E, Fliegel L (2002) Structure and function of the NHE1 isoform of the Na⁺/H⁺ exchanger. *Biochem Cell Biol* 80: 499–508.
32. Fliegel L (2001) Regulation of myocardial Na⁺/H⁺ exchanger activity. *Basic Res Cardiol* 96: 301–305.
33. Pang T, Su X, Wakabayashi S, Shigekawa M (2001) Calcineurin homologous protein as an essential cofactor for Na⁺/H⁺ exchangers. *J Biol Chem* 276: 17367–17372.
34. Pang T, Wakabayashi S, Shigekawa M (2002) Expression of calcineurin B homologous protein 2 protects serum deprivation-induced cell death by serum-independent activation of Na⁺/H⁺ exchanger. *J Biol Chem* 277: 43771–43777.
35. Zhu WH, Loh TT (1995) Effects of Na⁺/H⁺ antiport and intracellular pH in the regulation of HL-60 cell apoptosis. *Biochim Biophys Acta* 1269: 122–128.
36. Jonkers J, Berns A (2004) Oncogene addiction: Sometimes a temporary slavery. *Cancer Cell* 6: 535–538.
37. Amundson SA, Myers TG, Scudiero D, Kitada S, Reed JC, et al. (2000) An informatics approach identifying markers of chemosensitivity in human cancer cell lines. *Cancer Res* 60: 6101–6110.
38. Zamo A, Chiarle R, Piva R, Howes J, Fan Y, et al. (2002) Anaplastic lymphoma kinase (ALK) activates Stat3 and protects hematopoietic cells from cell death. *Oncogene* 21: 1038–1047.
39. Coluccia AM, Perego S, Cleris L, Gunby RH, Passoni L, et al. (2004) Bcl-XL downregulation suppresses the tumorigenic potential of NPM/ALK in vitro and in vivo. *Blood* 103: 2787–2794.
40. Bai J, Sui J, Demirjian A, Vollmer CM Jr., Marasco W, et al. (2005) Predominant Bcl-XL knockdown disables antiapoptotic mechanisms: Tumor necrosis factor-related apoptosis-inducing ligand-based triple chemotherapy overcomes chemoresistance in pancreatic cancer cells in vitro. *Cancer Res* 65: 2344–2352.
41. Warburg O (1930) *The metabolism of tumours*: London: Constable Press. 327 p.
42. Griffiths JR (1991) Are cancer cells acidic? *Br J Cancer* 64: 425–427.
43. Abraham KM, Levin SD, Marth JD, Forbush KA, Perlmutter RM (1991) Delayed thymocyte development induced by augmented expression of p56lck. *J Exp Med* 173: 1421–1432.
44. Chow S, Hedley D, Tannock I (1996) Flow cytometric calibration of intracellular pH measurements in viable cells using mixtures of weak acids and bases. *Cytometry* 24: 360–367.
45. He X, Dave VP, Zhang Y, Hua X, Nicolas E, et al. (2005) The zinc finger transcription factor Th-POK regulates CD4 versus CD8 T-cell lineage commitment. *Nature* 433: 826–833.

Supplementary Figure 1

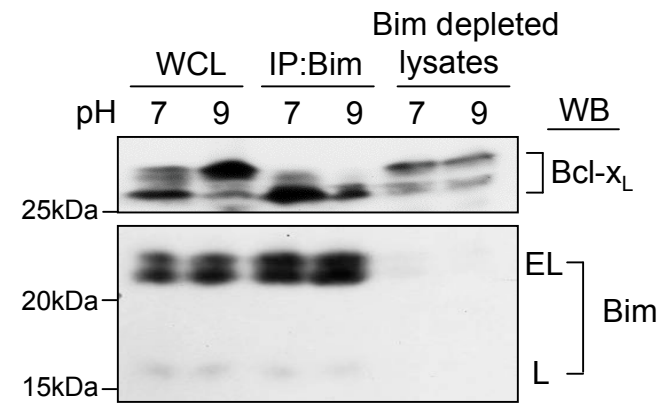


Supplementary Figure 2

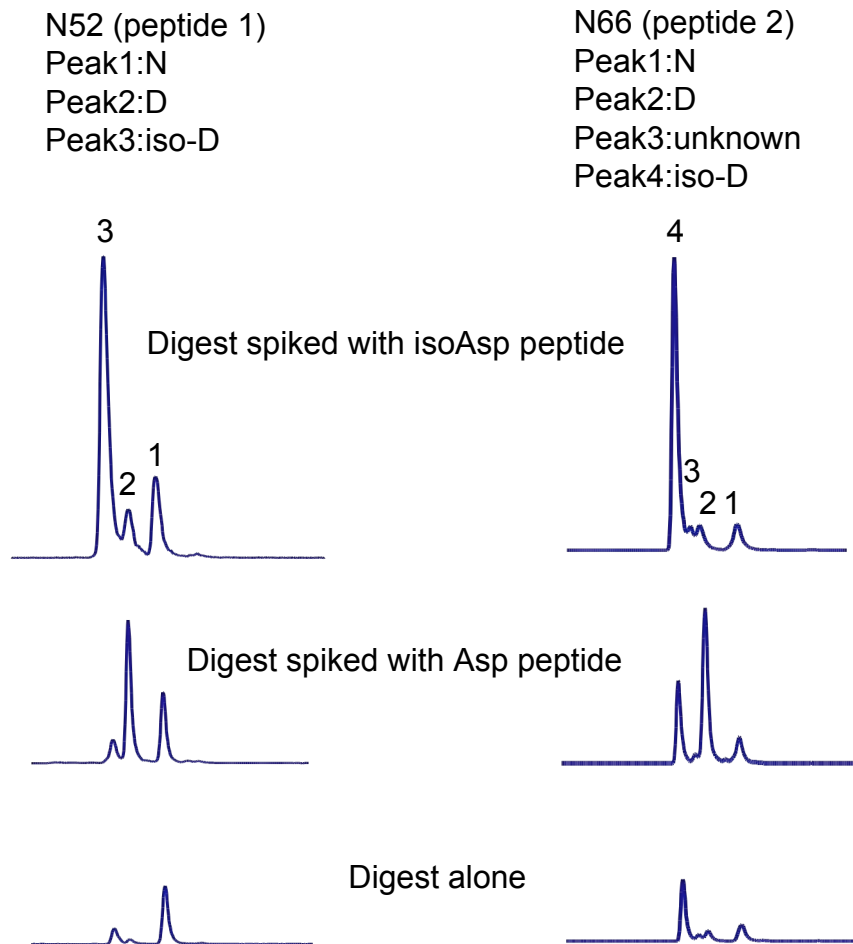
A



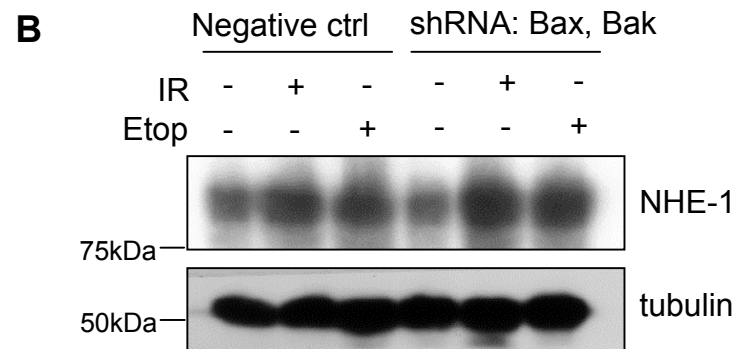
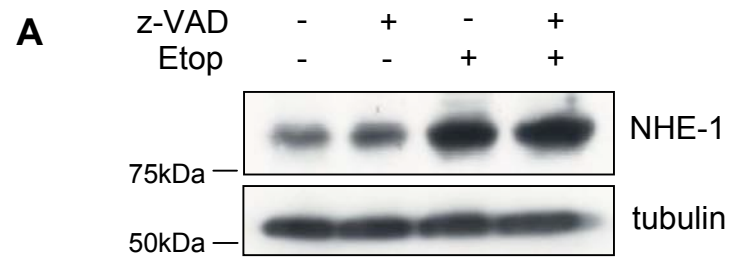
B



Supplementary Figure 3

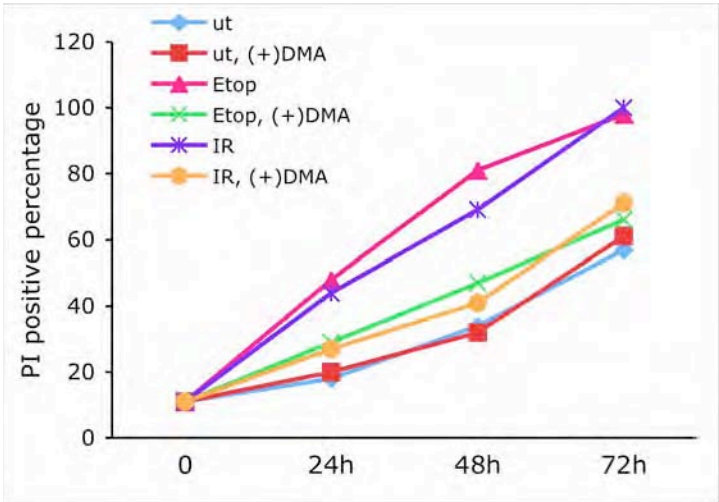


Supplementary Figure 4

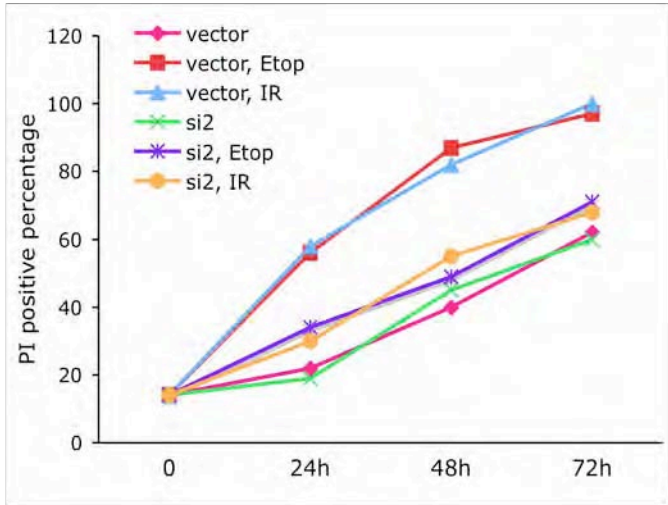


Supplementary Figure 5

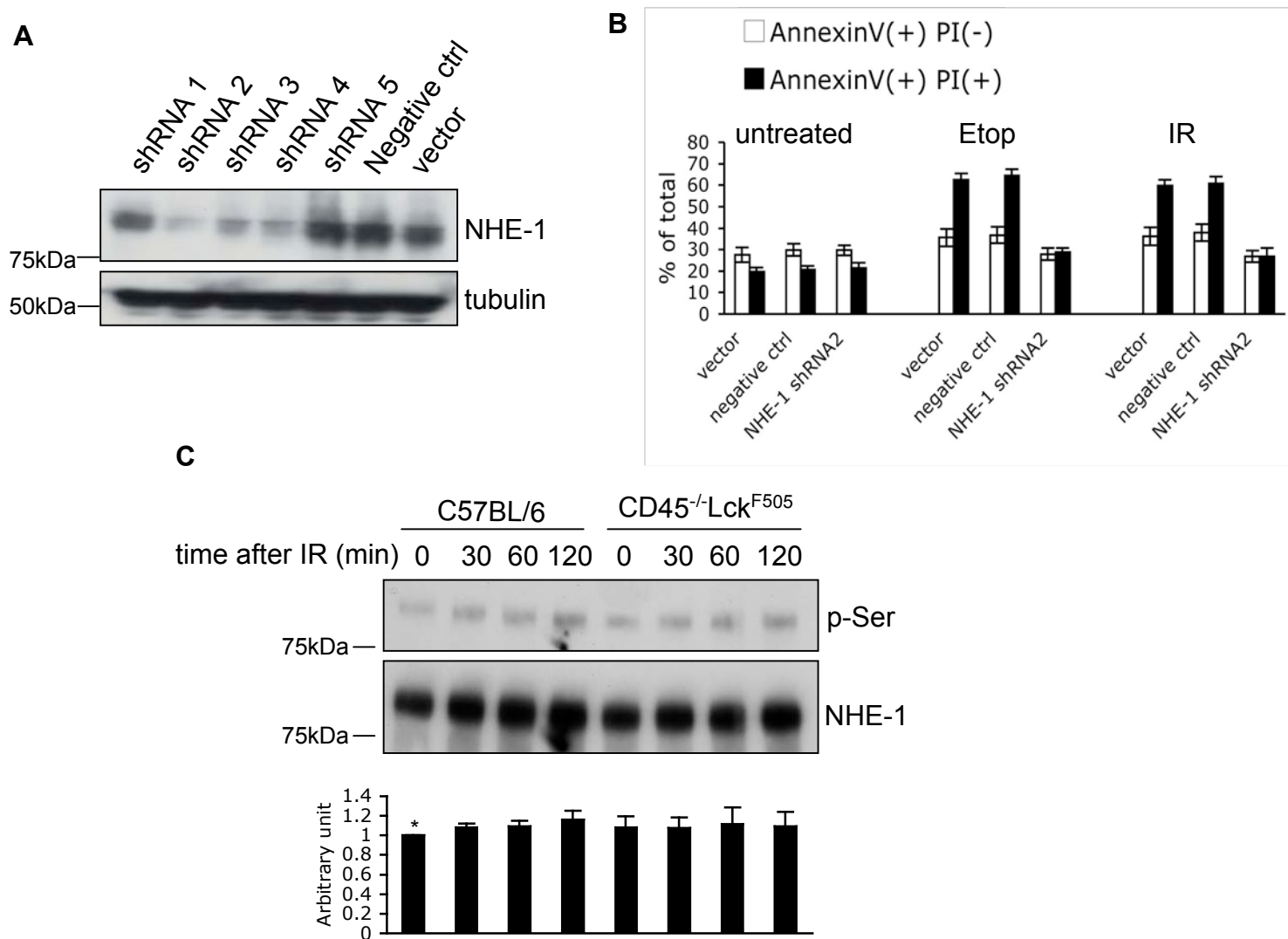
A



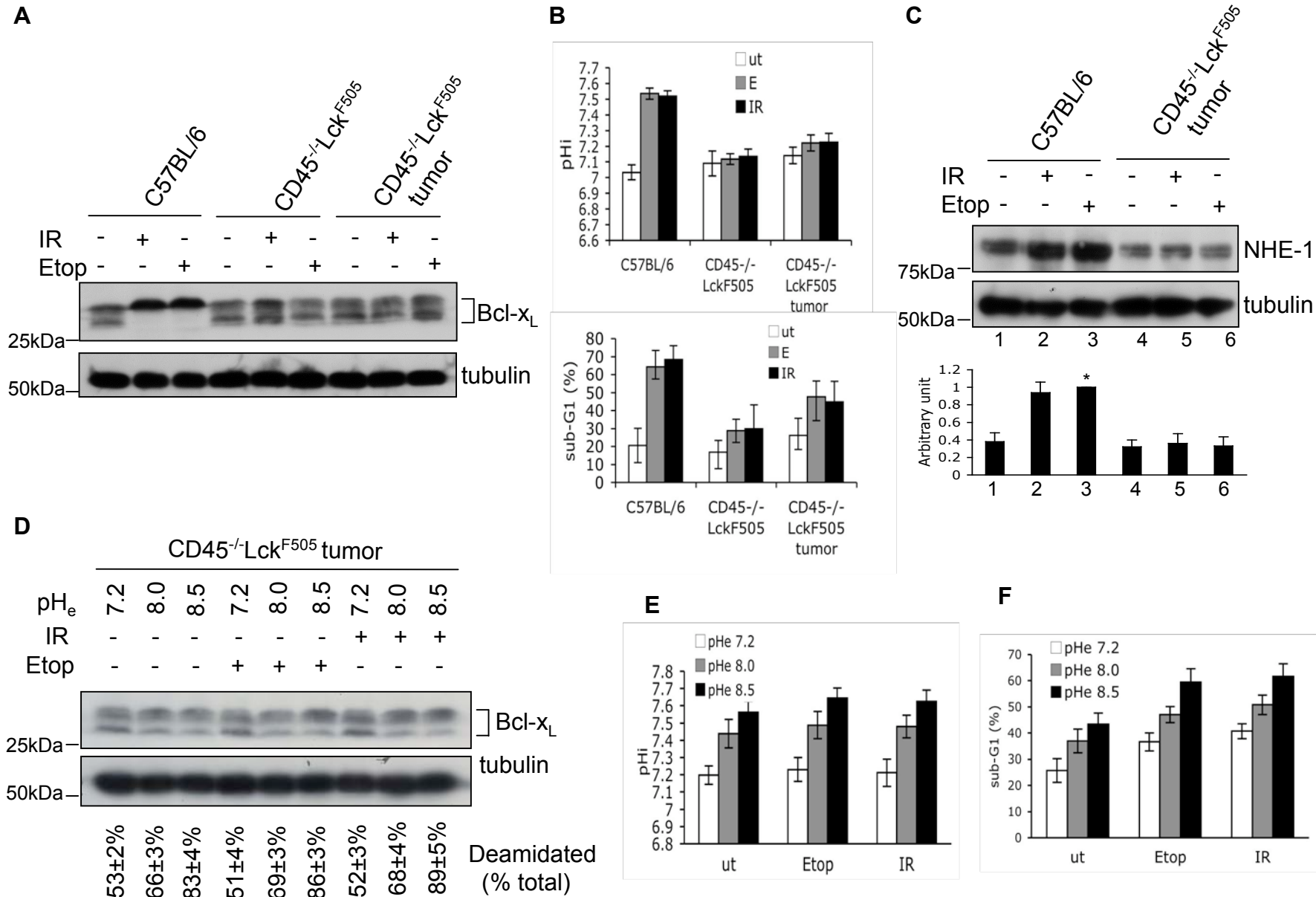
B



Supplementary Figure 6

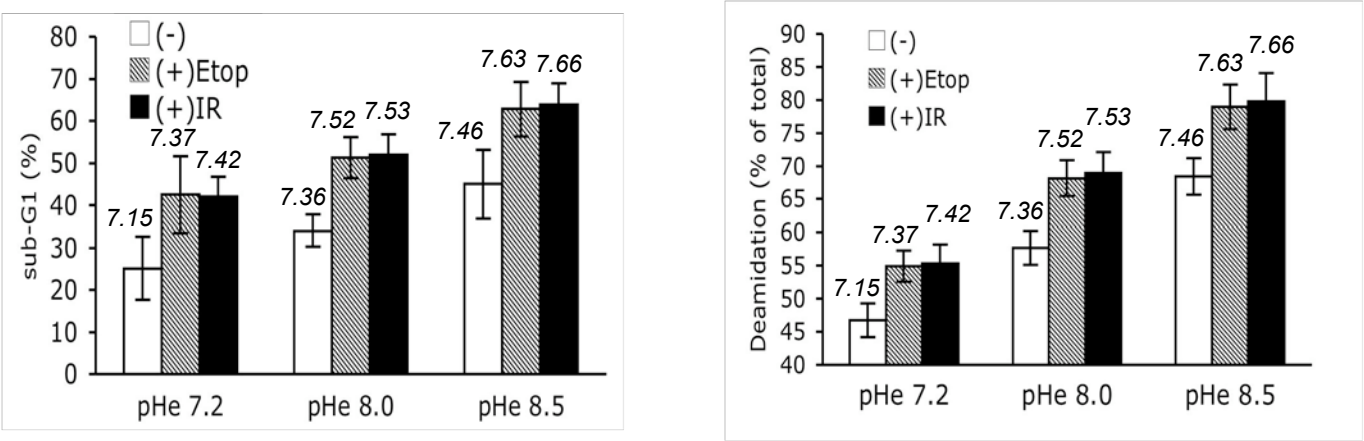


Supplementary Figure 7

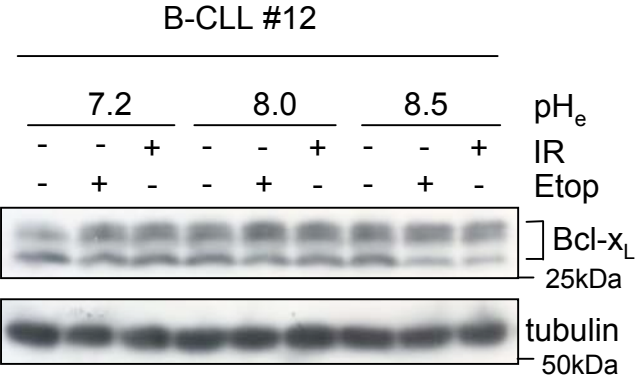


Supplementary Figure 8

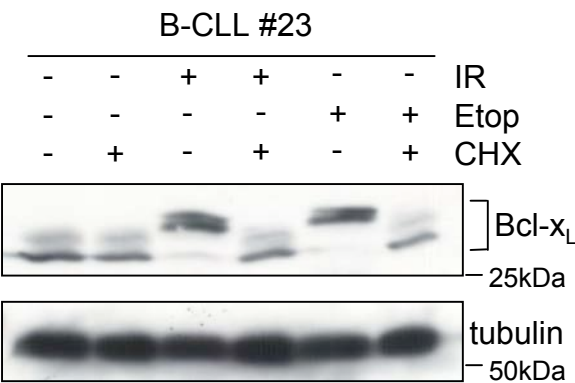
A



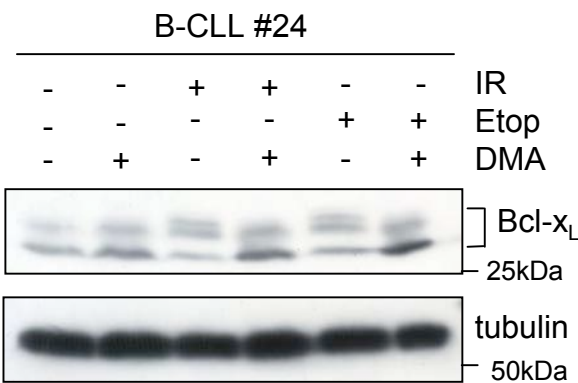
B



C



D



ORIGINAL ARTICLE

Inhibition of the Bcl-x_L Deamidation Pathway in Myeloproliferative Disorders

Rui Zhao, M.D., George A. Follows, M.R.C.P., M.R.C.Path.,
Philip A. Beer, M.R.C.P., M.R.C.Path., Linda M. Scott, Ph.D.,
Brian J.P. Huntly, M.R.C.P., M.R.C.Path., Anthony R. Green, F.R.C.Path., F.Med.Sci.,
and Denis R. Alexander, Ph.D.

ABSTRACT

BACKGROUND

From the Laboratory of Lymphocyte Signalling and Development, Babraham Institute (R.Z., D.R.A.), and the Cambridge Institute for Medical Research, Addenbrooke's Hospital (G.A.F., P.A.B., L.M.S., B.J.P.H., A.R.G.), University of Cambridge, Cambridge, United Kingdom. Address reprint requests to Dr. Zhao at the Laboratory of Lymphocyte Signalling and Development, Babraham Institute, Cambridge CB2 4AT, United Kingdom, or at rui.zhao@bbsrc.ac.uk; or to Dr. Green at the Cambridge Institute for Medical Research, Hills Rd., Cambridge CB2 2XY, United Kingdom, or at arg1000@cam.ac.uk.

Drs. Green and Alexander contributed equally to this article.

N Engl J Med 2008;359:2778-89.
Copyright © 2008 Massachusetts Medical Society.

The myeloproliferative disorders are clonal disorders with frequent somatic gain-of-function alterations affecting tyrosine kinases. In these diseases, there is an increase in DNA damage and a risk of progression to acute leukemia. The molecular mechanisms in myeloproliferative disorders that prevent apoptosis induced by damaged DNA are obscure.

METHODS

We searched for abnormalities of the proapoptotic Bcl-x_L deamidation pathway in primary cells from patients with chronic myeloid leukemia (CML) or polycythemia vera, myeloproliferative disorders associated with the BCR-ABL fusion kinase and the Janus tyrosine kinase 2 (JAK2) V617F mutation, respectively.

RESULTS

The Bcl-x_L deamidation pathway was inhibited in myeloid cells, but not T cells, in patients with CML or polycythemia vera. DNA damage did not increase levels of the amiloride-sensitive sodium-hydrogen exchanger isoform 1 (NHE-1), intracellular pH, Bcl-x_L deamidation, and apoptosis. Inhibition of the pathway was reversed by enforced alkalization or overexpression of NHE-1, leading to a restoration of apoptosis. In patients with CML, the pathway was blocked in CD34+ progenitor cells and mature myeloid cells. Imatinib or JAK2 inhibitors reversed inhibition of the pathway in cells from patients with CML and polycythemia vera, respectively, but not in cells from a patient with resistance to imatinib because of a mutation in the BCR-ABL kinase domain.

CONCLUSIONS

BCR-ABL and mutant JAK2 inhibit the Bcl-x_L deamidation pathway and the apoptotic response to DNA damage in primary cells from patients with CML or polycythemia vera.

CHRONIC MYELOID LEUKEMIA (CML) AND polycythemia vera are clonal myeloproliferative disorders that are associated with the activation of distinct tyrosine kinases, the BCR-ABL fusion kinase¹ and the Janus tyrosine kinase 2 (JAK2) mutation,^{2,3} respectively. In both disorders, patients usually present with chronic disease, which is readily controlled. However, for reasons that are unclear, both diseases carry a risk of progression to a blastic phase resembling acute leukemia that resists further therapy. The cellular prosurvival protein Bcl-x_L is up-regulated in patients with CML and polycythemia vera and is thought to inhibit apoptosis.⁴⁻⁷ Moreover, BCR-ABL protein expression is associated with a reduced apoptotic response to genotoxic drugs,⁸ and quiescent CML stem cells, thought to be responsible for residual disease, are resistant to the apoptosis that tyrosine kinase inhibitors induce.⁹⁻¹¹

A pathway regulating the function of Bcl-x_L has been described in several studies.¹²⁻¹⁴ In normal mouse thymocytes, DNA damage increases the activity of the amiloride-sensitive sodium-hydrogen exchanger isoform 1 (NHE-1), thus raising the intracellular pH, which in turn causes nonenzymatic deamidation of Bcl-x_L. In this context, the importance of deamidation (the removal of an amide functional group from an organic compound) is due to its conversion of the amino acid asparagine into isoaspartic acid. Such an alteration reduces the ability of the antiapoptotic Bcl-x_L protein to sequester and inhibit the Bcl-2 homology 3 (BH3)-only family of proapoptotic proteins, thereby promoting apoptosis. A link with tumorigenesis was suggested by the observation that the normal response of the NHE-1-Bcl-x_L pathway to DNA damage was abolished in a mouse model of T-cell lymphoma.^{13,14} Thymocytes that were transformed by an activated Lck tyrosine kinase were unable to respond to DNA damage by increasing NHE-1 levels, Bcl-x_L deamidation, or apoptosis. Inhibition of the NHE-1-Bcl-x_L pathway does not appear to be a general feature of cancer, since Bcl-x_L deamidation that is induced by damaged DNA is intact in cell lines of osteosarcoma and cervical, bladder, and ovarian cancers^{12,15} and in primary chronic lymphocytic leukemia cells.¹⁴ Because the relevance of Bcl-x_L deamidation for human cancers associated with activated tyrosine kinases remains unclear, we examined the Bcl-x_L deamidation pathway in cells from patients with CML and polycythemia vera.

METHODS

REAGENTS AND ANTIBODIES

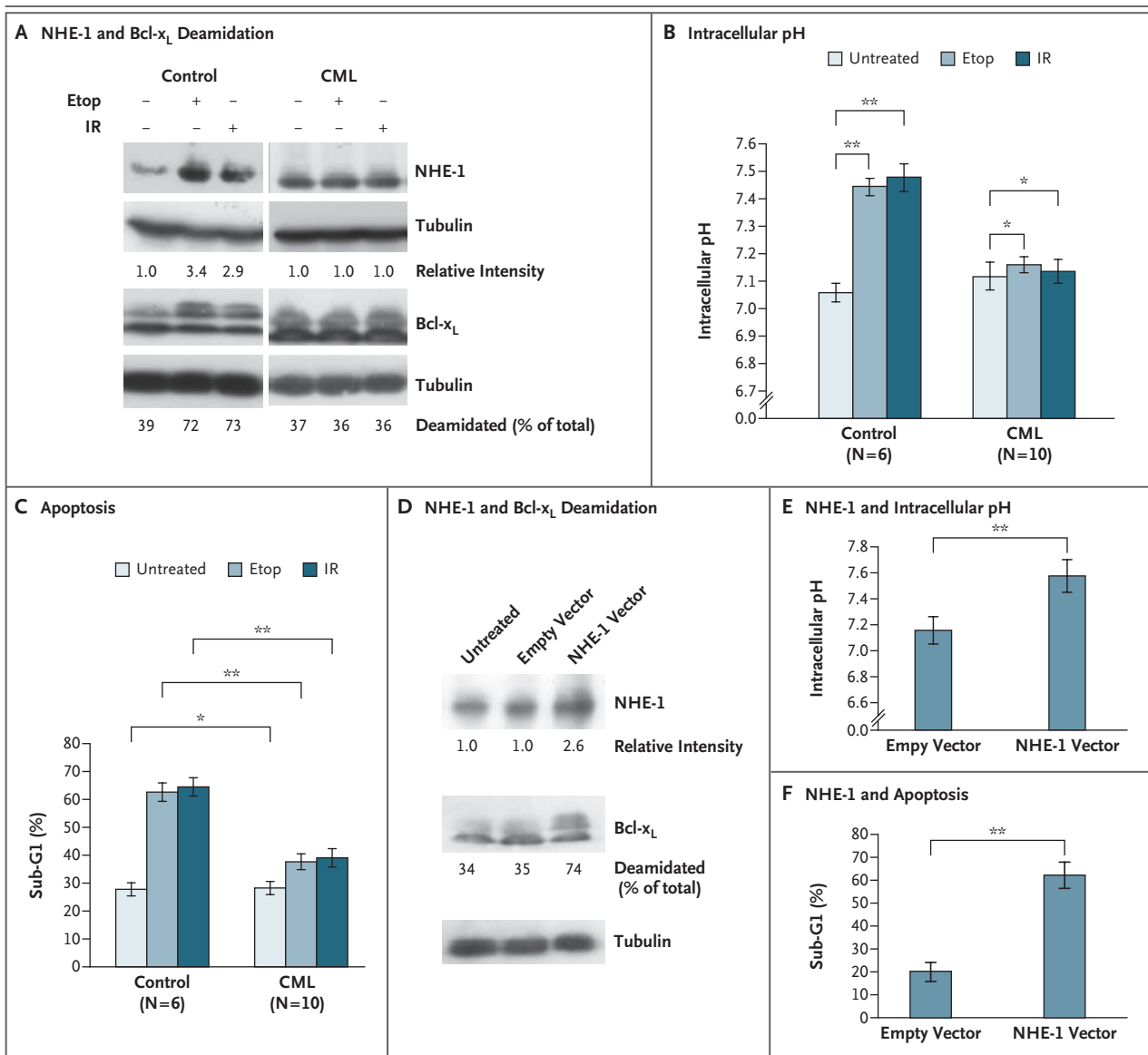
We obtained etoposide, propidium iodide, and nigericin from Sigma; SNARF-1 from Molecular Probes; imatinib from Novartis; JAK inhibitor 1 from Calbiochem; and JAK2 inhibitors TG101209 and AT9283 from Astex Therapeutics. For Western blot analysis, we used antibodies Bcl-x_L (610212) and NHE-1 (clone 54) from BD Transduction Laboratories and β -actin and α -tubulin from Sigma. For flow cytometry, we used antibodies CD2-FITC (product code, CD0201), CD3-FITC (product code, MHCD0301), CD19-FITC (product code, MHCD1901), CD13-PE (product code, MHCD1304), and CD14-APC (product code, MHCD1405) (Caltag).

PATIENTS

We collected peripheral-blood samples from patients with either CML or polycythemia vera and from healthy control subjects. All subjects provided written informed consent. The study was approved by the Cambridge and Eastern Region ethics committee. Of the 10 CML samples for which data are presented in Figure 1, 6 were from patients with newly diagnosed chronic-phase CML, 1 was from a patient in the accelerated phase, and 3 were from patients in the chronic phase who were receiving therapy. All patients with polycythemia vera whose data are presented in Figure 2 had stable, nontransformed disease and were receiving hydroxycarbamide therapy at the time of blood sampling. The six patients with CML whose data are presented in Figure 3 had newly diagnosed chronic-phase CML, and the patient with the imatinib resistance mutation (E255V) in Figure 4 was in the accelerated phase. All patients with CML had the BCR-ABL rearrangement; patients with polycythemia vera and idiopathic myelofibrosis had received a diagnosis on the basis of criteria that have been reported previously.² The quantitative pyrosequencing assay for the JAK2 V617F mutation was performed as described previously.¹⁶

CELL PURIFICATION

Peripheral-blood samples from the patients and control subjects were centrifuged through Lymphoprep (Axis-Shield PoC), and the cells in the pellets (granulocytes) or the interphase (peripheral-blood mononuclear cells [PBMCs]) were then harvested for subsequent experiments. The myeloid origin



of PBMCs and the purity of the granulocyte populations were checked by staining with CD2, CD3, and CD19 monoclonal antibodies, conjugated with fluorescein isothiocyanate, together with CD13-PE and CD14-APC, followed by flow cytometry. Of the PBMCs, 85 to 95% were of myeloid origin, and the granulocytes were more than 90% pure. (Representative flow cytometric data of cell preparations are shown in Fig. 1 in the Supplementary Appendix, available with the full text of this article at www.nejm.org.) Mobilized peripheral-blood samples from control subjects and samples of CML peripheral blood were used to purify CD34⁺ cells, first using a MACS CD34 Micro-

Bead Kit (Miltenyi Biotec), followed by cell sorting to obtain 95% pure CD34⁺ cells maintained in RPMI medium with 10% fetal-calf serum.

CELL LINES

We used human hematopoietic cancer-cell lines K562, HEL, Daudi, DU528, Jum2, Karpas299, OPM2, and DOHH2 (for details, see Table 1 in the Supplementary Appendix). Cells were cultured in RPMI medium with 10% fetal-calf serum. Murine BaF3 cells expressing the thrombopoietin receptor (BaF3-TpoR) were cultured in RPMI medium with 10% fetal-calf serum containing 1 ng per milliliter of recombinant interleukin-3.

Figure 1 (facing page). Inhibition of the NHE-1–Bcl-x_L Deamidation Pathway Induced by DNA Damage in CML Cells.

In Panel A, NHE-1 up-regulation and Bcl-x_L deamidation induced by DNA damage are inhibited in cells from patients with CML in representative blots. Purified granulocytes (from 6 control subjects and 10 patients with CML) that were cultured in RPMI medium were either treated with etoposide (Etop) for 24 hours or exposed to 5 Gy of irradiation (IR) and then cultured for 24 hours. Cells were lysed and subjected to immunoblotting for NHE-1 and Bcl-x_L. Tubulin was reprobated as a loading control. Representative blots from a control subject and a patient with CML are shown. Since these are two different blots, densities cannot be compared between blots. NHE-1 relative intensities that were normalized for protein loading are shown below the immunoblots, with the relative intensity for untreated control samples set at a value of 1.0. In the Bcl-x_L analysis, the upper bands (deamidated) and lower bands (native) were quantified and the deamidated species expressed as a percentage of total Bcl-x_L, as shown. In Panel B, intracellular alkalinization induced by DNA damage is inhibited in CML cells, as compared with cells from control subjects. Intracellular pH was measured in aliquots of the same cells used in the analysis shown in Panel A. The mean (±SD) values from 6 control subjects and 10 patients with CML are shown. Single asterisks indicate $P > 0.05$, and double asterisks $P < 0.001$. In Panel C, DNA damage-induced apoptosis is inhibited in CML cells. Apoptosis was measured in aliquots of the same cells used in the analysis shown in Panel A by DNA staining in the sub-G1 region with the use of flow cytometry. The mean (±SD) values from 6 control subjects and 10 patients with CML are shown. The single asterisk indicates $P > 0.05$, and double asterisks indicate $P < 0.001$. In Panel D, overexpression of NHE-1 antiporter causes Bcl-x_L deamidation in CML cells. Peripheral-blood mononuclear cells (PBMCs) from patients with CML were either untreated or were transfected with empty vector or with plasmid NHE-1–internal ribosome entry site–enhanced green fluorescent protein (NHE-1 vector) with the use of a Nucleofector kit (Amaxa Biosystems).¹⁴ Green fluorescent protein–positive cells were then sorted and subjected to immunoblotting for NHE-1 or Bcl-x_L. Tubulin was reprobated as a loading control. Densitometric values that were normalized for protein loading are shown under the immunoblots. In Panel E, overexpression of NHE-1 causes intracellular alkalinization in CML cells. Intracellular pH was measured in aliquots of the same cells used in the analysis shown in Panel D. The graph represents mean (±SD) values for three patients with CML. Double asterisks indicate $P < 0.001$. In Panel F, overexpression of NHE-1 causes apoptosis in CML cells. Apoptosis of cells in the sub-G1 phase was measured in aliquots of the same cells used in the analysis shown in Panel D. The graph represents mean (±SD) values. Double asterisks indicate $P < 0.001$.

DNA DAMAGE TREATMENTS

Cells were irradiated with 5 Gy with the use of a cesium source or treated with 50 μ M of etoposide in dimethyl sulfoxide (DMSO) for the times indicated. Carrier DMSO was added to control cells.

IMMUNOBLOTTING AND MEASURES OF pH AND APOPTOSIS

These analyses were performed as described previously.¹⁴ Intracellular pH was measured with the use of a pH-sensitive dye in conjunction with flow cytometry.

TRANSFECTION AND RETROVIRAL TRANSDUCTION

Peripheral-blood mononuclear cells from patients with CML were transfected with plasmid NHE-1–internal ribosome entry site–enhanced green fluorescent protein (pNHE-1–IRES–EGFP) with the use of a Nucleofector kit (K562) (Amaxa Biosystems). GFP-positive cells were sorted by flow cytometry with the use of a FACSaria flow cytometer (BD Biosciences). Murine stem-cell virus–IRES–GFP–based retroviral vectors MIG-BCR-ABL, MIG-Jak2^{V617F}, and MIG-NPM-ALK were transfected into the Phoenix cell line with the use of Lipofectamine (Invitrogen), and culture supernatants were harvested 24 hours later. Viral infection of Baf3–TpoR cells was performed by spinoculation (1200 g for 90 minutes at 30°C). GFP-positive cells were cultured in RPMI medium with 10% fetal-calf serum and sorted 2 days later by flow cytometry with the use of a FACSaria flow cytometer.

STATISTICAL ANALYSIS

We performed all statistical analyses using Student's t-test. All P values are two-sided. A P value of less than 0.05 was considered to indicate statistical significance.

RESULTS

DNA DAMAGE

To assess the activity of the NHE-1–Bcl-x_L pathway in normal myeloid cells, we studied the effect of DNA damage on purified peripheral-blood granulocytes from healthy control subjects. Both etoposide and irradiation increased levels of NHE-1, intracellular pH, deamidation of Bcl-x_L, and the percentage of apoptotic cells, findings that were consistent with results in mouse thymocytes that were reported previously.¹⁴ However, no

irradiation caused significantly less apoptosis in CML granulocytes than in normal granulocytes (Fig. 1C), which was consistent with the genotoxic resistance for BCR-ABL-positive cells reported previously.⁸ In contrast, T lymphocytes from the same patients with CML did not resist alkalinization.

Bcl-x_L deamidation, and apoptosis induced by damaged DNA (Fig. 3 in the Supplementary Appendix).

To investigate the level at which the NHE-1–Bcl-x_L deamidation pathway was blocked in CML cells, we exposed granulocytes from patients with CML to varying levels of external pH. Enforced alkalinization reversed the inhibition and restored Bcl-x_L deamidation and apoptosis even in the absence of DNA damage, suggesting that the block was at the level of the NHE-1 antiport (Fig. 4 in the Supplementary Appendix). Consistent with this interpretation, transfection of NHE-1 complementary DNA (cDNA) into CML cells resulted in an increase in NHE-1 levels by a factor of 2 to 3 and was accompanied by increased intracellular pH, Bcl-x_L deamidation, and apoptosis (Fig. 1D to 1F).

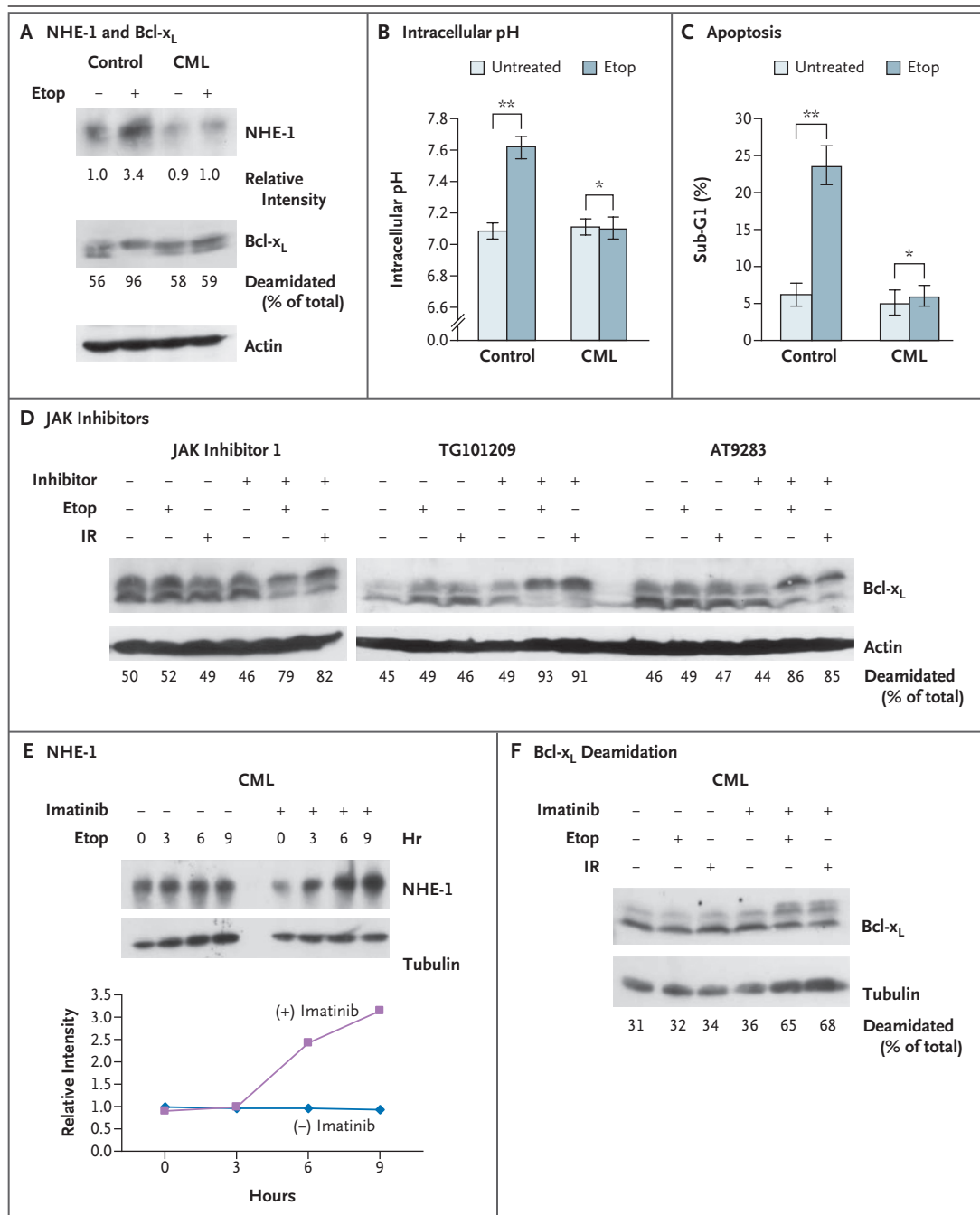
We next studied patients with polycythemia vera, a disease that is associated with a gain-of-function point mutation in the cytoplasmic tyrosine kinase JAK2.^{17–20} Since peripheral-blood granulocytes and bone marrow progenitors from many patients with polycythemia vera contain a mixture of normal and mutant cells,^{17,21} we selected patients in whom JAK2 pyrosequencing demonstrated that the majority of peripheral-blood granulocytes carried the JAK2 mutation (Fig. 5 in the Supplementary Appendix). In contrast to granulocytes from control subjects, those from all eight patients with polycythemia vera who fulfilled these criteria consistently did not have a response to DNA damage by increasing NHE-1 levels, intracellular pH, or Bcl-x_L deamidation (Fig. 2A to 2C). In addition, both etoposide and irradiation produced significantly less apoptosis in polycythemia vera granulocytes than in normal granulocytes (Fig. 2D). In contrast to the granulocytes, T cells from the same patients showed no defect in DNA damage–induced Bcl-x_L deamidation, intracellular alkalinization, or apoptosis (Fig. 3 in the Supplementary Appendix).

As with CML cells, enforced alkalinization of polycythemia vera granulocytes overcame inhibition of the NHE-1–Bcl-x_L deamidation pathway and was accompanied by increased Bcl-x_L deamidation and apoptosis (Fig. 6 in the Supplementary Appendix). The Bcl-x_L deamidation pathway was also inhibited in granulocytes from two patients with idiopathic myelofibrosis with the JAK2 V617F mutation but not in two patients with this disease without the JAK2 mutation (Fig. 7 in the Supplementary Appendix).

To elucidate further the correlation between tyrosine kinase expression and inhibition of the NHE-1–Bcl-x_L pathway, we investigated eight cell lines representing different hematologic cancers associated with distinct molecular mechanisms (Table 1 and Fig. 8 in the Supplementary Appendix). The NHE-1–Bcl-x_L pathway was inhibited in K562 cells carrying BCR-ABL and derived from a patient with CML in blast crisis and also in human erythroleukemia (HEL) cells, which carry the JAK2 V617F mutation and were derived from a patient with acute myeloid leukemia. These data suggest that the pathway remains inhibited after leukemic transformation, which was confirmed using blasts from a patient with CML in blast crisis (data not shown). In contrast, the pathway was intact in four other cell lines that are not thought to express oncogenic tyrosine kinases (Table 1 and Fig. 8 in the Supplementary Appendix). The pathway was also intact in a T-lymphoma cell line (Karpas-299), which expresses the NPM-ALK tyrosine kinase fusion protein, and in a myeloma cell line (OPM-2), which overexpresses the fibroblast growth factor receptor 3 (FGFR3) tyrosine kinase. These results suggest that inhibition of the Bcl-x_L deamidation pathway is not a general feature of hematologic cancers and is mediated by a subgroup of tyrosine kinases or is dependent on a particular cellular context.

To address whether inhibition of the NHE-1–Bcl-x_L pathway is influenced by kinase strength, we performed a series of experiments using a Baf3–TPoR cell line transduced with BCR-ABL, JAK2 V617F, or NPM-ALK tyrosine kinases, giving rise to several cell populations with varying kinase expression levels (Fig. 9 in the Supplementary Appendix). Levels of BCR-ABL and JAK2 V617F expression correlated well with the degree of inhibition of the Bcl-x_L deamidation pathway, whereas NPM-ALK caused no inhibition even at its highest expression level.

Both CML and polycythemia vera are thought to arise from a transformed multipotent stem cell. BCR-ABL is expressed at high levels in stem and progenitor cells and induces expansion of the progenitor compartment during chronic-phase CML.^{22–24} We therefore assessed the status of the NHE-1–Bcl-x_L pathway in normal and CML progenitors that expressed the CD34 stem-cell antigen. In normal CD34+ cells, but not in those derived from patients with CML, etoposide treatment increased NHE-1 levels, Bcl-x_L deamidation,



intracellular alkalinization, and apoptosis (Fig. 3A to 3C). Furthermore, in normal CD34⁺ cells, apoptosis that was triggered by DNA damage was significantly inhibited by dimethylamiloride, a selective NHE-1 antiport inhibitor (Fig. 10 in the Supplementary Appendix). These data demonstrate that the Bcl-x_L deamidation pathway operates in normal CD34⁺ cells and is inhibited in CD34⁺ cells from patients with CML.

We next addressed whether inhibition of the Bcl-x_L deamidation pathway was dependent on aberrant kinase activity. Granulocytes from three patients with polycythemia vera were exposed to three different JAK2 inhibitors. All three inhibitors reversed the block of the pathway: Bcl-x_L deamidation, intracellular pH, and apoptosis all increased in response to DNA damage (Fig. 3D, and Fig. 11 in the Supplementary Appendix).

Figure 3 (facing page). The Effect of Imatinib or JAK2 Inhibitors on NHE-1 Up-Regulation and Bcl-x_L Deamidation in CML Cells Induced by DNA Damage.

In Panel A, purified CD34+ cells from a patient with CML and granulocyte colony-stimulating factor–mobilized peripheral-blood cells from a control subject were treated with etoposide (Etop) for 24 hours, and cell aliquots were then processed for NHE-1 and Bcl-x_L immunoblotting. Actin was reprobed as a loading control. The data are representative of three separate experiments. In Panel B, aliquots of the cells used for the analysis shown in Panel A were assessed for intracellular pH. The graph represents mean (±SD) values of intracellular pH for three patients with CML. The single asterisk indicates $P>0.05$, and double asterisks indicate $P<0.001$. In Panel C, aliquots of the cells used for the analysis shown in Panel B were assessed for apoptosis. The graph represents mean (±SD) percentages for sub-G1 DNA staining. The single asterisk indicates $P>0.05$, and double asterisks indicate $P<0.001$. In Panel D, JAK inhibitors reverse the inhibition of DNA damage–induced Bcl-x_L deamidation in polycythemia vera granulocytes. Three JAK inhibitors were tested at the following concentrations: JAK inhibitor 1 (Calbiochem), 0.5 μ M; TG101209 (Targagen), 20 nM; and AT9283 (Astex), 20 nM. Separate titrations were carried out to determine optimal inhibitory concentrations. Granulocytes from three patients with polycythemia vera that were cultured in RPMI with 10% fetal-calf serum, with or without an inhibitor, were treated with etoposide or irradiation (IR). Cells were harvested and processed for immunoblotting of Bcl-x_L and actin (loading control). A representative blot from three independent experiments is shown. The percentages of deamidated Bcl-x_L were calculated as described in Figure 1A and are shown below the blots. In Panel E, imatinib is shown to reverse inhibition of DNA damage–induced NHE-1 up-regulation. PBMCs from three patients with CML that were cultured in RPMI with 10% fetal-calf serum, with or without imatinib added simultaneously (1.5 μ M), were treated with etoposide for 3, 6, or 9 hours, as shown, and NHE-1 expression was then assessed by immunoblotting. A representative blot and relative quantification (normalized for tubulin loading control) are shown. In Panel F, imatinib is shown to reverse inhibition of DNA damage–induced Bcl-x_L deamidation. PBMCs that were cultured with or without imatinib (as shown in Panel E) were treated with etoposide or irradiation. Cells were harvested and processed for immunoblotting of Bcl-x_L or tubulin (loading control). A representative blot is shown. The percentages of deamidated Bcl-x_L that were calculated as described in Figure 1A are shown below the blots.

PBMCs (>85% myeloid) that were obtained at the time of diagnosis from four patients with CML were also exposed to imatinib, a selective tyrosine kinase inhibitor.²⁵ In contrast to untreated cells, imatinib-treated cells increased NHE-1 levels and Bcl-x_L deamidation in response to DNA damage

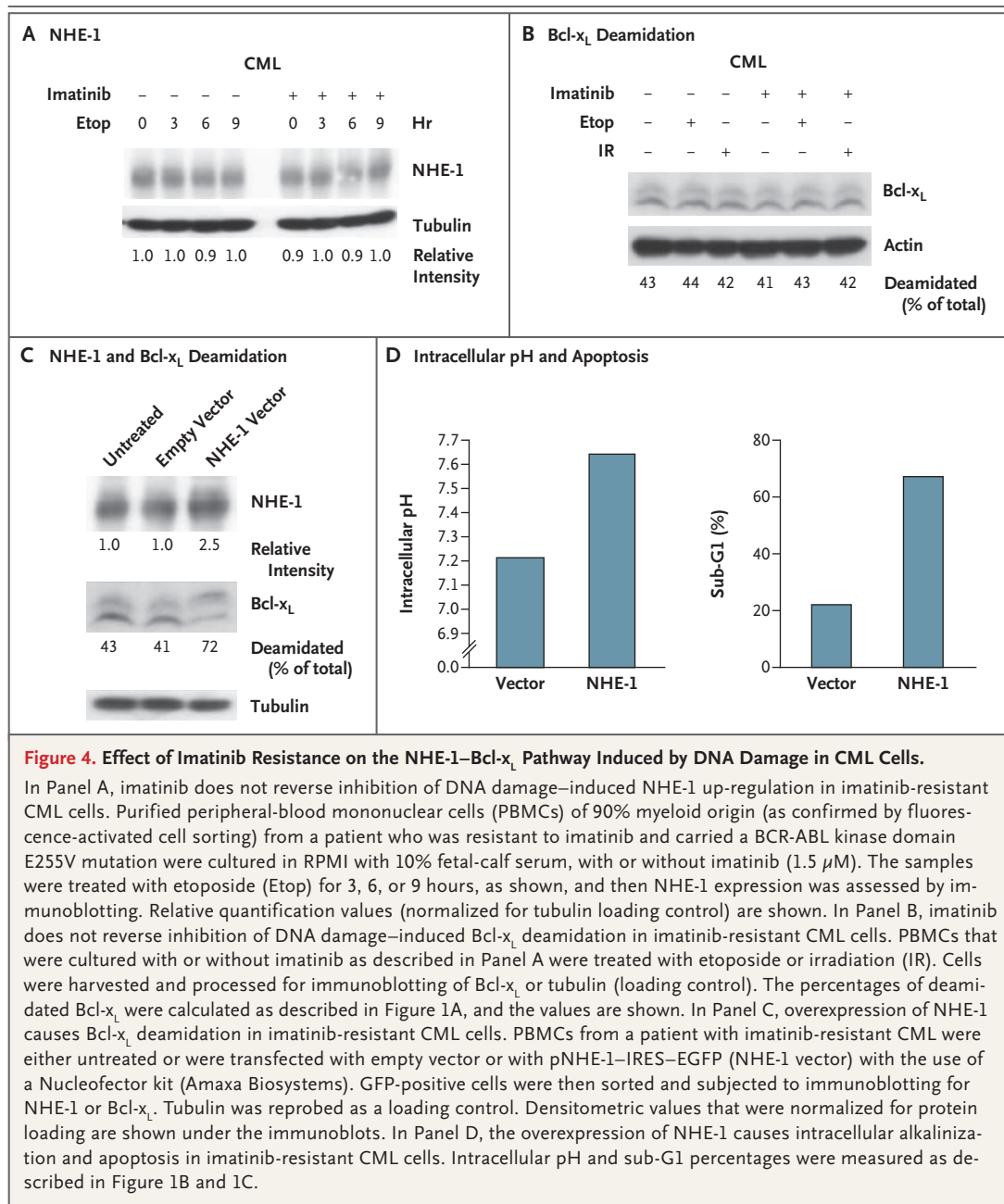
(Fig. 3E and 3F). These results demonstrate a causal link between tyrosine kinase activity and repression of the Bcl-x_L deamidation pathway.

Imatinib and the JAK2 inhibitors inhibit the activity of several kinases in addition to BCR-ABL and JAK2, respectively, raising the possibility that inhibition of other kinases may contribute to the observed effects. We therefore studied a patient who had become resistant to imatinib as a consequence of an E255V mutation in the BCR-ABL kinase domain. Imatinib-treated PBMCs from this patient did not have increased NHE-1 levels in response to etoposide or Bcl-x_L deamidation in response to either etoposide or irradiation (Fig. 4A and 4B). However, the effects of imatinib resistance could be bypassed by NHE-1 overexpression, which caused increased intracellular pH and apoptosis (Fig. 4C and 4D), or by enforced alkalization, which caused increased Bcl-x_L deamidation and apoptosis (Fig. 12 in the Supplementary Appendix). These data demonstrate that BCR-ABL kinase activity is essential for inhibition of the Bcl-x_L deamidation pathway in CML cells.

DISCUSSION

Deamidation of internal asparagine or glutamine residues can have a profound influence on protein function and has been implicated in a wide range of biologic processes.^{26–28} Rates of asparagine deamidation were initially thought to be fixed and determined solely by the structural context of a given asparagine residue, but an active role in the regulation of biologic processes was suggested by the observations that DNA damage can trigger rapid deamidation of Bcl-x_L¹² and that Bcl-x_L deamidation plays a central role in the apoptotic response of normal mouse thymocytes to DNA damage.^{13,14}

In our study, we found that the signaling pathway leading from DNA damage to Bcl-x_L deamidation and consequent apoptosis is inhibited in two myeloproliferative disorders associated with different tyrosine kinases and activated by distinct mechanisms (Fig. 5). We demonstrated this defect in cells from all 20 patients bearing either BCR-ABL or the JAK2 V617F mutation, whereas no defect was observed in cells expressing other oncogenic tyrosine kinases, such as NPM-ALK. To suppress the apoptotic response to DNA damage, it is insufficient for BCR-ABL or mutant JAK2 merely to up-regulate or maintain Bcl-x_L expres-



sion levels. In addition, both oncogenic tyrosine kinases must prevent deamidation of Bcl-x_L to preserve its antiapoptotic function. These observations not only shed light on the accumulation of DNA damage that is characteristic of these cancers^{29,30} but also have potential therapeutic relevance.

CML and polycythemia vera are associated with an increased risk of leukemic transformation, which is thought to reflect the accrual of

additional genetic lesions. However, it is not clear why stem cells from patients with chronic-phase CML and polycythemia vera are prone to accumulate DNA damage.²⁹ Normal cells undergo many DNA strand breaks per genome per cell division, and adequate DNA repair mechanisms, combined with the removal of damaged cells by apoptosis, are therefore essential for homeostasis.³¹ Inhibition of the Bcl-x_L deamidation pathway in chronic-phase CML and polycythemia vera

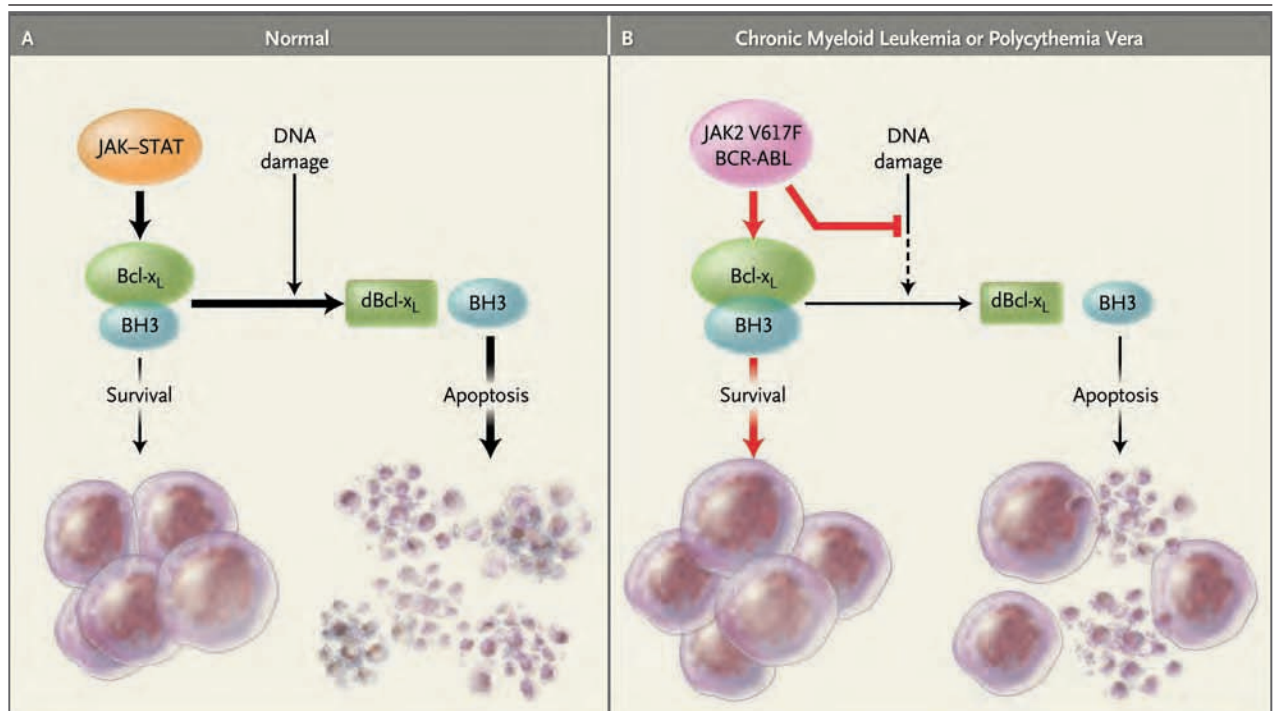


Figure 5. Effects of Inhibition of Bcl-x_L Deamidation in Patients with CML or Polycythemia Vera.

In Panel A, a normal signaling pathway leads from DNA damage to Bcl-x_L deamidation, which reduces the ability of the antiapoptotic Bcl-x_L protein to sequester and inhibit the Bcl-2 homology 3 (BH3)-only family of proapoptotic proteins, thereby promoting apoptosis. In Panel B, in patients with CML or polycythemia vera, the BCR-ABL fusion kinase and the Janus tyrosine kinase 2 (JAK2) V617F mutation, respectively, are associated with the inhibition of Bcl-x_L deamidation, which in turn reduces apoptosis. The deamidated version of Bcl-x_L is denoted as dBcl-x_L. The thickness of the black horizontal arrow is proportional to Bcl-x_L deamidation.

provides a mechanism for circumventing the apoptotic response and permitting accumulation of DNA damage within the malignant clone.

It has been reported that cells expressing oncogenic tyrosine kinases, including BCR-ABL, are resistant to DNA damage.³²⁻³⁴ Resistance to DNA-damaging agents depends on BCR-ABL catalytic activity.³² Consistent with this finding, the combination of antileukemic chemotherapy with the tyrosine kinase inhibitor imatinib produces increased or synergistic apoptosis.³⁵⁻³⁸ Our results shed light on the molecular basis for the effectiveness of such combination therapies. Inhibition of BCR-ABL by imatinib is associated with increased levels of proapoptotic BH3-only proteins, such as Bim and Bad.³⁹⁻⁴¹ The activity of these molecules is constrained by their binding to Bcl-x_L. Optimal apoptosis in response to DNA damage requires that imatinib restore the normal Bcl-x_L deamidation pathway, thus minimizing sequestration by Bcl-x_L and maximizing apoptosis in response to DNA-damaging agents.

The use of tyrosine kinase inhibitors in CML faces two main challenges. Acquired resistance to imatinib therapy can result in relapse, often as a consequence of kinase-domain mutations in BCR-ABL.⁴² In addition, treatment of CML with tyrosine kinase inhibitors is usually associated with persistence of residual disease, which is thought to reflect quiescent BCR-ABL-positive stem cells that resist current tyrosine kinase inhibitors.⁹⁻¹¹ It is therefore notable that an increase in the expression of NHE-1 by a factor of 2 to 3 was sufficient to increase Bcl-x_L deamidation and triple the level of apoptosis in imatinib-resistant CML cells (Fig. 4D). Therefore, targeted stimulation of Bcl-x_L deamidation provides a potential route for circumventing resistance to tyrosine kinase inhibitors and perhaps also for eradicating leukemic stem cells.

The NHE-1 antiport itself represents a potential therapeutic target. Small-molecule inhibitors already exist, although the development of agonists may be more challenging. The NHE-1 anti-

port can also be activated by phosphorylation,⁴³ which suggests the possibility of other therapeutic approaches. The fact that modulation of the NHE-1-Bcl-x_L signaling pathway can bypass resistance to apoptosis in patients with CML and polycythemia vera raises the possibility of new therapeutic approaches that could be of general relevance to any cancer in which Bcl-x_L plays an important role in genotoxic resistance. Indeed, Bcl-x_L expression in a wide range of cancers has a striking correlation with resistance to genotoxic compounds,⁴⁴ which suggests that our findings are likely to have relevance well beyond the myelo-proliferative disorders.

Supported by the Association for International Cancer Research, the Biotechnology and Biological Sciences Research Council, the U.K. Leukaemia Research Fund, the Wellcome Trust, the U.K. Medical Research Council, Cancer Research UK, the National Institute for Health Research Cambridge Biomedical Research Center, and the U.S. Leukemia and Lymphoma Society.

No potential conflict of interest relevant to this article was reported.

We thank Geoff Morgan and Mary Janes for their assistance with fluorescence-activated cell sorting and cell culture, respectively; Dr. Suzanne Turner for providing the NPM-ALK construct; the Addenbrooke's Haematological Disorders Sample Bank for storage and provision of samples; and Drs. J. Lyons and M. Squires for providing JAK2 inhibitors.

REFERENCES

- Goldman JM, Melo JV. Chronic myeloid leukemia — advances in biology and new approaches to treatment. *N Engl J Med* 2003;349:1451-64.
- Campbell PJ, Green AR. The myeloproliferative disorders. *N Engl J Med* 2006;355:2452-66.
- Scott LM, Tong W, Levine RL, et al. JAK2 exon 12 mutations in polycythemia vera and idiopathic erythrocytosis. *N Engl J Med* 2007;356:459-68.
- Amarante-Mendes GP, McGahon AJ, Nishioka WK, Afar DE, Witte ON, Green DR. Bcl-2-independent Bcr-Abl-mediated resistance to apoptosis: protection is correlated with up regulation of Bcl-xL. *Oncogene* 1998;16:1383-90.
- Oetzel C, Jonuleit T, Götz A, et al. The tyrosine kinase inhibitor CGP 57148 (ST1 571) induces apoptosis in BCR-ABL-positive cells by down-regulating BCL-X. *Clin Cancer Res* 2000;6:1958-68.
- Silva M, Richard C, Benito A, Sanz C, Olalla I, Fernández-Luna JL. Expression of Bcl-x in erythroid precursors from patients with polycythemia vera. *N Engl J Med* 1998;338:564-71.
- Garçon L, Rivat C, James C, et al. Constitutive activation of STAT5 and Bcl-xL overexpression can induce endogenous erythroid colony formation in human primary cells. *Blood* 2006;108:1551-4.
- Skorski T. BCR/ABL regulates response to DNA damage: the role in resistance to genotoxic treatment and in genomic instability. *Oncogene* 2002;21:8591-604.
- Holyoake T, Jiang X, Eaves C, Eaves A. Isolation of a highly quiescent subpopulation of primitive leukemic cells in chronic myeloid leukemia. *Blood* 1999;94:2056-64.
- Copland M, Hamilton A, Elrick LJ, et al. Dasatinib (BMS-354825) targets an earlier progenitor population than imatinib in primary CML but does not eliminate the quiescent fraction. *Blood* 2006;107:4532-9.
- Jørgensen HG, Allan EK, Jordanides NE, Mountford JC, Holyoake TL. Nilotinib exerts equipotent antiproliferative effects to imatinib and does not induce apoptosis in CD34+ CML cells. *Blood* 2007;109:4016-9.
- Deverman BE, Cook BL, Manson SR, et al. Bcl-xL deamidation is a critical switch in the regulation of the response to DNA damage. *Cell* 2002;111:51-62.
- Zhao R, Yang FT, Alexander DR. An oncogenic tyrosine kinase inhibits DNA repair and DNA-damage-induced Bcl-xL deamidation in T cell transformation. *Cancer Cell* 2004;5:37-49.
- Zhao R, Oxley D, Smith TS, Follows GA, Green AR, Alexander DR. DNA damage-induced Bcl-xL deamidation is mediated by NHE-1 antiport regulated intracellular pH. *PLoS Biol* 2006;5:e1.
- Chang CY, Lin YM, Lee WP, Hsu HH, Chen EI. Involvement of Bcl-X(L) deamidation in E1A-mediated cisplatin sensitization of ovarian cancer cells. *Oncogene* 2006;25:2656-65.
- Jones AV, Kreil S, Zoi K, et al. Widespread occurrence of the JAK2 V617F mutation in chronic myeloproliferative disorders. *Blood* 2005;106:2162-8.
- Baxter EJ, Scott LM, Campbell PJ, et al. Acquired mutation of the tyrosine kinase JAK2 in human myeloproliferative disorders. *Lancet* 2005;365:1054-61.
- James C, Ugo V, Le Couédic JP, et al. A unique clonal JAK2 mutation leading to constitutive signalling causes polycythemia vera. *Nature* 2005;434:1144-8.
- Kralovics R, Passamonti F, Buser AS, et al. A gain-of-function mutation of JAK2 in myeloproliferative disorders. *N Engl J Med* 2005;352:1779-90.
- Levine RL, Wadleigh M, Cools J, et al. Activating mutation in the tyrosine kinase JAK2 in polycythemia vera, essential thrombocythemia, and myeloid metaplasia with myelofibrosis. *Cancer Cell* 2005;7:387-97.
- Scott LM, Scott MA, Campbell PJ, Green AR. Progenitors homozygous for the V617F mutation occur in most patients with polycythemia vera, but not essential thrombocythemia. *Blood* 2006;108:2435-7.
- Jaiswal S, Traver D, Miyamoto T, Akashi K, Lagasse E, Weissman IL. Expression of BCR/ABL and BCL-2 in myeloid progenitors leads to myeloid leukemias. *Proc Natl Acad Sci U S A* 2003;100:10002-7.
- Jamieson CH, Ailles LE, Dylla SJ, et al. Granulocyte-macrophage progenitors as candidate leukemic stem cells in blast-crisis CML. *N Engl J Med* 2004;351:657-67.
- Koschmieder S, Göttgens B, Zhang P, et al. Inducible chronic phase of myeloid leukemia with expansion of hematopoietic stem cells in a transgenic model of BCR-ABL leukemogenesis. *Blood* 2005;105:324-34.
- Druker BJ, Tamura S, Buchdunger E, et al. Effects of a selective inhibitor of the Abl tyrosine kinase on the growth of Bcr-Abl positive cells. *Nat Med* 1996;2:561-6.
- Hoffmann C, Pop M, Leemhuis J, Schirmer J, Aktories K, Schmidt G. The Yersinia pseudotuberculosis cytotoxic necrotizing factor (CNFY) selectively activates RhoA. *J Biol Chem* 2004;279:16026-32.
- Robinson NE, Robinson AB. Molecular clocks: deamidation of asparaginyl and glutaminyl residues in peptides and proteins. Cave Junction, OR: Althouse Press, 2004.
- Moss CX, Matthews SP, Lamont DJ, Watts C. Asparagine deamidation perturbs antigen presentation on class II major histocompatibility complex molecules. *J Biol Chem* 2005;280:18498-503.
- Melo JV, Barnes DJ. Chronic myeloid leukaemia as a model of disease evolution in human cancer. *Nat Rev Cancer* 2007;7:441-53.
- Plo I, Nakatake M, Malivert L, et al. JAK2 stimulates homologous recombination and genetic instability. *Blood* 2008;112:1402-12.
- McGlynn P, Lloyd RG. Recombination-

- al repair and restart of damaged replication forks. *Nat Rev Mol Cell Biol* 2002;3:859-70.
32. Bedi A, Barber JP, Bedi GC, et al. BCR-ABL-mediated inhibition of apoptosis with delay of G2/M transition after DNA damage: a mechanism of resistance to multiple anticancer agents. *Blood* 1995;86:1148-58.
33. Nishii K, Kabarowski JH, Gibbons DL, et al. BCR-ABL kinase activation confers increased resistance to genotoxic damage via cell cycle block. *Oncogene* 1996;13:2225-34.
34. Amarante-Mendes GP, Naekyung Kim C, Liu L, et al. Bcr-Abl exerts its antiapoptotic effect against diverse apoptotic stimuli through blockage of mitochondrial release of cytochrome C and activation of caspase-3. *Blood* 1998;91:1700-5.
35. Fang G, Kim CN, Perkins CL, et al. CGP57148B (STI-571) induces differentiation and apoptosis and sensitizes Bcr-Abl-positive human leukemia cells to apoptosis due to antileukemic drugs. *Blood* 2000;96:2246-53.
36. Slupianek A, Hoser G, Majsterek I, et al. Fusion tyrosine kinases induce drug resistance by stimulation of homology-dependent recombination repair, prolongation of G(2)/M phase, and protection from apoptosis. *Mol Cell Biol* 2002;22:4189-201.
37. Topaly J, Zeller WJ, Fruehauf S. Synergistic activity of the new ABL-specific tyrosine kinase inhibitor STI571 and chemotherapeutic drugs on BCR-ABL-positive chronic myelogenous leukemia cells. *Leukemia* 2001;15:342-7.
38. Kano Y, Akutsu M, Tsunoda S, et al. In vitro cytotoxic effects of a tyrosine kinase inhibitor STI571 in combination with commonly used antileukemic agents. *Blood* 2001;97:1999-2007.
39. Aichberger KJ, Mayerhofer M, Krauth MT, et al. Low-level expression of proapoptotic Bcl-2-interacting mediator in leukemic cells in patients with chronic myeloid leukemia: role of BCR/ABL, characterization of underlying signaling pathways, and reexpression by novel pharmacologic compounds. *Cancer Res* 2005;65:9436-44.
40. Kuroda J, Puthalakath H, Cragg MS, et al. Bim and Bad mediate imatinib-induced killing of Bcr/Abl+ leukemic cells, and resistance due to their loss is overcome by a BH3 mimetic. *Proc Natl Acad Sci U S A* 2006;103:14907-12.
41. Kuroda J, Kimura S, Strasser A, et al. Apoptosis-based dual molecular targeting by INNO-406, a second-generation Bcr-Abl inhibitor, and ABT-737, an inhibitor of antiapoptotic Bcl-2 proteins, against Bcr-Abl-positive leukemia. *Cell Death Differ* 2007;14:1667-77.
42. Schiffer CA. BCR-ABL tyrosine kinase inhibitors for chronic myelogenous leukemia. *N Engl J Med* 2007;357:258-65.
43. Putney LK, Denker SP, Barber DL. The changing face of the Na⁺/H⁺ exchanger, NHE1: structure, regulation, and cellular actions. *Annu Rev Pharmacol Toxicol* 2002;42:527-52.
44. Amundson SA, Myers TG, Scudiero D, Kitada S, Reed JC, Fornace AJ Jr. An informatics approach identifying markers of chemosensitivity in human cancer cell lines. *Cancer Res* 2000;60:6101-10.

Copyright © 2008 Massachusetts Medical Society.

FULL TEXT OF ALL JOURNAL ARTICLES ON THE WORLD WIDE WEB

Access to the complete text of the *Journal* on the Internet is free to all subscribers. To use this Web site, subscribers should go to the *Journal*'s home page (www.nejm.org) and register by entering their names and subscriber numbers as they appear on their mailing labels. After this one-time registration, subscribers can use their passwords to log on for electronic access to the entire *Journal* from any computer that is connected to the Internet. Features include a library of all issues since January 1993 and abstracts since January 1975, a full-text search capacity, and a personal archive for saving articles and search results of interest. All articles can be printed in a format that is virtually identical to that of the typeset pages. Beginning 6 months after publication, the full text of all Original Articles and Special Articles is available free to nonsubscribers.

Supplementary Appendix

This appendix has been provided by the authors to give readers additional information about their work.

Supplement to: Zhao R, Follows GA, Beer PA, et al. Inhibition of the Bcl-x_L deamidation pathway in myeloproliferative disorders. N Engl J Med 2008;359:2778-89.

Supplementary data

Figure S1. FACS analysis of the cells purified from normal donors and CML patients.

(a) Granulocytes were purified from the peripheral blood of normal and CML patient donors. The similar cell surface marker phenotype of the normal and CML granulocytes was confirmed by staining with anti-CD2, CD3, CD19, conjugated to FITC; anti-CD13, conjugated to PE; and anti-CD14, conjugated to APC. The analysis was carried out on a FACScalibur.

(b) Peripheral blood mononuclear cells were isolated from CML patients and stained and analysed as in (a).

Figure S2. Expression levels of NHE-1 and extent of Bcl-x_L deamidation in CML and PV patients.

(a) Western blots showing the NHE-1 expression level of representative CML patients and PV patients. Tubulin was reprobbed as a loading control. NHE-1 relative intensities normalised for protein loading are shown below the immunoblot with untreated controls set at a value of 1 (*). Basal NHE-1 expression was comparable between normal donor, CML and PV cells.

(b) NHE-1 relative intensities (quantified from the western blots) of the normal donors, CML, and PV patients utilised in this study are shown as mean values with untreated controls set at a value of 1. Comparison of normal donors' and CML or PV patients' etoposide and irradiation treated sample values generates * $p < 0.001$.

(c) Percentages of deamidated Bcl-x_L measured in aliquots of the samples used in (b) are shown as mean values. Comparison of normal donors' and CML or PV patients' etoposide and irradiation treated Bcl-x_L deamidation values generates * $p < 0.001$.

There was no significant difference in basal Bcl-x_L deamidation values between donor, CML and PV patients' values ($p = > 0.05$).

Figure S3. DNA damage induces the Bcl-x_L deamidation pathway in T lymphocytes from CML and PV patients.

(a) DNA damage induces intracellular alkalinisation in T lymphocytes from CML and PV patients. PBMC were purified from patients' blood and stained with CD3-FITC,

before T cells were purified by flow cytometry. The cells were then processed as in Fig 1a . Intracellular pH was measured as in Fig 1b. The mean values \pm S.D. from 7 PV and 3 CML patients are shown in the histogram. * $p < 0.001$.

(b) DNA damage induces Bcl-x_L deamidation in T lymphocytes from CML and PV patients. Cell aliquots as used for (a) were subjected to immunoblotting for Bcl-x_L. A representative blot is shown with actin as a loading control.

(c) DNA damage induces apoptosis in T lymphocytes from CML and PV patients. Apoptosis was measured using aliquots of the same cells used in (a) by sub-G1 DNA staining using flow cytometry. The mean values \pm S.D. from 7 PV and 3 CML patients are shown in the histogram. * $p < 0.001$.

Figure S4. Enforced intracellular alkalinisation of CML cells causes Bcl-x_L deamidation and apoptosis.

(a) Enforced intracellular alkalinisation of CML cells causes Bcl-x_L deamidation. Purified granulocytes from CML patients were cultured in RPMI/10% Fetal Calf Serum with the extracellular pH (pH_e) as shown, treated with irradiation or etoposide as in Fig1a, and analysed for Bcl-x_L deamidation by immunoblotting. The deamidated species of Bcl-x_L were quantified as in Fig1a .

(b) Enforced intracellular alkalinisation of CML cells causes apoptosis. Aliquots of the cells used for (a) were assessed for apoptosis. The histograms represent sub-G1 % mean values \pm S.D. (n=10). The numbers above the histogram bars show the mean intracellular pH values. Statistical comparison of values between cells cultured in media with pH_e 7.2 and pH_e 8.0, and between cells cultured in media with pH_e 7.2 and pH_e 8.5, generated * $p < 0.001$; ** $p < 0.0001$.

Figure S5. Analysis of mutations in JAK2 from polycythaemia vera patients.

(a) Representative granulocyte sequencing traces from a normal control and 3 PV patient used in Figure 2, showing the somatic G to T transversion (black arrow) that causes phenylalanine to be substituted for valine at position 617 of JAK2 (V617F). (b) Pyrosequencing results for the PV patients are shown in the table. The allele burden was at least 62% in all patients. Since the granulocytes will include both homozygous and heterozygous mutant cells, these results indicate that the vast majority of granulocytes are likely to contain at least one mutant allele.

Figure S6. Enforced intracellular alkalinisation of polycythaemia vera cells causes Bcl-x_L deamidation and apoptosis.

(a) Enforced intracellular alkalinisation of PV cells causes Bcl-x_L deamidation. Purified granulocytes from PV patients were cultured in RPMI/10% Fetal Calf Serum with the extracellular pH (pH_e) as shown, treated with irradiation or etoposide as in Fig1a, and analysed for Bcl-x_L deamidation by immunoblotting. The deamidated species of Bcl-x_L were quantified as in Fig1a .

(b) Enforced intracellular alkalinisation of PV cells causes apoptosis. Apoptosis (sub-G1) was measured using aliquots of the same cells used in (a), analysed as in Fig 1c. The histograms represent sub-G1 % mean values \pm S.D. (n=8). The numbers above the histogram bars show the mean intracellular pH values. Statistical comparison of values between cells cultured in media with pH_e 7.2 and pH_e 8.0, and between cells cultured with pH_e 7.2 and pH_e 8.5, generated * p<0.01; ** p<0.001.

Figure S7. Analysis of the Bcl-x_L deamidation pathway in IMF patients' granulocytes.

(a) Granulocytes from 2 IMF patients without JAK2^{V617F} mutation and 2 IMF patients with the JAK2^{V617F} mutation were treated with etoposide and irradiation and analysed as in Fig 1a.

(b) Intracellular pH was measured using aliquots of the same cells used in (a).

(c) Apoptosis was measured using aliquots of the same cells used in (a) by sub-G1 DNA staining using flow cytometry.

Figure S8. Analysis of the Bcl-x_L deamidation pathway in cancer cell lines.

(a) Representative western blots showing Bcl-x_L deamidation in the 8 cell lines analysed. Cell lines were maintained in RPMI/10% Fetal Calf Serum. Cells were either treated with 50μM etoposide for 24h, or exposed to 5 Gy of irradiation and then cultured for 24h. Cells were lysed and subjected to immunoblotting for Bcl-x_L and tubulin (loading control). The deamidated Bcl-x_L values were calculated as in Fig 1a.

(b) Intracellular pH was measured in the same cell aliquots from (a) as for Fig. 1b.

(c) Apoptosis (sub-G1 percentages) was measured in the same cell aliquots from (a) as for Fig. 1c. The histograms in both (b) and (c) show the mean values \pm S.D. from at least 3 separate measurements.

Figure S9. Kinase expression levels correlate with the degree of inhibition of DNA damage-induced Bcl-x_L deamidation.

(a) Flow cytometric analysis of sub-populations of BaF3/TpoR cells transfected with different expression levels of Bcr-Abl. Retroviral vector MIG-BCR-ABL was transduced into BaF3/TPoR cells at a range of retroviral titers. The cells were then sorted using a FACS Aria into four populations with different expression levels of GFP.

(b) The four populations of cells from (a) were processed for immunoblotting with a BCR-ABL antibody and the immunoblots reprobed for actin as loading control.

(c) The BCR-ABL expression level correlates with the degree of inhibition of DNA damage-induced Bcl-x_L deamidation. The same cell aliquots as shown in (b) were treated with etoposide and irradiation as in Fig 1a, and processed for immunoblotting with Bcl-x_L. One representative blot from 3 independent experiments is shown and the percentage of deamidation was quantified as in Fig 1a.

(d) The BCR-ABL expression level correlates with the degree of inhibition of DNA damage-induced intracellular alkalinisation. Intracellular pH was measured in the same cell aliquots as in (b). The mean values \pm S.D. from 3 independent experiments are shown in the histogram.

(e) Jak2^{V617F} and NPM-ALK were expressed in BaF3/TpoR cells by retroviral transduction. Three cell populations with different GFP levels (labelled as #1, #2 and #3) were sorted by flow cytometry from each kinase-transduced BaF3/TpoR cells.

(f) A comparison of different BCR-ABL, mutant Jak2 and NPM-ALK expression levels on the DNA damage-induced Bcl-x_L deamidation pathway. Cells expressing Jak2^{V617F} and NPM-ALK shown in (e) and cells expressing BCR-ABL shown in (a) and (b) were treated with etoposide for 24h, then processed for immunoblotting with Bcl-x_L. A representative blot is shown with the percentage of deamidation below. Note that with increased kinase expression, Jak2^{V617F} and BCR-ABL show increased inhibition of the pathway, whereas NPM-ALK shows no inhibition even at its highest expression level..

Figure S10. DNA damage-triggered apoptosis in normal CD34-positive cells is inhibited by DMA.

CD34-positive cells from three normal donors were treated with or without DMA (100 μ M), and with or without etoposide (50 μ M) for 24 h. Percentage of sub-G1 DNA was measured by FACS. Statistical evaluation of the difference between 'etoposide alone' and 'etoposide+DMA' generated $p = <0.05$.

Figure S11. JAK2 inhibitors (JAK inhibitor 1, TG101209 and AT9283) reverse the inhibition of the DNA damage-induced Bcl-x_L deamidation pathway in PV granulocytes.

(a) JAK2 inhibitors reverse the inhibition of DNA damage-induced intracellular alkalisation in PV granulocytes. Intracellular pH was measured using aliquots of the same cells used in Fig 3f. The mean values \pm S.D. from 3 PV patients are shown in the histogram. Statistical comparison of values in the presence or absence of JAK2 inhibitors revealed $p = <0.01$.

(b) JAK2 inhibitors reverse the inhibition of DNA damage-induced apoptosis in PV granulocytes. Apoptosis was measured using aliquots of the same cells used in Fig 3f by sub-G1 DNA staining using flow cytometry. The mean values \pm S.D. from 3 PV patients are shown in the histogram. Statistical comparison of values in the presence or absence of JAK2 inhibitors revealed $p = <0.01$.

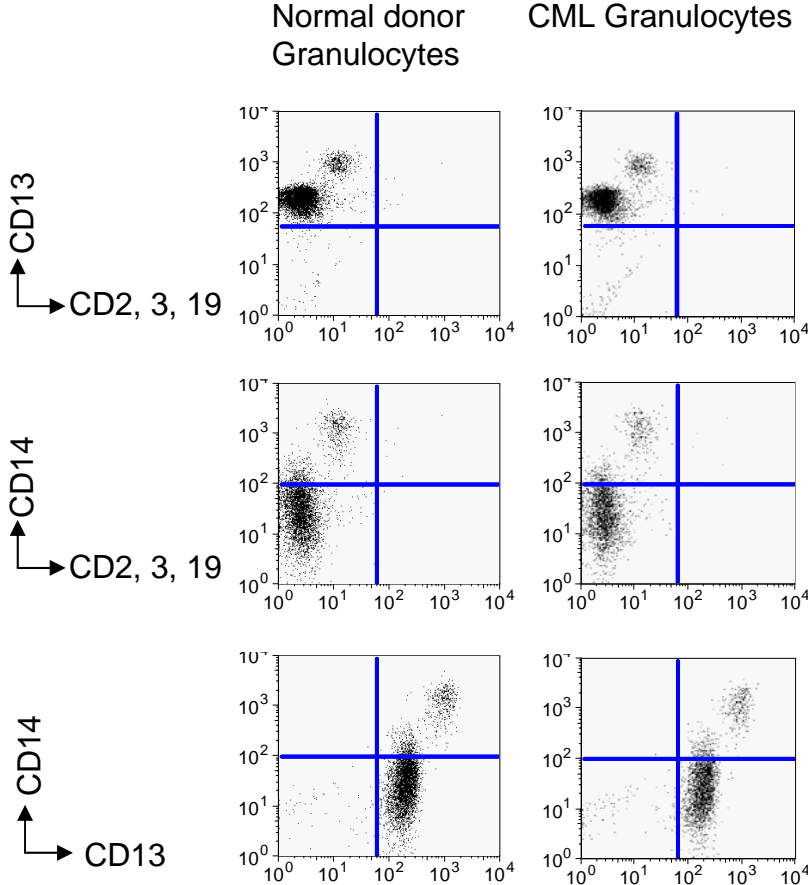
Figure S12. Enforced intracellular alkalisation reverses the effects of imatinib-resistance in CML cells.

(a) Enforced intracellular alkalisation of imatinib-resistant CML cells causes Bcl-x_L deamidation. PBMCs from an imatinib-resistant CML patient were cultured in RPMI/10% Fetal Calf Serum with the extracellular pH (pH_e) as shown, treated with irradiation or etoposide as in Fig 1a, and analysed for Bcl-x_L deamidation by immunoblotting. The deamidated species of Bcl-x_L were quantified as in Fig. 1a.

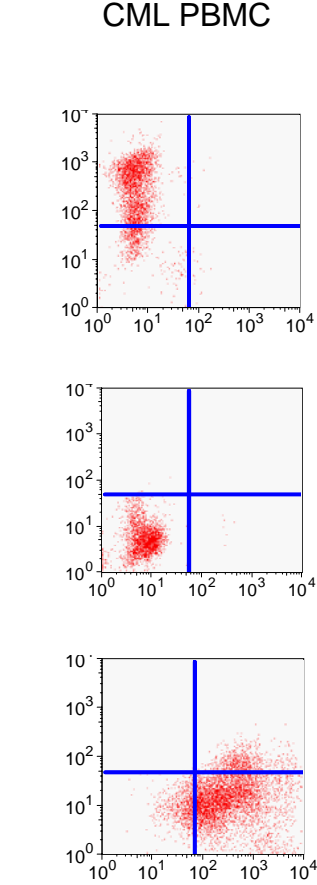
(b) The intracellular pH and apoptosis (sub-G1 percentage) were measured in the same cell aliquots as in Fig 1 (b) and (c) respectively. The numbers above the histogram bars show the mean intracellular pH values.

Supplementary Figure S1

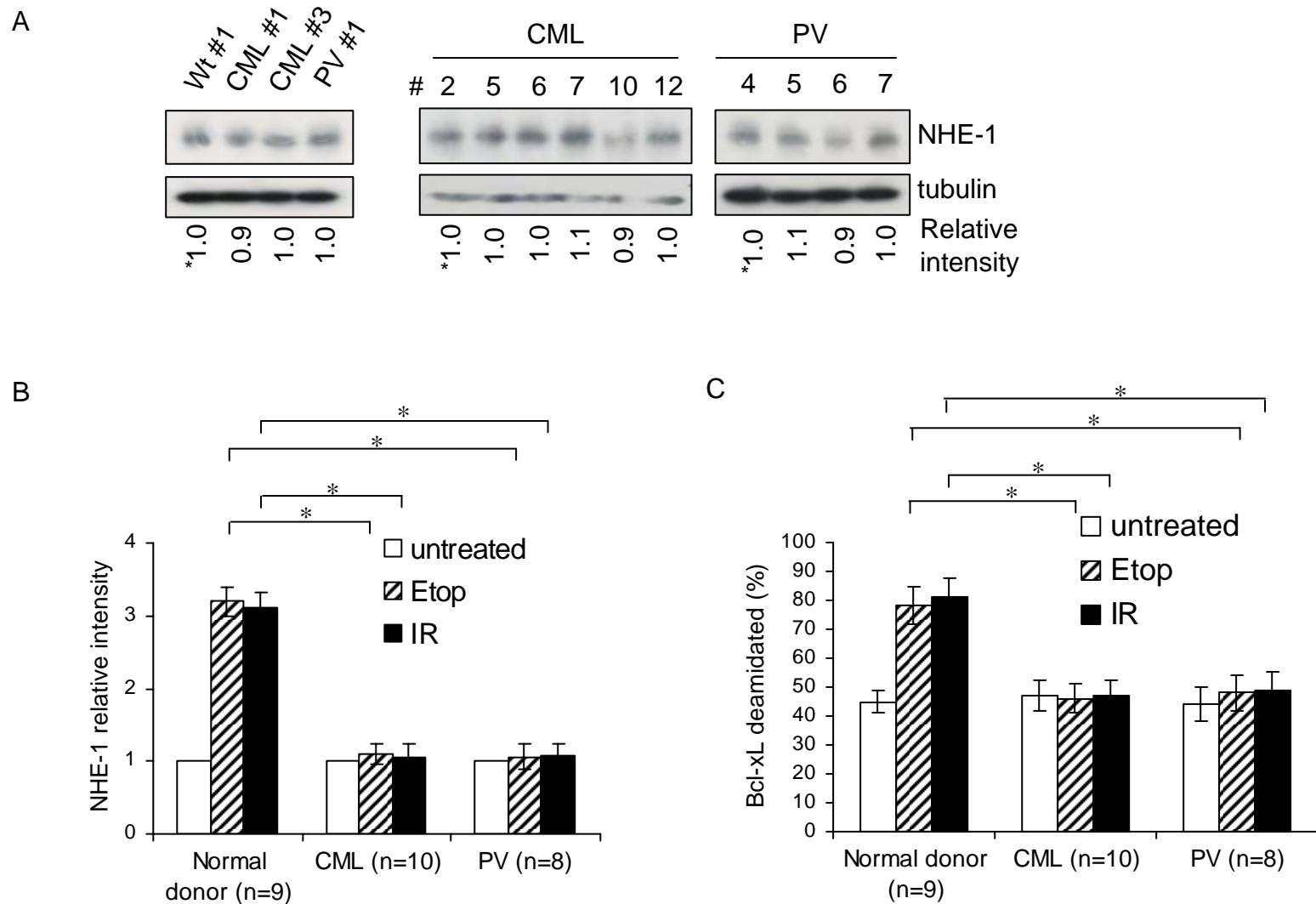
A



B

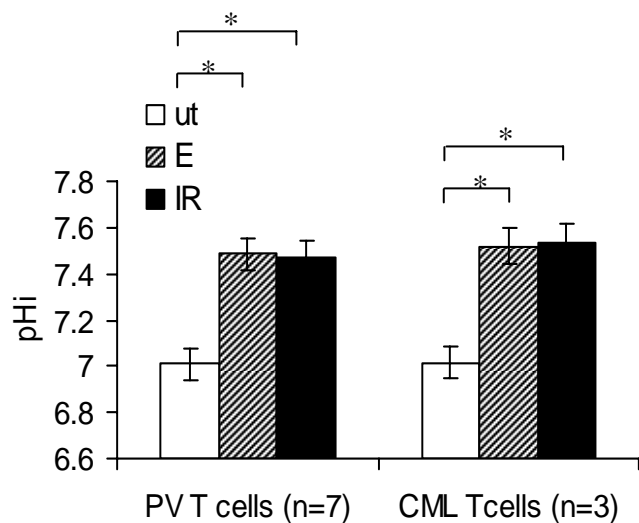


Supplementary Figure S2

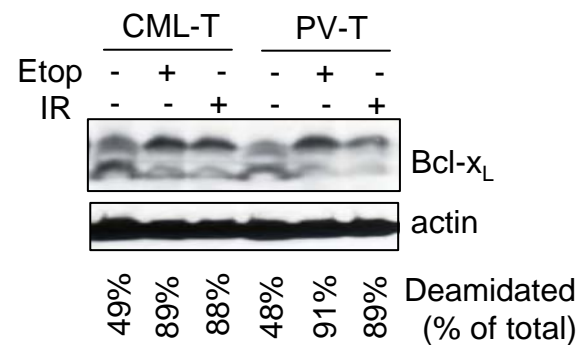


Supplementary Figure S3

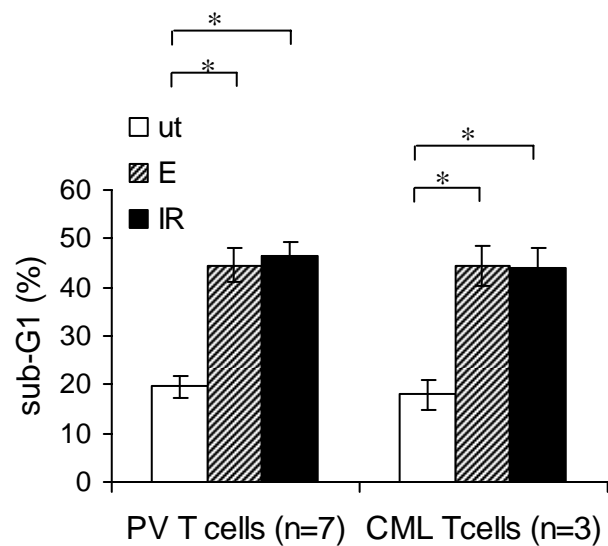
A



B

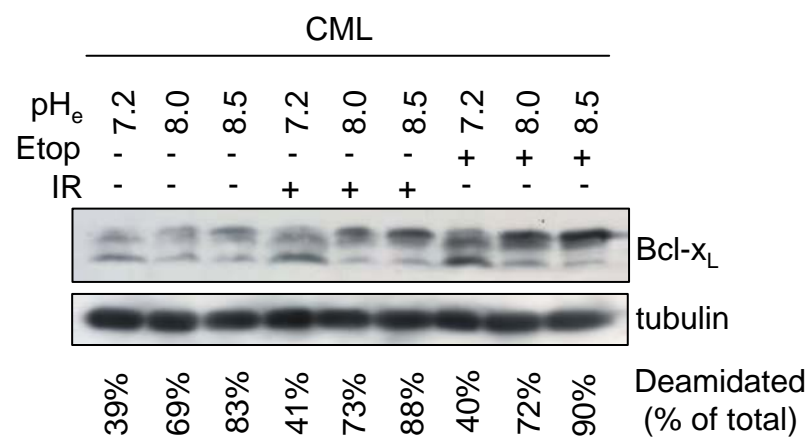


C

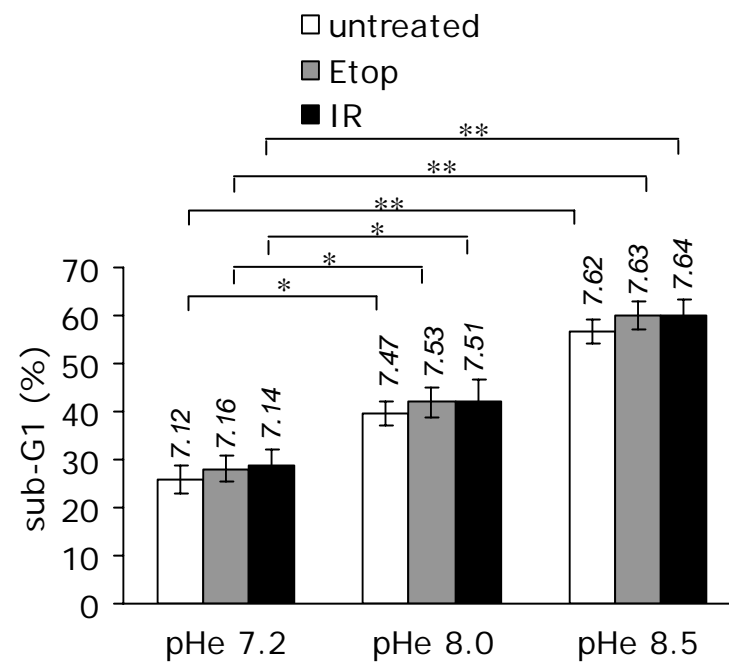


Supplementary Figure S4

A



B

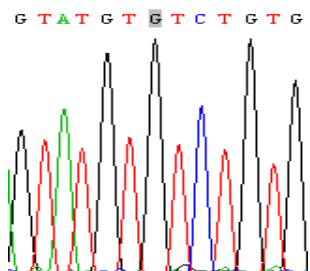


Supplementary Figure S5

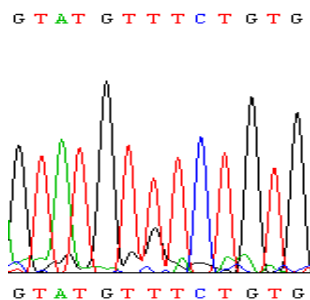
A



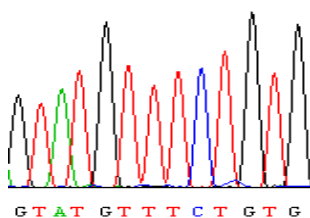
Normal control



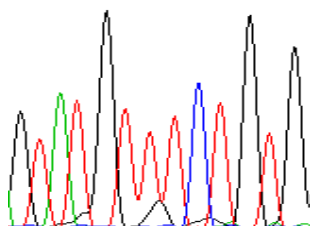
PV # 2



PV # 3



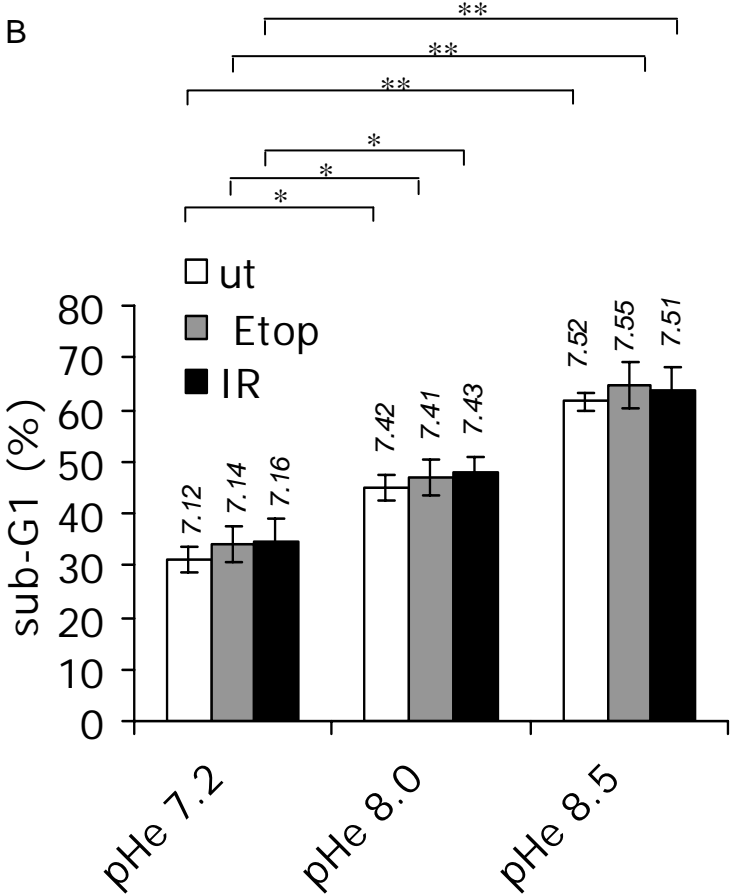
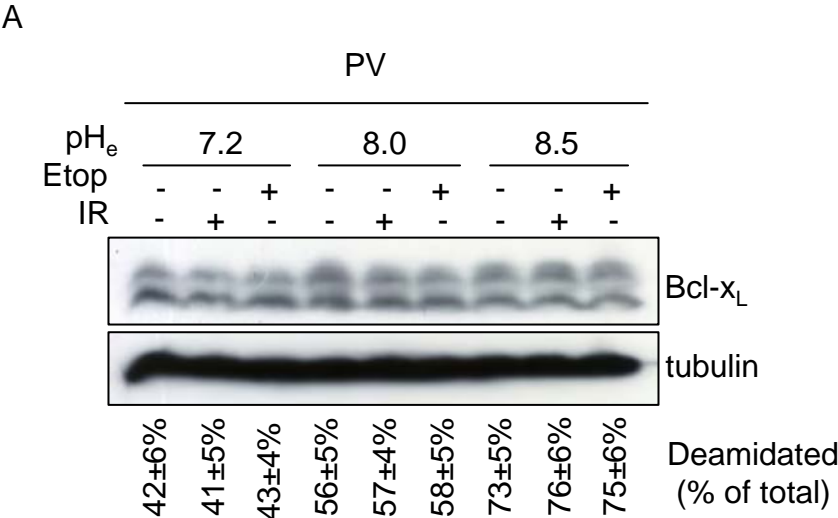
PV # 4



B

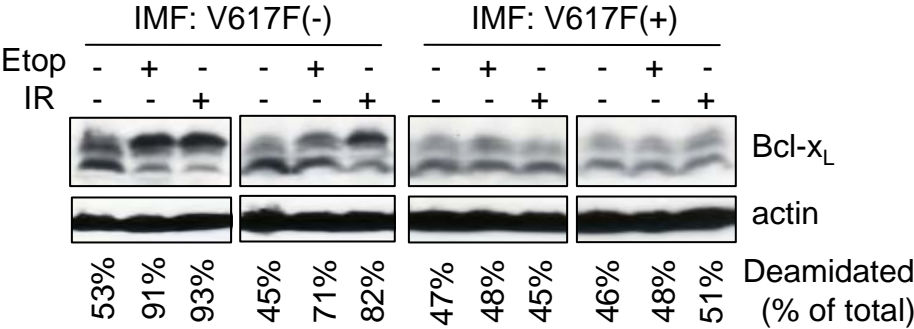
Patient No.	Mutant allele burden
#1	90%
#2	96%
#3	93%
#4	100%
#5	72%
#6	98%
#7	77%
#8	62%

Supplementary Figure S6

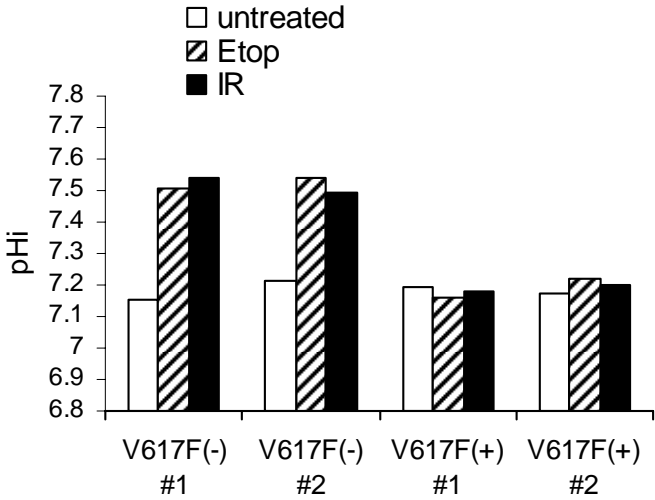


Supplementary Figure S7

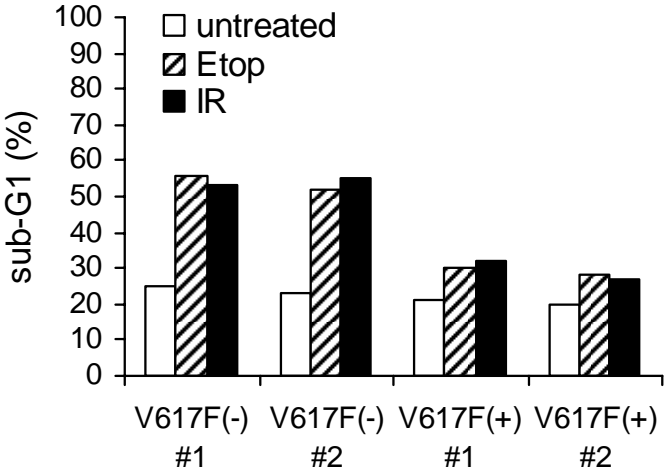
A



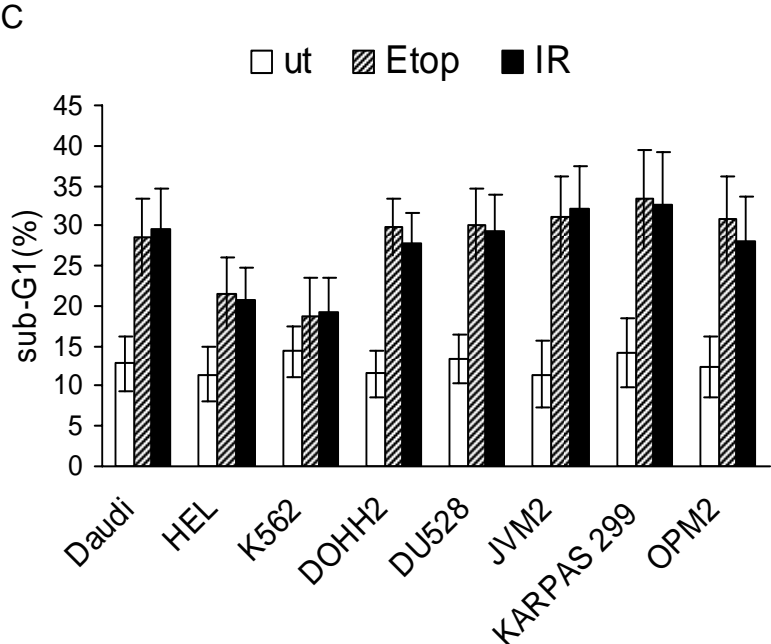
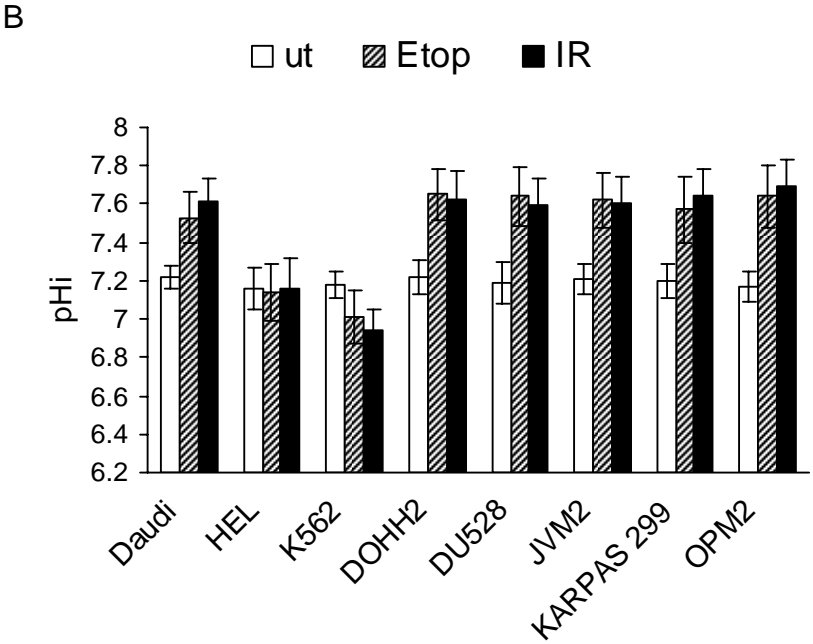
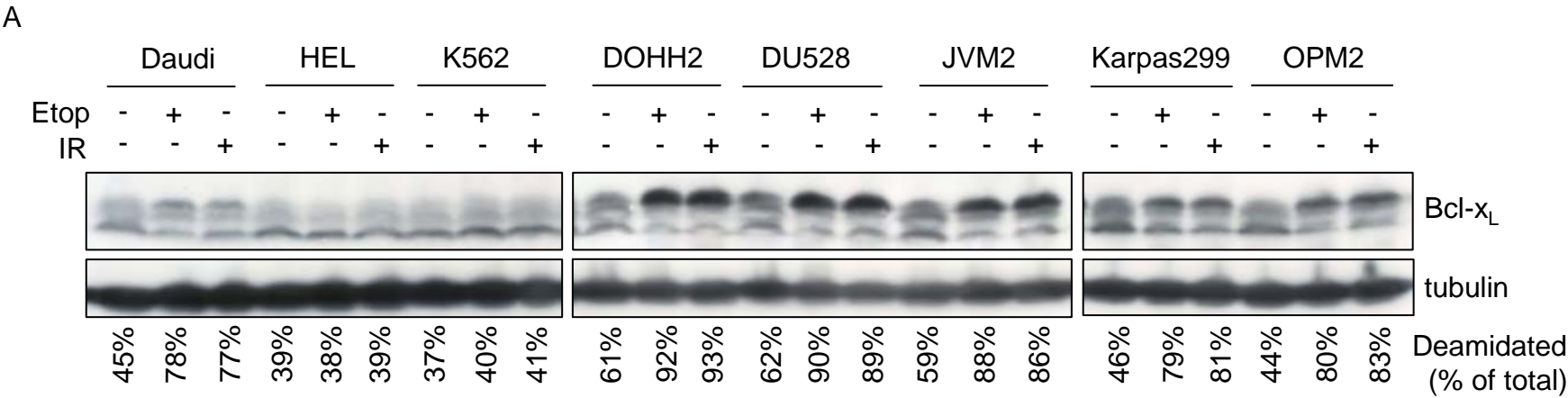
B



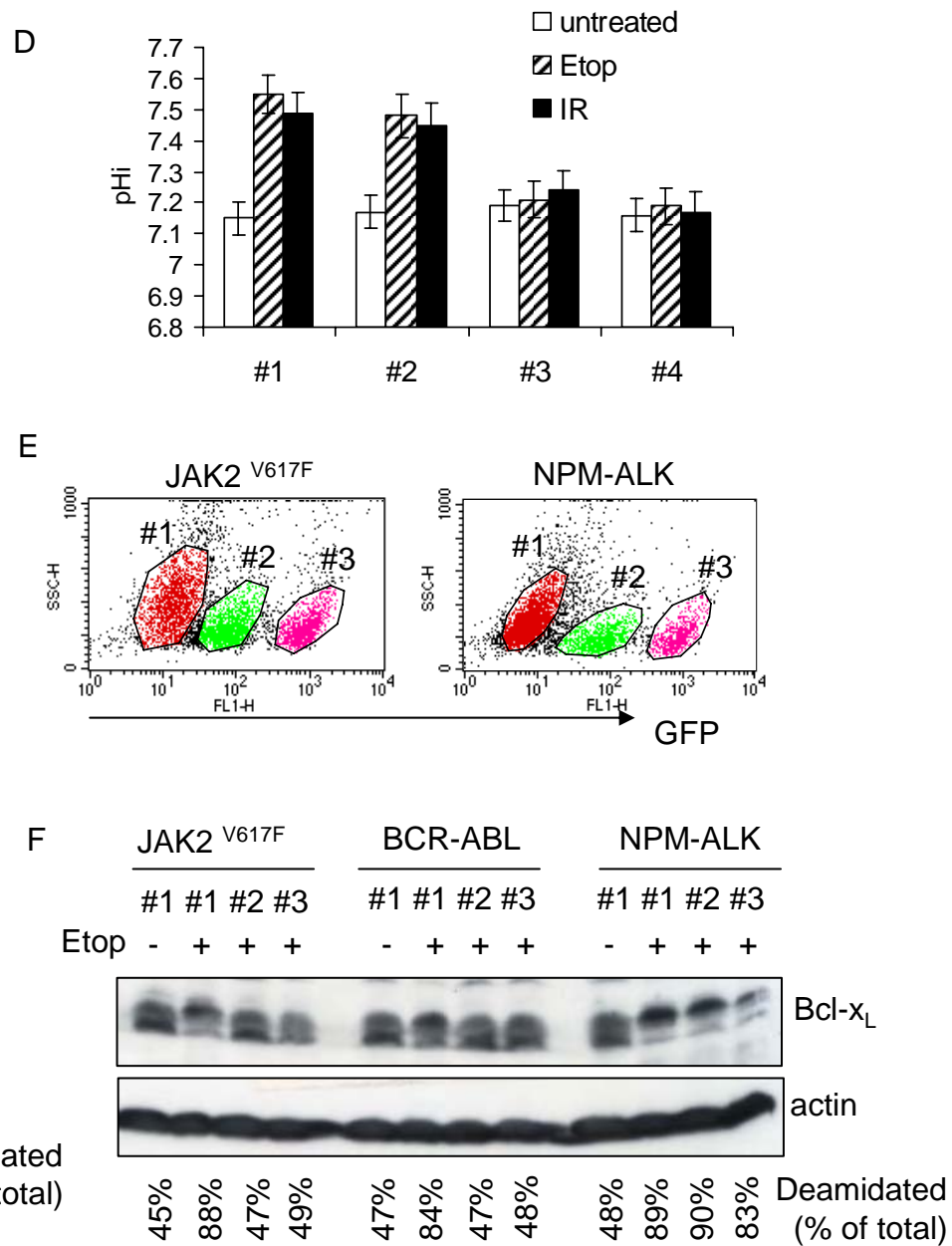
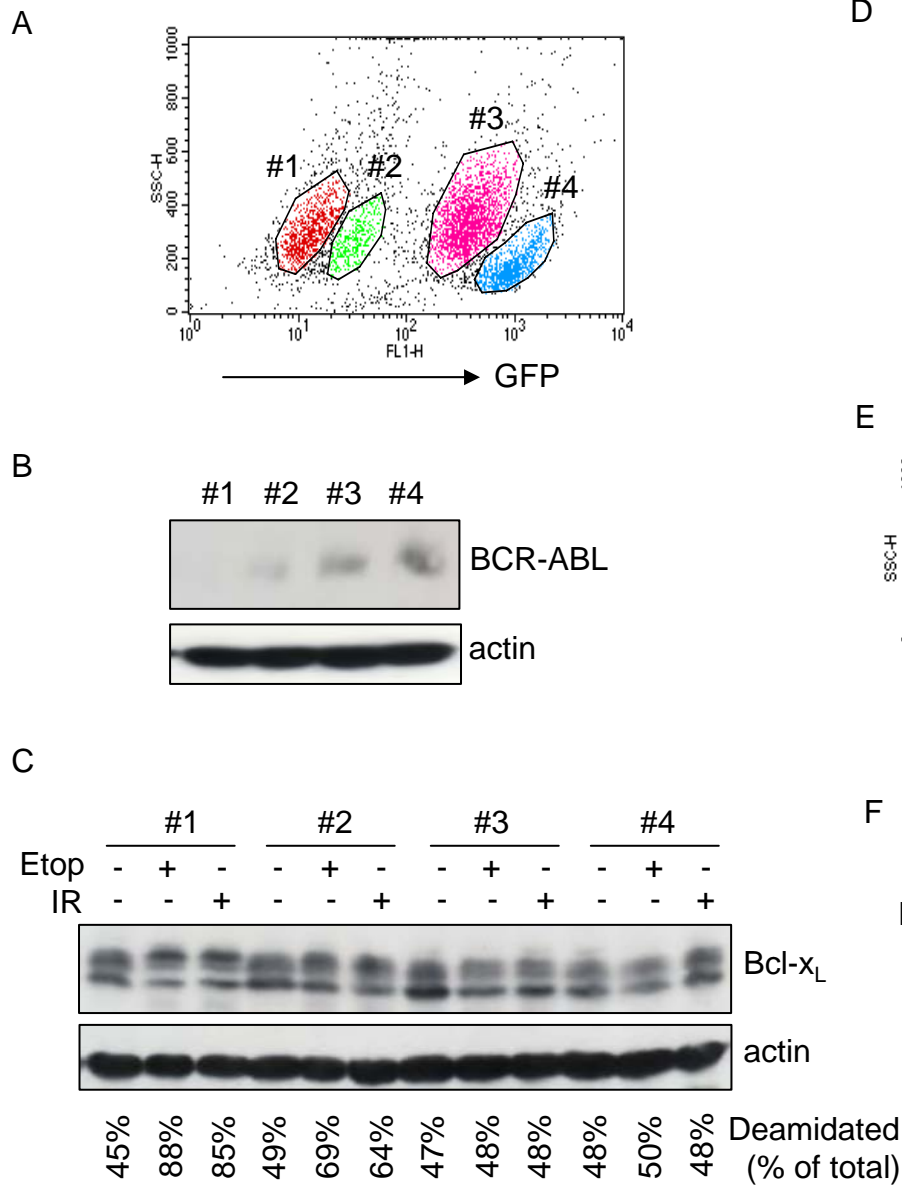
C



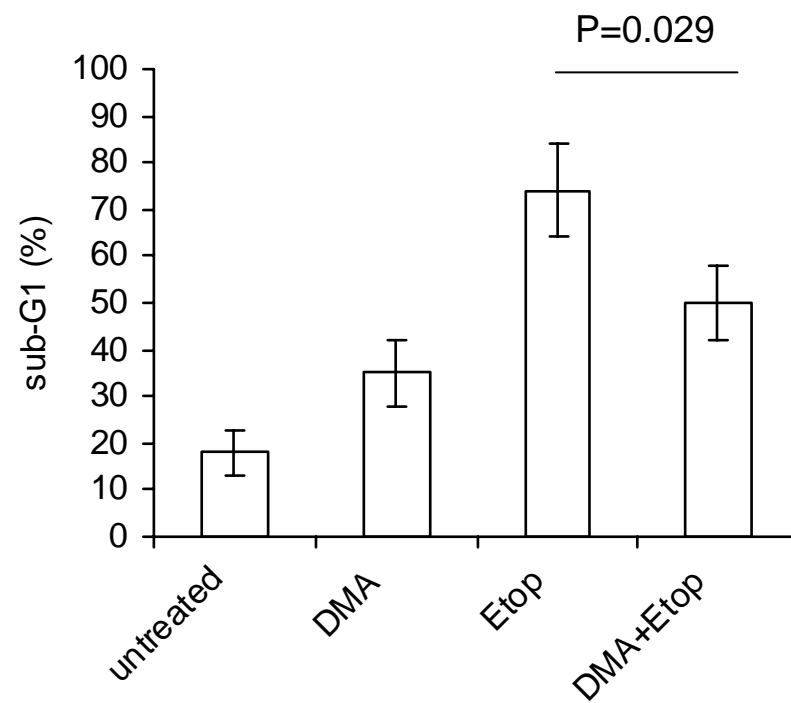
Supplementary Figure S8



Supplementary Figure S9

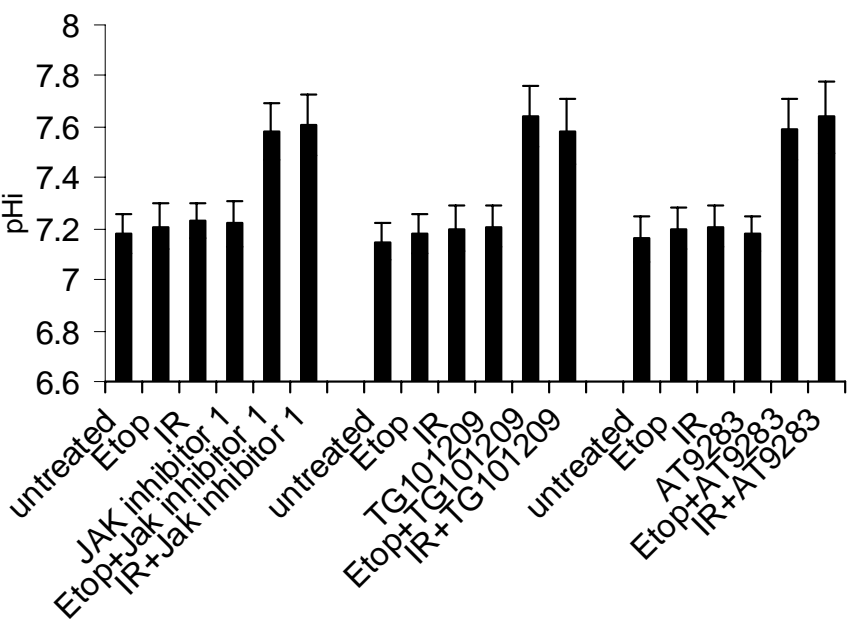


Supplementary Figure S10

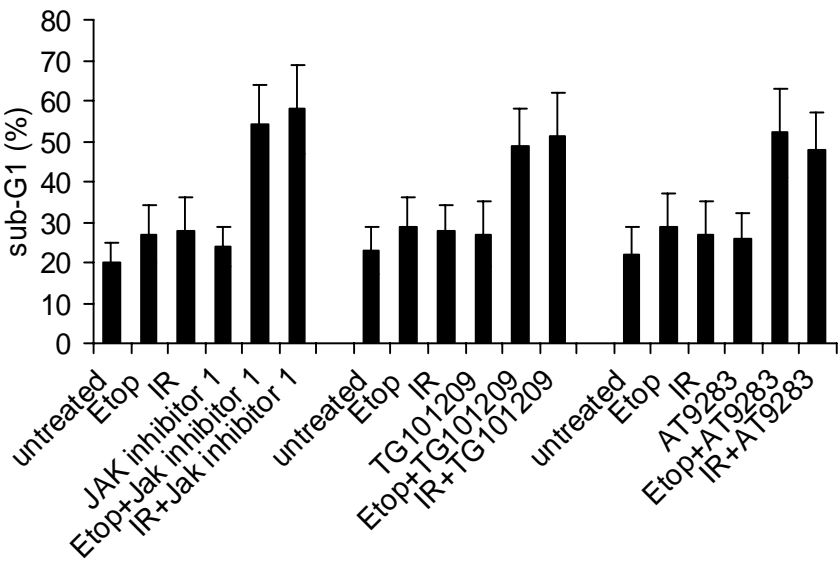


Supplementary Figure S11

A

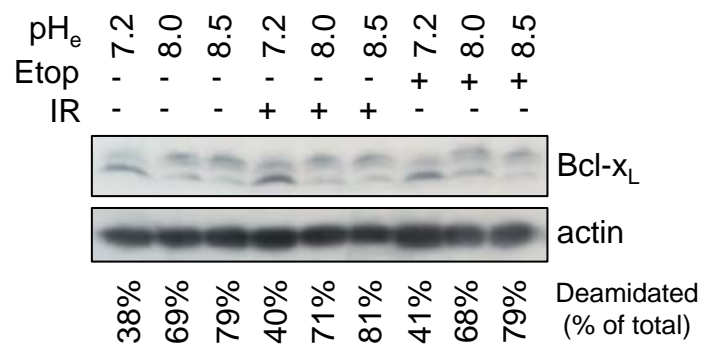


B

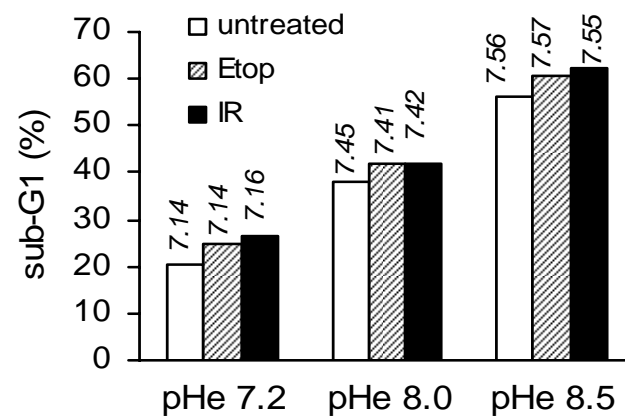


Supplementary Figure S12

A



B



Supplementary Table 1. Description of cell lines used for investigation of the Bcl-x_L deamidation pathway

Cell lines	Hematological cancers	Chromosomal defects	Dysfunctional / deregulated gene
K562 ¹	Chronic Myeloid Leukaemia	t(9;22)(q34;q11)	BCR-ABL*
HEL ²	Polycythaemia Vera	JAK2 V617F homozygous	JAK2*
Daudi ³	Burkitt lymphoma/Burkitt cell leukemia	t(8;14)(q24;q32)	c-myc
DU528 ⁴	Precursor T-cell acute lymphoblastic leukemia	t(1;14)(p34;q11)	TAL1
JVM2 ⁵	Mantle-cell lymphoma	t(11;14)(q13;q32)	cyclinD1
Karpas299 ⁶	Anaplastic large-cell lymphoma	t(2;5)(p23;q35)	NPM-ALK*
OPM2 ⁷	Multiple myeloma	t(4;14)(p16;q32)	FGFR3*
DOHH2 ⁸	Follicular lymphoma	t(14;18)(q32;q21)	BCL2

* signifies dysfunctional / deregulated gene is a tyrosine kinase

1. Lozzio, C.B. & Lozzio, B.B. Human chronic myelogenous leukemia cell-line with positive Philadelphia chromosome. *Blood* **45**, 321-34 (1975).
2. Martin, P. & Papayannopoulou, T. HEL cells: a new human erythroleukemia cell line with spontaneous and induced globin expression. *Science* **216**, 1233-5 (1982).
3. Klein, E. et al. Surface IgM-kappa specificity on a Burkitt lymphoma cell in vivo and in derived culture lines. *Cancer Res* **28**, 1300-10 (1968).
4. Begley, C.G. et al. The gene SCL is expressed during early hematopoiesis and encodes a differentiation-related DNA-binding motif. *Proc Natl Acad Sci U S A* **86**, 10128-32 (1989).
5. Melo, J.V. et al. Two new cell lines from B-prolymphocytic leukaemia: characterization by morphology, immunological markers, karyotype and Ig gene rearrangement. *Int J Cancer* **38**, 531-8 (1986).
6. Fischer, P. et al. A Ki-1 (CD30)-positive human cell line (Karpas 299) established from a high-grade non-Hodgkin's lymphoma, showing a 2;5 translocation and rearrangement of the T-cell receptor beta-chain gene. *Blood* **72**, 234-40 (1988).
7. Chesi, M. et al. Frequent translocation t(4;14)(p16.3;q32.3) in multiple myeloma is associated with increased expression and activating mutations of fibroblast growth factor receptor 3. *Nat Genet* **16**, 260-4 (1997).
8. Kluin-Nelemans, H.C. et al. A new non-Hodgkin's B-cell line (DoHH2) with a chromosomal translocation t(14;18)(q32;q21). *Leukemia* **5**, 221-4 (1991).